



A Comprehensive Review of the Tunicate Swarm Algorithm: Variations, Applications, and Results

Rong Zheng^{1,2} · Abdelazim G. Hussien^{3,4} · Anas Bouaouda⁵ · Rui Zhong⁶ · Gang Hu⁷

Received: 18 November 2024 / Accepted: 24 January 2025

© The Author(s) under exclusive licence to International Center for Numerical Methods in Engineering (CIMNE) 2025

Abstract

The development of new metaheuristic algorithms and their enhancements has seen significant growth, yet many of these algorithms share similar limitations. This is largely due to insufficient studies analyzing their structures and performance prior to proposing modifications. The Tunicate Swarm Algorithm (TSA), a recently developed nature-inspired algorithm, offers a simple structure, distinctive stabilizing features, and impressive efficiency. Inspired by the social behaviors of tunicates and their jet propulsion for movement and foraging, the TSA employs a dynamic weighting mechanism to simulate their influence during the search process. Its notable traits, including simplicity, adaptability, minimal parameters, and independence from derivatives, have contributed to its rapid adoption across various optimization problems. This review focuses on the foundational research underlying the TSA, exploring its development and effectiveness as highlighted in existing studies. It also examines enhancements to the algorithm's behavior, particularly efforts to align search space geometry with practical optimization challenges. Finally, potential directions for future improvements and adaptations are proposed to further advance the TSA's capabilities.

Abbreviations

✉ Rong Zheng
zhengr@fjsmu.edu.cn

Abdelazim G. Hussien
abdelazim.hussien@liu.se

Anas Bouaouda
anas.bouaouda-etu@etu.univh2c.ma

Rui Zhong
zhongrui@iic.hokudai.ac.jp

Gang Hu
hugang@xaut.edu.cn

¹ New Engineering Industry College, Putian University, Putian 351100, Fujian, China

² School of Information Engineering, Sanming University, Sanming 365004, Fujian, China

³ Department of Computer and Information Science, Linköping University, Linköping, Sweden

⁴ Faculty of Science, Fayoum University, Fayoum, Egypt

⁵ Faculty of Science and Technology, Hassan II University of Casablanca, Mohammedia, Morocco

⁶ Information Initiative Center, Hokkaido University, Sapporo, Japan

⁷ Department of Applied Mathematics, Xi'an University of Technology, Xi'an 710054, PR China

AOA	Arithmetic optimization algorithm
BHA	Black hole attack
CCC	Complex correlation coefficient
CB	Capacitor bank
CH	Cluster head
CNN	Convolutional neural network
CRNN	Convolutional-recurrent neural network
CS	Cuckoo search
DNN	Deep neural network
DE	Differential algorithm
DEED	Dynamic economic emission dispatch
DG	Distributed generators
DL	Deep learning
DNR	Distribution network reconfiguration
DR	Diabetic retinopathy
DRINA	Distributed routing information acquisition
DWT	Discrete wavelet transform
E2E	End-to-end
EGTBoost	Extreme gradient tree boost classifier
ELM	Extreme learning machine
EV	Electric vehicle
FA	Firefly algorithm
FCM	Fuzzy C-mean

FPR	False positive rate
GBDT	Gradient boosting decision tree
GA	Genetic algorithm
GHA	Gray hole attack
GSA	Gravitational search algorithm
GWO	Grey wolf optimizer
HHO	Harris Hawks optimization
KNN	k-nearest neighbor
LEO	Local escaping operator
LSTM	Long short-term memory
MAPE	Mean absolute percentage error
MANET	Mobile adhoc network
MBO	Monarch butterfly optimization
MFO	Moth-flame optimization
ML	Machine learning
NL	Network lifetime
OPF	Optimal power flow
OBL	Opposition based learning
PDR	Packet delivery ratio
PLR	Packet loss rate
PSNR	Peak signal-to-noise ratio
QC	Quantum computing
QKM	Quantum kernel method
RDS	Radial distribution system
RMSE	Root mean square error
RoI	Region of interest
SA	Simulated annealing
SCA	Sine cosine algorithm
SRM	Switched reluctance motor
SVM	Support vector machine
TPR	True positive rate
TSA	Tunicate swarm algorithm
VIF	Variance inflation factor
WOA	Whale optimization algorithm
WHA	Wormhole attacks
WSN	Wireless sensor networks

1 Introduction

In recent decades, the utilization of optimization techniques has expanded significantly to address complex problems across various domains, including science, engineering, economics, and business [1]. Optimization plays a pivotal role in assisting companies and institutions in improving profitability, operational efficiency, and cost-effectiveness, ultimately saving valuable time and resources. Consequently, a diverse array of optimization methods has emerged, categorized into distinct types such as deterministic, heuristic, and meta-heuristic optimization approaches [2].

Deterministic methods distinguish themselves from randomized approaches and can be further categorized into

linear and nonlinear optimization methods. Typically, deterministic methods employ gradient-based algorithms tailored for linear, nonlinear, and differentiable optimization problems. However, these methods are vulnerable to being ensnared in local optima during the optimization process [3]. On the other hand, heuristic algorithms are typically tailored to specific problems and operate without requiring random elements. They yield consistent results with the same input, following predefined steps. Similar to other deterministic techniques, heuristic algorithms may encounter challenges as they can become trapped in local optima due to their rigid implementation, hindering their ability to reach global optima [4].

Considering the aforementioned factors, meta-heuristic methods prove more advantageous compared to deterministic approaches. These methods iteratively navigate the search space using various operators to minimize or maximize a given function. During the exploration phase, the algorithm broadly and randomly explores the solution space, resulting in more diverse solution sets and faster convergence [5]. In contrast, the exploitation phase allows the algorithm to conduct a more precise search within the promising regions identified during exploration, reducing randomness while improving accuracy. Therefore, the efficient design of exploration and exploitation processes is crucial for the success of any meta-heuristic algorithm, emphasizing the importance of finding the right balance between these two aspects [6].

The widespread adoption of meta-heuristic algorithms can be attributed to their inherent flexibility, independence from problem-specific characteristics, freedom from reliance on gradient information, and demonstrated ability to escape local optima in complex optimization problems [7, 8]. Their flexibility enables efficient problem-solving across a wide range of scenarios without necessitating extensive modifications to their core components. Furthermore, meta-heuristics do not require derivative computations in problem search spaces, as they operate as stochastic algorithms utilizing stochastic operators. This quality proves particularly valuable for real-world problems, which often feature numerous local optima. Notably, simplicity and ease of use are additional advantages, as many meta-heuristics draw inspiration from simple rules and collective behaviors observed in natural systems.

In the literature, meta-heuristic algorithms are often categorized based on several factors [9], including their inspiration from nature or non-nature sources, utilization of population-based or single-point search strategies, adaptability to dynamic or static objective functions, exploration of multiple neighborhoods, and incorporation of memory. Moreover, meta-heuristics can be classified into three key trends: enhancing existing methods by optimizing their control parameters, combining different methods to leverage their strengths, and introducing entirely new approaches.

When categorized based on the source of inspiration, these algorithms are typically grouped into five main classes as shown in Fig. 1.

The first category comprises evolutionary-based algorithms, drawing inspiration from natural phenomena and biological processes. These algorithms leverage concepts from biology, genetics, natural selection laws, and random operators to tackle optimization problems. Key examples include the differential evolution (DE) [10] and Genetic Algorithm (GA) [11], widely employed algorithms that emulate principles of reproduction, natural selection, and Darwinian evolution. These algorithms utilize random operators such as selection, crossover, and mutation to navigate complex search spaces. Additional noteworthy algorithms in this category include the Artificial Immune System (AIS) [12], Biogeography-Based Optimization (BBO) [13], Backtracking Search Algorithm (BSA) [14], Monkey King Evolution (MKE) [15], Wildebeests Herd Optimization (WHO) [16], and Human Felicity Algorithm (HFA) [17].

The second category of metaheuristic algorithms which is mathematics-based algorithms draws inspiration from numerical techniques, mathematical operators, and mathematical programming processes to address diverse constraints and optimization challenges in real-world applications. This diverse category includes a variety of algorithms such as the Gradient-based Optimizer (GBO) [18], Generalized Normal Distribution Optimization (GNDO) [19], Arithmetic Optimization Algorithm (AOA) [20], Runge Kutta Optimizer (RUN) [21], Circle Search Algorithm (CSA) [22], weIghted meaN oF vectOr (INFO) [23], Exponential Distribution Optimizer (EDO) [24], and Sinh Cosh Optimizer (SCHO) [25].

The third category involved physics-based algorithms, drawing inspiration from physical models and incorporating various motions, concepts, phenomena, processes, and laws related to mechanics, heat, electromagnetism, optics, and atomic physics. A widely used algorithm in this category is Simulated Annealing (SA) [26], which applies thermodynamics laws, mimicking the annealing process used in material sciences to enhance crystal size through controlled heating and cooling. SA, renowned for its effective local search capabilities, proves valuable in discovering potential solutions to diverse engineering problems. Other noteworthy physics-based algorithms include the Transient Search Algorithm (TSO) [27], Equilibrium Optimizer (EO) [28], Lichtenberg Algorithm (LA) [29], Archimedes Optimization Algorithm (AOA) [30], Homonuclear Molecules Optimization (HMO) [31], Light Spectrum Optimizer (LSO) [32], Fick's Law Algorithm (FLA) [33], and Optical Microscope Algorithm (OMA) [34].

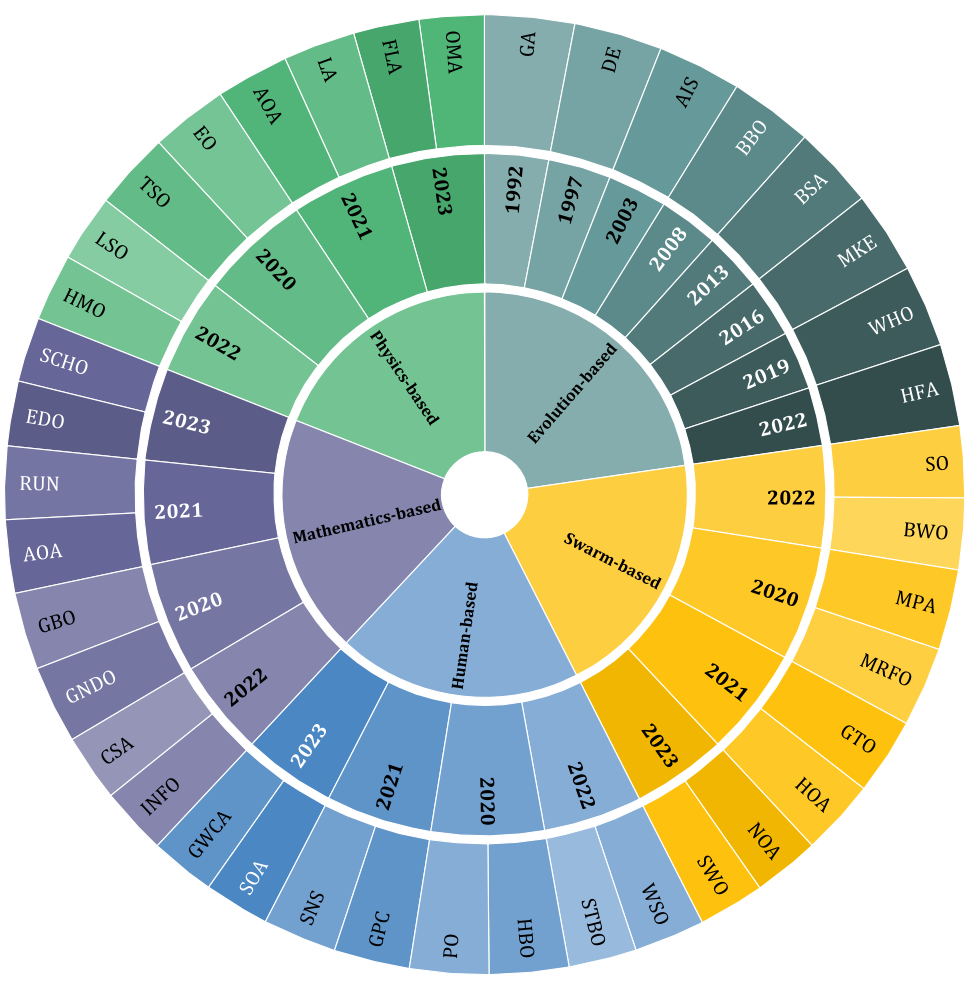
In addition to the previously discussed categories of optimization algorithms, a distinct approach has emerged with human-based algorithms. These algorithms are designed

by simulating mathematical models of human behaviors, activities, and interactions within individual and social settings. Teaching-learning-based optimization (TLBO) [35] is a prominent example of a human-based algorithm, conceptualizing a classroom learning environment and the interactions between teachers and students to enhance knowledge acquisition, mirroring the optimization process. Other notable human-based algorithms include Heap-Based Optimizer (HBO) [36], Political Optimizer (PO) [37], Giza Pyramids Construction (GPC) [38], Social Network Search (SNS) [39], War Strategy Optimization (WSO) [40], Sewing training-based optimization (STBO) [41], Skill optimization algorithm (SOA) [42], and Great Wall Construction Algorithm (GWCA) [43].

The final category encompasses swarm-based algorithms, representing one of the most rapidly evolving families of metaheuristic algorithms. These algorithms draw inspiration from collective behaviors observed in biological populations across the natural world, including animals, plants, and microorganisms. Classic swarm-based algorithms have made significant contributions to optimization. Ant Colony Optimization (ACO) [44], for instance, mimics the foraging behavior of ant colonies, where ants deposit pheromones on paths to guide others toward food sources. Another prominent example is the Whale Optimization Algorithm (WOA) [45], which emulates the predatory tactics of whales, including encircling prey, bubble-net hunting techniques, and prey searching. This diverse category includes well-established algorithms such as the Marine Predator Algorithm (MPA) [46], Manta Ray Foraging Optimization (MRFO) [47], Gorilla Troops Optimizer (GTO) [48], Horse Herd Optimization Algorithm (HOA) [49], Snake Optimizer (SO) [9], Beluga Whale Optimization (BWO) [50], Nutcracker Optimization Algorithm (NOA) [51], and Spider Wasp Optimization (SWO) [52].

Although most metaheuristic algorithms are derived from the five fundamental categories previously mentioned, many others are inspired by a diverse range of unique sources [53]. These sources include plant-based algorithms such as the Waterwheel Plant Algorithm (WWPA) [54], Strawberry Algorithm (SBA) [55], and Willow Catkin Optimization (WCO) [56]; music-based/art-based algorithms such as the Stochastic Paint Optimizer (SPO) [57], Melody Search algorithm (MS) [58], and Musical Composition Algorithm (MMC) [59]; sport-based algorithms such as the Alpine Skiing Optimization (ASO) [60], Football Team Training Algorithm (FTTA) [61], and Running City Game Optimizer (RCGO) [62]; and chemistry-based algorithms such as Chemical Reaction Optimization (CRO) [63], Ray Optimization (RO) [64], Smell Agent Optimization (SAO), and Gases Brownian Motion Optimization (GBMO) [65].

Fig. 1 Classification of metaheuristic algorithms



On the other hand, hybrid algorithms represent a distinct category in which multiple optimization methods or metaheuristic frameworks are combined to leverage their advantages. These algorithms typically aim to balance exploration and exploitation better or to be more tailored to specific problem domains [2]. For example, Khaleel [66] combined the Sparrow Search Algorithm (SSA) with DE to create a hybrid algorithm called CSSA-DE, which was used to solve the load balancing problem. Hasanien et al. [67] developed a hybrid approach by merging PSO with the Hippocampus Optimizer to address the reactive power problem in electric vehicles, successfully reducing voltage fluctuations and power losses. Guo and Chiu [68] introduced a hybrid optimization method called HJPSO by integrating Jellyfish Search (JS) with PSO to address PSO's tendency to get stuck in local optima when tackling problems such as feature selection and parameter optimization in large datasets. The studies highlighted demonstrate the strong performance of hybrid algorithms in addressing real-world optimization issues.

The Tunicate Swarm Algorithm (TSA) is another swarm-based optimization algorithm introduced by Satnam Kaur et al. [69]. Drawing inspiration from the jet propulsion and

swarm behaviors observed in tunicates, this algorithm aims to achieve optimal solutions by effectively mimicking the movement patterns of these marine organisms. TSA's mechanism involves guiding search agents towards the position of the best-performing tunicate, while simultaneously preventing conflicts among agents and maintaining proximity to the optimal search agent [69]. This unique approach has garnered considerable attention since TSA's inception due to its straightforward structure, robust search performance, rapid iteration capabilities, and minimal parameter requirements. Researchers have successfully applied TSA to a wide range of optimization problems across diverse fields, demonstrating its efficacy in addressing practical application challenges. As of November 18, 2023, TSA has accumulated an impressive 795 citations on Google Scholar, underscoring its impact and relevance within the optimization research community. The introduction of TSA has spurred extensive research across various disciplines, leading to a multitude of scholarly achievements and advancements in the field.

This survey offers a comprehensive review of the TSA and its adaptations, covering research conducted from 2020 to the present. The motivation for this effort arises from the

absence of a dedicated and comprehensive review or survey paper on TSA. The study systematically compiles and critically analyzes the existing TSA literature, categorizing its variants, and evaluating their applications in various optimization problems. By exploring the practical applications of TSA across diverse domains, the research aims to illuminate its real-world effectiveness. The survey concludes by proposing potential avenues for future research in this field.

The following sections of this survey are organized as follows: sect. 2 provides a comprehensive exposition of the TSA algorithm, detailing its structure and underlying methodologies. Sect. 3 shows the expansion of Tunicate Swarm Algorithm whereas sect. 4 explores delves into the realm of TSA variants, modifications, and enhancements, offering an overview of the diverse adaptations and advancements that have expanded the algorithm's capabilities. Section 5 explores the practical applications of TSA, showcasing its effectiveness in various domains and highlighting improvements achieved in specific fields. Section 6 analyze delves into the theoretical framework underpinnings of TSA, examining its assessment and evaluation methodologies. Section 7 engages in a discussion of future research directions, identifying promising avenues for further exploration. Finally, Sect. 8 summarizes the key findings and conclusions drawn from this comprehensive survey.

2 Overview of Tunicate Swarm Algorithm

Tunicate Swarm Algorithm (TSA) is a swarm intelligence approach inspired by the swarm behavior of tunicates in the deep ocean [69]. Tunicates are bioluminescent creatures that can emit a soft blue-green light. Each tunicate draws water from the surrounding sea and expels it through its atrial siphons, which creates a form of jet propulsion. This unique mechanism allows tunicates to move through the ocean with fluid and jet-like movements. The propulsion is powerful enough to enable vertical migration in the water column. Individual tunicates are only a few millimeters in size, but they possess a common gelatinous tunic that connects them, which allows them to exhibit coordinated swarm behavior. Inspired by the unique behaviors of tunicates, Kaur et al. [69] proposed TSA, which mainly contains two phases: jet propulsion and swarm intelligence. A demonstration of TSA is presented in Fig. 2.

2.1 Avoiding the Individual Conflicts

To avoid conflicts among tunicate individuals during the search phase, \vec{A} is employed to support the location of the

offspring tunicate individual, as formulated in Eq. (1).

$$\begin{aligned}\vec{A} &= \frac{\vec{G}}{\vec{M}} \\ \vec{G} &= \vec{c}_2 + \vec{c}_3 - \vec{F} \\ \vec{F} &= 2 \cdot c_1\end{aligned}\quad (1)$$

where \vec{G} and \vec{F} represent the gravity force and water flow advection, respectively. c_1 is a random number in $[0, 1]$, \vec{c}_2 and \vec{c}_3 are random vectors where each element is within $[0, 1]$. \vec{M} denotes social forces between tunicate individuals, as formulated in Eq. (2).

$$\vec{M} = \lfloor P_{\min} + c_1 \cdot P_{\max} - P_{\min} \rfloor \quad (2)$$

where P_{\min} and P_{\max} denote the initial and subordinate speeds of social interaction among tunicate individuals.

2.2 Movement Towards the Best Neighbor

After the conflicts among tunicate individuals are avoided in the previous phase, tunicate individuals move towards the best neighbor using Eq. (3).

$$\vec{P_D} = \left| \vec{FS} - \text{rand} \cdot \vec{P}_P(x) \right| \quad (3)$$

where $\vec{P_D}$ indicates the distance between the food source and the tunicate individual, \vec{FS} denotes the location of the food source (i.e., the optimum found so far), $\vec{P}_P(x)$ is the position of the tunicate individual, and rand is a random number in $[0, 1]$.

2.3 Movement Towards the Best Tunicate

Once the distance between the food source and the tunicate individual is determined, tunicate individuals move towards the current best tunicate individual using Eq. (4).

$$\vec{P}_p(x') = \begin{cases} \vec{FS} + \vec{A} \cdot \vec{P_D}, & \text{if rand} \geq 0.5 \\ \vec{FS} - \vec{A} \cdot \vec{P_D}, & \text{if rand} < 0.5 \end{cases} \quad (4)$$

where $P_p(x')$ is the updated position of tunicate individuals.

2.4 Swarm Intelligence

In the swarm intelligence phase, the tunicate swarm ensures the survival of the best and the second-best tunicate individuals, which corresponds to the concept of “survival of the fittest”, and the remaining tunicate individuals are updated

Movement to the best tunicate:

$$\overrightarrow{PD} = |\overrightarrow{FS} - \text{rand} \cdot \vec{P}_p(x)|$$

$$\vec{P}_p(x) = \begin{cases} \overrightarrow{FS} + \vec{A} \cdot \overrightarrow{PD}, & \text{if rand} \geq 0.5 \\ \overrightarrow{FS} - \vec{A} \cdot \overrightarrow{PD}, & \text{if rand} < 0.5 \end{cases}$$

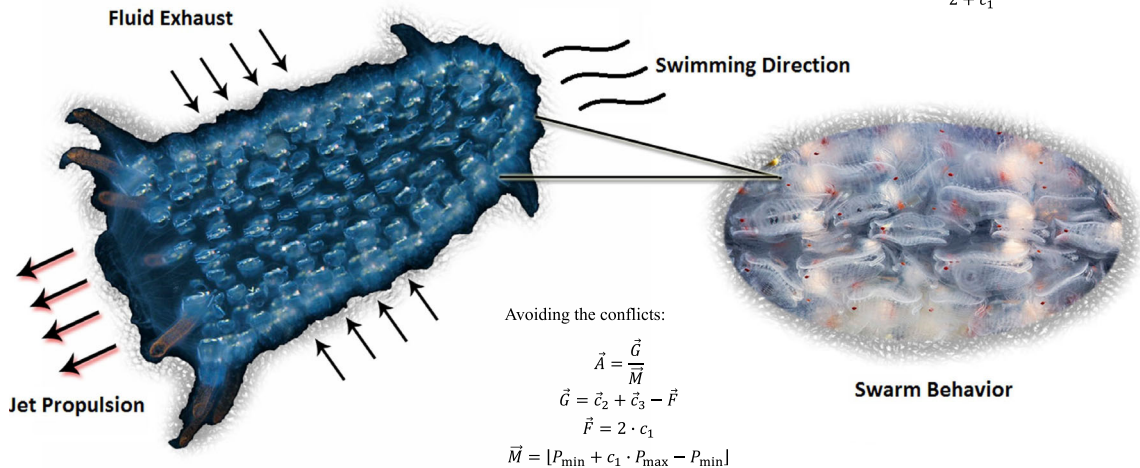


Fig. 2 A demonstration of TSA [69]

using Eq. (5).

$$\vec{P}_P(x+1) = \frac{\vec{P}_P(x) + \vec{P}_P(x')}{2 + c_1} \quad (5)$$

In summary, the flowchart of TSA is shown in Fig. 3, and its pseudocode is presented in Algorithm 1.

2.5 Time Complexity of TSA

Supposing the size of the Tunicate swarm is N , the dimension size of the problem is D , and the maximum iteration is T . The main steps in TSA are as follows.

- Tunicate swarm initialization: $O(N \times D)$.
- Computational complexity for avoiding conflicts: $O(D)$.
- Computational complexity for moving towards the best neighbor: $O(N \times D)$.

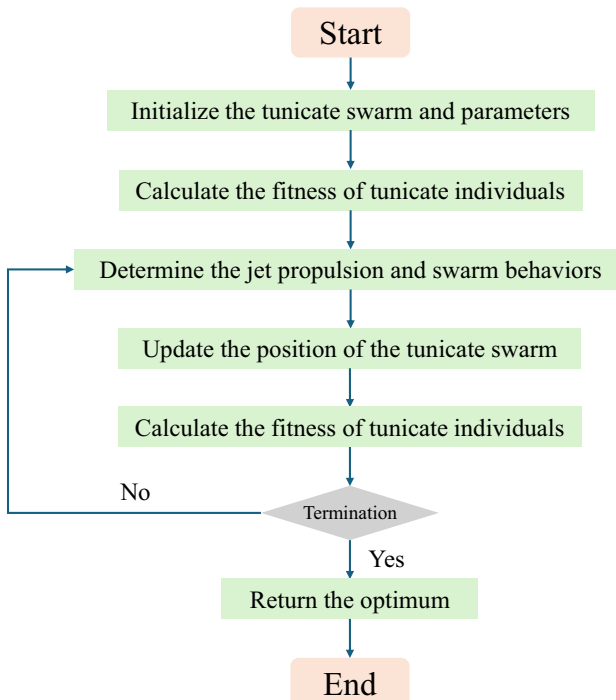
Algorithm 1 Tunicate Swarm Algorithm (TSA)

Function TSA():

```

Initialize  $t_{Max}$ ,  $N$ ,  $D$ , Fitness Function
Initialize tunicate swarm randomly
while  $t < t_{Max}$  do
    for  $i = 0$  to  $D$  do
         $c_1, c_2, c_3, rand \leftarrow \text{rand}()$ 
        Determine  $\vec{A}, \vec{G}, \vec{F}$  using Eq. (1)
        Determine  $\vec{M}$  using Eq. (2)
        Determine  $\overrightarrow{PD}$  using Eq. (3)
        Update  $\vec{P}_p(x')$  using Eq. (4)
    end
    Update  $\vec{P}_P(x+1)$  using Eq. (5)
    Update parameters  $\vec{A}, \vec{G}, \vec{F}$ , and  $\vec{M}$ 
    Record the current best agent
end
Return the best agent

```

**Fig. 3** The flowchart of TSA

- Computational complexity for moving towards the best tunicate: $O(N \times D)$.
- Computational complexity of swarm intelligence phase: $O(N)$.

In summary, the computational complexity of TSA is computed in Eq. (6).

$$\begin{aligned} O(N \times D + T \times (D + N \times D + N \times D + N)) \\ := O(T \times N \times D) \end{aligned} \quad (6)$$

3 The Expansion of Tunicate Swarm Algorithm

The TSA has gained substantial attention and widespread recognition since its introduction in 2020. As of 31 August 2024, Google Scholar reports that the original paper has been cited 1043 times. These citations include 900 journal articles, 102 conference papers, and 25 book chapters. Due to its strengths, the paper has been acknowledged as one of the top-ranked works in both Web of Science¹ and Scopus².

Table 1 The top seven journals with the highest number of manuscripts on TSA

No.	Source documents	Count
1	IEEE access	48
2	Expert systems with applications	22
2	Multimedia tools and applications	22
3	Engineering applications of artificial intelligence	21
4	Biomimetics	19
4	Scientific reports	19
4	Soft computing	19
5	Knowledge based systems	18
6	Computers materials and continua	17
7	Artificial intelligence review	16
7	Mathematics	16

This section offers an in-depth analysis of the growth of TSA from 2020 to 2024. It addresses several key aspects, such as the TSA's distribution of citations since its appearance in 2020, the yearly number of articles on TSA, the top journals interested in TSA algorithm, number of papers by different publishers. Furthermore, it includes various other statistical data related to TSA research.

Figure 4 presents the yearly citation distribution of the TSA paper, based on data from the Google Scholar database, with a total of 1043 citations. Figure 5 illustrates the increase in TSA-related publications since its initial release. Moreover, Table 1 presents the top 7 journals with the highest number of publications on TSA. Figure 6 provides an overview of the major publishers featuring research on TSA in their journals. Springer ranks first with 231 articles, followed by Elsevier with 202 articles, MDPI with 147 papers, IEEE with 89 papers, and Wiley with 37 papers. Additional contributions are spread across various other publishers, as shown in Fig. 6.

4 Variants of Tunicate Swarm Algorithm

Due to its extensive application in addressing optimization problems of various sizes and complexities across multiple domains, TSA has been modified or hybridized to navigate the challenging search spaces of real-world optimization issues effectively. A multi-objective version of TSA has been developed also to address problems with multiple objectives. The following subsections provide a comprehensive

¹ <https://www.webofscience.com/wos/woscc/full-record/WOS:000528194400031>

² [https://www.scopus.com/record/display.uri?eid=2-s2.0-85079402816&origin=resultslist&sort=plf-f&src=s&sid=c3f02358e2fb6041b84b7c46f9cf38f9&relpos=1](https://www.scopus.com/record/display.uri?eid=2-s2.0-85079402816&origin=resultslist&sort=plf-f&src=s&sid=c3f02358e2fb6041b84b)

Footnote 2 continued

7c46f9cf38f9&sot=b&sdt=b&s=TITLE-ABS-KEY%28Tunicate+Swarm+Algorithm%3A+A+new+bio-inspired+based+metaheuristic+paradigm+for+global+optimization%29&sl=112&sessionSearchId=c3f02358e2fb6041b84b7c46f9cf38f9&relpos=1

Fig. 4 Distribution of citations by TSA

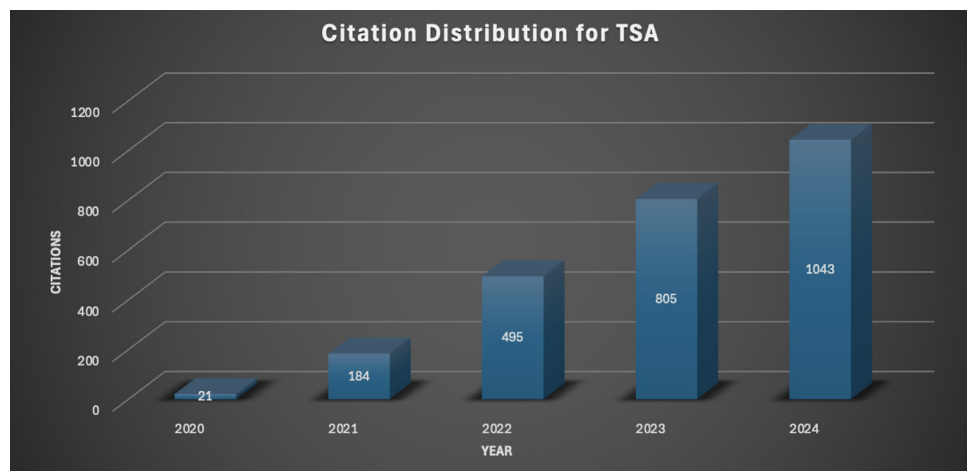


Fig. 5 TSA's citations growing

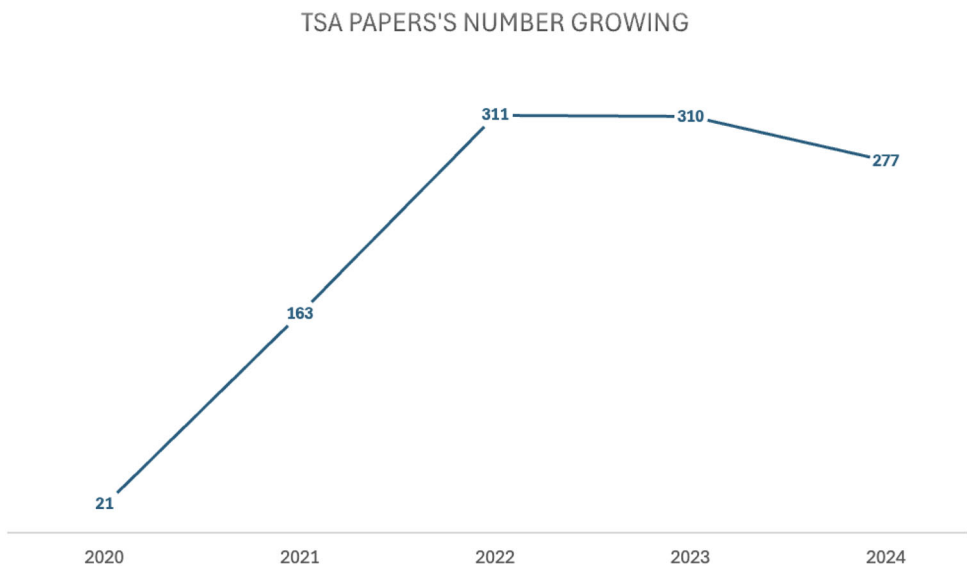
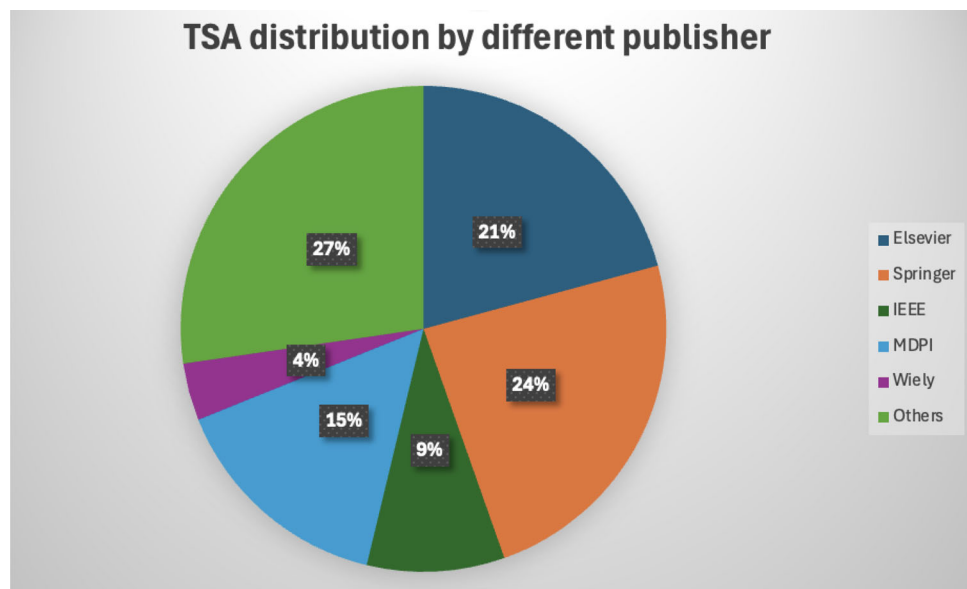
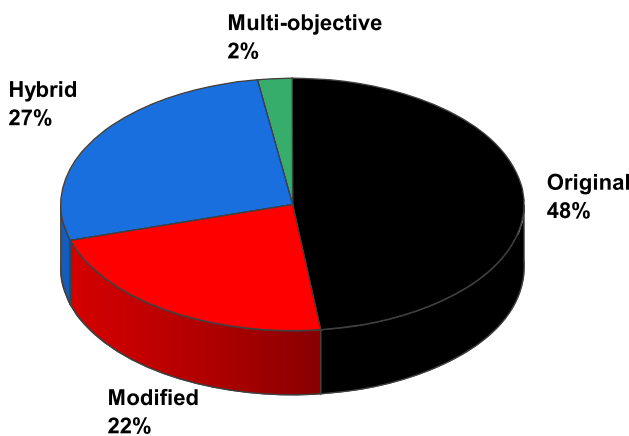


Fig. 6 Publishers distributions



**Fig. 7** Percentage of applying TSA variants in diverse domains

summary of TSA variants across different areas. Figure 7 illustrates the distribution of TSA usage in various real-world problems: original TSA accounts for approximately 48%, modified TSA for around 2%, hybridized TSA for about 27%, and multi-objective versions for the remaining proportion (2%).

4.1 Modified Versions of Tunicate Swarm Algorithm

Modified versions of TSA have been introduced, focusing on adjustments to certain parameters or operators within the algorithm. These minor modifications do not fundamentally alter the TSA algorithm's core mechanism. Instead, they enhance TSA's ability to better balance exploration and exploitation within the complex search spaces of various applications. The modified TSA variants include opposition-based learning TSA, chaotic TSA, Levy-flight-based TSA, adaptive TSA, and multi-strategy TSA, among others. Table 2 provides an overview of the conventional TSA alongside various enhancement strategies. The following subsections discuss research articles based on these methodologies.

4.1.1 Opposition Based Learning Tunicate Swarm Algorithm

Tizhoosh [126] introduced the machine learning technique known as Opposite-Based Learning (OBL). OBL enhances an algorithm's optimization capability by exploring the search space in the direction opposite to a current solution, thereby investigating unfamiliar areas. This approach increases the diversity of solutions within a population, providing the algorithm with a better chance of escaping local optima. Numerous studies have integrated OBL with TSA, improving convergence rates and solution quality, as discussed below.

Table 2 Summary of the modified TSA variants

No.	Strategies used	References
1	Opposition-based learning	[70–76]
2	Binary	[77, 78]
3	Chaotic theory	[79, 80]
4	Levy-Flight	[81–85]
5	Adaptive	[86–93]
6	Q-learning	[94, 95]
7	Dynamic perturbation strategy	[96]
8	Crossover and mutation operators	[97]
9	Chronological mechanism	[98]
10	Adaptive weights	[99]
11	Quantum theory	[100]
12	Reference set	[101]
13	Two distinct random numbers	[102]
14	Taylor strategy	[103]
15	Crossover operator	[104]
16	Fitness-distance balance strategy	[105]
17	Elite opposition learning strategy and exponential function steps strategy	[106]
18	Self-adaptive method and enhanced exploration phase strategy	[107]
19	Tent map, Gray Wolf Optimizer, and Levy flight	[108]
20	Lévy mutation operator, Cauchy mutation operator, and Gaussian mutation operator	[109]
21	Cosine mutation, adaptive grouping technique, Halton sequence, and arithmetic optimization strategy	[110]
22	Adaptive Gaussian Quantum Behaved Particle Swarm Optimization algorithm	[111]
23	Nine chaotic maps with the Lévy flight strategy	[112]
24	Opposition-based learning, Levy flight, and positive cosine operator	[113]
25	Differential evolution and quadratic interpolation strategies	[114]
26	Hyperbolic tangent domain adjustment, a nonlinear convergence factor, and the swarm update mechanism from the Harris Hawks Optimization	[115]
27	Adaptive weight parameters and mutation processes	[116]
28	Spiral technique, Levy flight, and Fish Aggregation Device effect	[117]
29	Reverse learning mechanism, non-linear self-learning factor, and Cauchy mutation strategy	[118]
30	Chaos theory, Opposition-based learning, and Cauchy mutation	[119]

Table 2 (continued)

No.	Strategies used	References
31	Tent map, quadratic interpolation, and Golden-Sine algorithm	[120]
32	Tent chaotic, golden sine partition factor, and nonlinear adaptive weight factor	[121]
33	Dynamic s-best mutation operator and directional mutation rule	[122]
34	Mutation and crossover operators	[123]
35	Differential sequencing alteration operator	[124]
36	Quasi-Oppositional Based Learning (QOBL) and Chaotic Local Search (CLS)	[125]

Houssein et al. [70] proposed TSA-OBL for disease classification using the k-nearest Neighbor (kNN) classifier. Evaluated on four datasets (Breast Cancer Wisconsin, Leukemia2, Base Brain T91, and Lung Cancer), TSA-OBL demonstrated superior accuracy to other methods, proving effective for disease classification.

Sharma et al. [71] proposed an opposition-based TSA for parameter estimation of photovoltaic modules to optimize solar power system performance. The algorithm enhances search space diversification through opposition-based learning. It successfully estimates parameters across different irradiance levels, showing good agreement with measured data. Comparative analysis reveals that opposition-based TSA outperforms other algorithms in robustness, statistical measures, and convergence speed, significantly reducing function costs compared to basic TSA.

Kanimozhi et al. [72] proposed the logistic regression-based oppositional tunicate fuzzy C-mean (LR-OTSFCM) methodology for efficient cloud intrusion detection. Addressing the need for robust security in cloud computing, LR-OTSFCM employs a four-stage process: preprocessing, feature selection, clustering using oppositional TSA (OPTSA) and fuzzy C-mean (FCM), and cluster handling to profile normal and abnormal behavior. Evaluated against benchmark problems and compared with state-of-the-art methods like ANN, LR-HID, ML-IDS, and En-ABC, LR-OTSFCM shows superior attack detection rates, enhancing cloud security.

Yasin et al. [73] proposed an intelligent framework for web page classification and re-ranking, consisting of classification and re-ranking phases. In classification, HTML tag removal, stemming, word-to-vector formation, and PCA are used for preprocessing and feature extraction. The Opposition-based TSA (O-TSA) optimizes feature selection, enhancing classification accuracy with the Enhanced Convolutional-Recurrent Neural Network (E-CRNN). In re-ranking, O-TSA optimizes the objective function for URL matching based on similarity, resulting in optimal web page retrieval. This approach improves classification and

re-ranking performance, reducing space requirements and search time compared to existing methods.

Suryawanshi et al. [74] evaluated heuristic-based expert systems for thermogram breast cancer detection. Using the DMR dataset, they employed preprocessing, segmentation, and entropy-based feature extraction. The Oppositional Improvement-based TSA (OI-TSA) optimized classifiers achieved 96% accuracy and 98.4% precision, demonstrating its effectiveness in enhancing classification accuracy and precision.

Mohanan et al. [75] studied the impact of the COVID-19 pandemic on HR management in IT firms in Tamil Nadu, focusing on work-from-home scenarios. Using a questionnaire for IT HR professionals, they analyzed nine key HRM categories: employee well-being and job loss. A Deep Neural Network (DNN) was optimized with the Oppositional Random Searched TSA (ORS-TSA) to minimize Root Mean Square Error (RMSE). ORS-TSA showed strong global optimization and fast convergence, outperforming traditional algorithms. The study effectively addressed HRM challenges during the pandemic.

Chandran et al. [76] introduced the Random Opposition-Based TSA (ROBTSA), an enhanced variant of TSA, to overcome premature convergence and local optima issues. By incorporating Random Opposition-Based Learning (ROBL) with a jumping probability mechanism, ROBTSA enhanced solution diversity and escaped local traps. The algorithm was tested on thirteen standard benchmark functions and applied to real-world engineering design problems, such as pressure vessel and spring optimization. ROBTSA demonstrated improved convergence, accuracy, and stability, outperforming other advanced algorithms in both benchmark and practical applications.

4.1.2 Binary Tunicate Swarm Algorithm

Prabhakaret al. [77] developed three systematic conglomerated models for cough sound classification, featuring the Binary TSA (BTSA) for effective feature selection. By integrating the Cross-Correlation Function (CCF) and machine learning techniques with the Tunable Q Wavelet Transform (TQWT), the models achieved an impressive classification accuracy of 98.99% using an arc-cosine Extreme Learning Machine (ELM) classifier. This research highlights the effectiveness of TSA variants in improving audio signal classification in medical applications, particularly for monitoring cough-related conditions.

Laishram et al. [78] developed a Binary TSA (BTSA) to enhance feature selection for computer-aided diagnosis (CAD) in mammographic mass classification. Utilizing pre-trained deep learning models and new fitness functions for suspicious lesions, the BTSA achieved sensitivity rates of 95.31% and 92.18%, with overall diagnostic accuracies of

97.86% and 93.86% on mini-MIAS and DDSM datasets. The F1 scores for malignancy reached 0.93 and 0.84, demonstrating the effectiveness of TSA variants in improving feature selection in medical imaging.

4.1.3 Chaotic Tunicate Swarm Algorithm

In chaotic theory, chaos denotes a deterministic approach exhibiting random behavior within dynamic, nonlinear systems [79]. These systems lack convergence and periodicity and have defined boundaries. Chaos serves primarily as a mechanism for generating randomness, operating as a straightforward deterministic dynamic system. It leverages a range of chaotic maps governed by distinct mathematical equations to produce sequences of elements [127]. This application of chaos aids optimization techniques in navigating problem search spaces with greater breadth and dynamism. The integration of chaos theory has bolstered the diversity control aspect of the TSA algorithm.

Gupta et al. [80] introduced the chaotic TSA (CTSA) to efficiently estimate solar PV cell parameters for improved PV system efficiency. CTSA addresses the challenge of flawed parameter estimation by introducing chaotic dynamics to optimize predictions. Using an adaptive weight mathematical model, CTSA balances exploitation and exploration effectively. Comparative analysis shows CTSA's superiority in computation time for both double-diode and triple-diode models. Ranking tests, error analysis, and sensitivity testing to temperature variation confirm CTSA as a promising solution for accurate PV cell parameter estimation.

4.1.4 Levy-Flight Tunicate Swarm Algorithm

A Levy flight is a random walk where step lengths follow a heavy power law distribution [128]. These occasional large steps can aid an algorithm in conducting a global search. Applying Levy flight trajectories can improve the trade-off between exploration and exploitation in algorithms, with the added benefit of avoiding local optima.

Fetouh et al. [81] introduced an Improved TSA (ITSA) to optimize Capacitor Banks (CBs), Distributed Generators (DGs), and Distribution Network Reconfiguration (DNR) in distribution systems. By incorporating Lévy flight distributions, ITSA enhances search diversity, mitigating stagnation risks. Tested on various distribution systems, ITSA outperforms existing algorithms, promising significant performance improvements in distribution system automation.

Jui et al. [82] introduced the Levy TSA (LTSA) by integrating Levy distribution into TSA to overcome local optima challenges in optimization. LTSA enhances TSA's exploration capabilities by incorporating Levy flight, improving efficiency and performance. Evaluation across benchmark

functions and a real-world engineering application, the twin-rotor system, shows LTSA's superiority over traditional TSA, indicating its effectiveness in numerical and real-world optimization scenarios.

Karthick et al. [83] introduced the Improved TSA (ITSA) for optimizing electric vehicles (EVs) powered by solar photovoltaic (PV) panels. ITSA enhances the conventional TSA with Lévy flight distributions to enable diversified search capabilities and mitigate stagnation risks. The goal is to minimize ripple in the supply current while optimizing photovoltaic power extraction. An enhanced cascaded converter configuration reduces voltage and dv/dt stresses. A Proportional-Integral (PI) controller tunes PI gain and generates a reference current signal, optimizing voltage gain and input current to mitigate the impact of varying solar irradiation in EV applications. MATLAB evaluation demonstrates the effectiveness of ITSA compared to existing methods.

Joseph et al. [84] proposed an innovative approach for classification and early identification, tackling the challenges of error-prone and time-consuming tasks associated with brain tumor detection from MRI scans. Their method includes pre-processing, K-means clustering-based segmentation, and tumor detection using an optimized convolutional neural network (CNN). Training is facilitated by a Levy-adopted TSA (L-TSA) for optimal weight tuning. Finally, 3D reconstruction is achieved using an improved marching cubes (MC) algorithm. MATLAB evaluation shows the superiority of the CNN+L-TSA algorithm over existing schemes, achieving approximately 0.934 accuracy.

Alohal et al. [85] introduced Enhanced TSA-based Lévy flight distribution with Deep Learning-based Rice Seedling Classification (ETSADL-RSC) to improve rice cultivation practices. Their approach integrates computer vision techniques and unmanned aerial vehicles (UAVs) to swiftly and accurately identify rice seedlings from UAV imagery. Through preprocessing steps and deep learning models like NASNet and Sparse Autoencoder (SAE), ETSADL-RSC achieves a high classification accuracy of 97.79%, surpassing other classifiers. This study underscores TSA's potential to modernize agricultural management through technological advancements.

4.1.5 Adaptive Tunicate Swarm Algorithm

In optimization, the notion of adaptive pertains to the algorithm's automatic adjustment of parameters throughout the search process. The TSA algorithm, lacking control parameters, relies on two algorithmic parameters: population size and maximum number of iterations. Consequently, adaptive variants of the TSA algorithm have been introduced to adjust the population size dynamically during the search.

Arabali et al. [86] introduced the Adaptive TSA (ATSA) algorithm for global optimization problems and optimizing shallow spread foundation designs. ATSA operates in two phases: an initial exploration phase covering the solution space and a refinement phase using the best tunicate's position. This adaptive approach enhances exploration while mitigating premature convergence. Evaluation using 23 mathematical test functions from the CEC 2017 benchmark suite and comparison with TSA and other algorithms demonstrate ATSA's effectiveness. Application in automating shallow spread foundation design, considering cost and CO₂ emissions, shows superior performance in a case study and sensitivity analysis, offering improved optimal solutions.

Das et al. [87] proposed the Self Adaptive-TSA (SA-TSA) to improve COVID-19 detection from medical imaging, which is crucial in countries like Bangladesh and India. They introduced Ensemble Learning with CNN-based Deep Features (EL-CNN-DF), leveraging chest X-ray images and deep learning classifiers for automatic COVID-19 detection. The method involves preprocessing, lung segmentation using Adaptive Activation Function-based U-Net (AAF-U-Net), and EL-CNN-DF for feature extraction. Three classifiers—Support Vector Machine (SVM), Autoencoder, and Naive Bayes (NB)—are employed, guided by a high-ranking strategy. SA-TSA boosts segmentation and detection performance, demonstrating superior precision over existing models in comparative analysis.

Arandian et al. [88] proposed an Improved TSA (ITSA) for the parameter identification of solar PV models, addressing the challenge of nonlinearity and complexity in PV parameter identification. ITSA enhances the exploration ability of the algorithm while preventing premature convergence through two main phases: exploring the search space based on randomly selected tunics and refining the search using the position of the best tunicate. The algorithm's efficacy is validated through comparisons with TSA and other optimization algorithms using ten mathematical test functions. Results demonstrate ITSA's superior convergence accuracy and stability in identifying various parameters in PV models, including single diode (SDM), double diode (DDM), and PV modules, highlighting its effectiveness in practical applications.

Bhujang et al. [89] proposed an unsupervised ensemble learning model for earthquake detection, combining random forests and LSTM networks. The model utilizes the Adaptive TSA (ATSOA) for selecting LSTM weights and clustering methods with weighted voting for transforming unlabeled datasets. The approach is tested on Southern California Seismic Network data and shows high potential for accurate seismic signal detection and phase identification. Experimental results demonstrate superior performance to other deep learning algorithms, particularly in earthquake detection and

seismic phase identification. The model's reliability in recognizing low-magnitude seismic phases suggests its potential for improving earthquake occurrence prediction, with implications for forecasting major earthquakes.

Jadhav et al. [90] introduced a machine learning-based method for accurately segmenting mangoes in challenging conditions. Their approach involves preprocessing with a guided Gabor bilateral filter, segmentation using the fuzzy level set method (FLSM), and feature extraction with the dual-tree complex transform (DT-CT). Optimal feature selection is achieved using the adaptive TSA (ATSO) and classification with an Extreme Gradient Tree Boost classifier (EGTBoost). Experimental results demonstrate high accuracy and precision, with values of 0.969 and 0.986 on Kaggle and real-time datasets, respectively.

Jakkulla et al. [91] proposed an approach for early diagnosis of thyroid disease, particularly prevalent in India. Using deep learning techniques, they emphasize early detection for timely treatment. Their method combines feature selection and categorization with the Adaptive TSA (ATSA) algorithm, comprising exploration and refinement phases to enhance exploration and avoid premature convergence. They employ a Deep Convolutional Neural Network (DeepCNN) for disease identification and GWO for training, achieving impressive accuracy and specificity of 95% and 92%, respectively, highlighting ATSA's potential in optimizing feature selection and improving thyroid disease prediction accuracy.

Kumar et al. [92] proposed a methodology for lung cancer identification. Their approach involves pre-processing, segmentation, feature extraction using a CNN, and detection. They optimized CNN weights with the self-adaptive TSA (SATSA) and tested on the LIDC-IDRI dataset in Python. Results show the effectiveness of the CNN + SATSA model in accurately identifying lung nodules, validated through various performance metrics.

Varaprasad et al. [93] introduced an Adaptive TSA (ATSA) to address potential disruptions in IoT networks caused by cooperative attacks at edge nodes. By efficiently solving global optimization problems and identifying malicious nodes, ATSA enhances network security. Leveraging Edge Computing, the model establishes a trustworthy environment, effectively defending against cooperative assaults and minimizing the risk of cyberattacks while reducing cloud connectivity overhead.

4.1.6 Multi-Strategy Tunicate Swarm Algorithm

A multi-strategy ensemble TSA, integrating multiple strategies, was proposed to enhance the TSA's capacity to explore and discover superior solutions for large-scale optimization problems. Wang et al. [106] introduced a novel wind speed forecasting model by integrating the modified TSA with benchmark models and Quantile regression. This model

addresses limitations of existing point forecast models by providing both deterministic and probabilistic interval forecasts, crucial for risk control in wind power grid connection. The modified TSA incorporates **elite opposition learning strategy and exponential function steps strategy** for location update, effectively capturing wind speed's nonlinear characteristics. Comparative experiments across three datasets and sixteen models demonstrate the proposed model's superior accuracy and interval forecast performance. Its capability to offer accurate point forecasts and uncertainty information enhances real-time wind turbine control and power grid dispatching.

Abdolinejad et al. [107] introduced SVR-MTSA, a hybrid method combining Support Vector Regression and Modified TSA, to optimize Pb recovery from liberator cell residue. This approach integrates a **self-adaptive method and an enhanced exploration phase strategy** to effectively handle the nonlinear relationship between recovery efficiency and temperature, processing time, and precursor composition parameters. Experimental results show precise lead recovery predictions, with optimal parameters yielding over 99% recovery rate. Sensitivity analysis using SVR-MTSA highlights the significant impact of temperature, coke content, processing time, Na₂CO₃ amount, and Fe content on recovery efficiency.

Li et al. [108] introduced the Improved TSA (ITSA) to tackle the Dynamic Economic Emission Dispatch (DEED) problem in power systems, aiming at minimizing fuel cost and pollutant emissions. ITSA enhances traditional approaches by employing several strategies. **Tent mapping** creates an initial population, enhancing optimization directionality. Additionally, the **Gray Wolf Optimizer** is employed to improve global exploration by generating the global search vector, while **Levy flight** is introduced to broaden the search range. ITSA's efficacy is demonstrated on test systems with varying generator units, showcasing competitive scheduling plans and optimal economic and environmental dispatch strategies.

Gharehchopogh et al. [109] proposed enhancing TSA by integrating **mutating operators, namely the Lévy mutation operator, the Cauchy mutation operator, and the Gaussian mutation operator**, aimed at addressing its tendency for premature convergence and local optimization. This modified version, termed the QLGCTSA algorithm, demonstrates improved performance in tackling global optimization problems. Through experimentation on benchmark functions and large-scale engineering problems, the QLGCTSA algorithm exhibited superior performance compared to other optimization algorithms, showcasing its effectiveness in diverse optimization scenarios.

Zhang et al. [110] proposed CG-TSA, an enhanced version of the TSA, for solving the airport gate assignment

problem. CG-TSA integrates **cosine mutation and adaptive grouping techniques** to optimize multiple objectives, such as minimizing flight conflicts and maximizing boarding bridge rate. It employs the **Halton sequence** for efficient initialization and dynamically divides the population into dominant and inferior groups. Inspired by the arithmetic optimization algorithm (AOA), CG-TSA applies an **arithmetic optimization strategy** to the dominant group and benefits from global optimal solutions for the inferior group. Validation tests demonstrate CG-TSA's effectiveness in addressing multi-objective optimization challenges in airport gate assignments.

Dohare et al. [111] proposed a novel approach named AGQPSOA-TS to optimize machining and cutting parameters and production costs for toughened glasses used in road transport and general purposes. The study aims to enhance compressive strength while minimizing tensile strength, which is crucial for improving toughened glass quality. Integrating the **Adaptive Gaussian Quantum Behaved Particle Swarm Optimization algorithm** and the TSA, the AGQPSOA-TS algorithm is devised for optimization. Experimental evaluations, adhering to Indian standards, involve a 5mm thick glass workpiece measuring 200mmx200mm. Comparative assessments for compressive strength, tensile strength, and production cost illustrate the efficiency of the proposed system, contributing to advancements in toughened glass manufacturing.

Cui et al. [112] proposed TLTSA to address premature convergence and local optima trapping issues. Initially, nine distinct TSAs based on a Chaotic-Lévy flight strategy (CLTSA) were derived by combining **nine chaotic maps with the Lévy flight strategy**. Among these, TLTSA exhibited superior performance. Comparative analyses were conducted with various meta-heuristic algorithms using benchmark functions and practical engineering problems. TLTSA demonstrated enhanced exploration and exploitation capabilities, outperforming TSA and other algorithms in finding global optimal solutions across diverse test functions. Engineering experiments further validated TLTSA's efficacy in solving constrained practical problems, underscoring its potential in real-world applications.

Wanget al. [113] proposed an enhanced version of TSA, named SLOTS, to address the challenges of low solution accuracy, slow convergence, and susceptibility to local extrema inherent in TSA. SLOTS integrates **opposition-based learning, Levy flight, and positive cosine operator** to improve TSA's performance. Comparative experiments on 10 benchmark functions validate the efficacy of the proposed enhancements. Furthermore, applying SLOTS to two practical industrial design problems demonstrates its wide applicability and effectiveness in tackling complex optimization challenges in industrial settings.

Hu et al. [114] introduced DQTSA, an enhanced hybrid TSA for shaping complex RQI-spline curves in engineering applications. DQTSA integrates **differential evolution and quadratic interpolation strategies** to overcome local minima challenges, demonstrating superior performance in benchmark and engineering optimization tasks, particularly in achieving optimal curves with minimal energy consumption.

Liu et al. [115] introduced MSHHOTSA to overcome the limitations of the TSA. MSHHOTSA aims to enhance optimization speed, accuracy, and convergence when tackling complex problems. The algorithm incorporates several innovative strategies: **the hyperbolic tangent domain adjustment** enhances convergence by ensuring similar distribution between new and old parameters, a **nonlinear convergence factor** replaces the original random factor to balance local exploitation and global exploration, and the **swarm update mechanism from the Harris Hawks Optimization (HHO) algorithm** further improves algorithmic performance. Evaluation of various benchmark functions and engineering problems demonstrates MSHHOTSA's superiority over existing metaheuristic algorithms, including HHO and TSA, in terms of local convergence, global exploration, robustness, and universality.

Dong et al. [116] proposed a novel environmental economic power dispatch (NEED) formulation for electricity trading, introducing environmental and economic indicators based on reactive power pricing. This innovative approach calculates total cost using reactive power pricing rather than pure fuel cost. To address the NEED problems, they introduced an Improved TSA (ITSA), overcoming limitations of the original TSA, such as fast convergence and susceptibility to local optima. ITSA incorporates **adaptive weight parameters and mutation processes**. By applying the Pareto dominance rule, ITSA effectively handles NEED problems. Simulation tests comparing ITSA, TSA, and PSO were conducted on the IEEE 30-node system. Objective functions optimized included total cost, pollution emission, and power loss. Results demonstrate that ITSA achieves better-distributed Pareto fronts and superior best-compromise solutions, showcasing its efficiency in addressing NEED problems.

Akdağ et al. [117] introduced a Modified TSA (M-TSA) to address limitations observed in the original TSA, such as being susceptible to local optima, slow convergence and inefficiency in solving complex engineering problems. M-TSA incorporates novel strategies to enhance tunate movement and herd behavior, introducing **spiral and Levy movement techniques**. Additionally, it considers the **Fish Aggregation Device (FAD) effect** to optimize performance further. The study evaluates M-TSA across various test suites, including CEC'2017, real-life engineering problems, and power system engineering challenges. Results demonstrate M-TSA's

improved exploration/exploitation balance and solution quality compared to other techniques, showcasing its efficacy in solving complex optimization problems. The experiments were conducted using MATLAB 2020b software.

Wang et al. [118] proposed a wind power prediction method aiming to mitigate the impact of wind power on power systems and alleviate scheduling challenges. Recognizing the growing importance of renewable energy amid the energy crisis, the study emphasizes the advantages of wind energy, including efficiency and cleanliness. However, the stochastic nature of wind energy complicates power system operations, underscoring the need for accurate wind power prediction. The proposed model integrates an improved TSA (ITSA) with an Extreme Learning Machine (ELM) to optimize random ELM parameters, enhancing prediction performance. ITSA addresses the limitations of the TSA by introducing a **reverse learning mechanism, a non-linear self-learning factor, and a Cauchy mutation strategy** to mitigate convergence issues and local optima susceptibility. Experimental results demonstrate the effectiveness of ITSA-ELM, achieving a reduction in Mean Absolute Percentage Error (MAPE) compared to TSA-ELM, thus offering promising implications for renewable energy development and power system scheduling.

Si et al. [119] introduced two improved variants of the TSA, leveraging **chaos theory and OBL alongside Cauchy mutation**. Named OCSTA and COCSTA, these algorithms incorporate static and dynamic OBL during initialization and generation jumping phases in OCTSA, while centroid opposition-based computing is integrated into COCTSA. The performance of these variants was evaluated on 30 IEEE CEC2017 benchmark optimization problems across different dimensions. Comparative analysis against classical TSA and several competitive algorithms, including TSA-LEO, SCA, and others, demonstrated the superior performance of OCSTA and COCSTA. Statistical analysis further confirmed their effectiveness in solving global optimization problems, with COCSTA showcasing robustness even in higher dimensions. This research contributes to enhancing the capabilities of TSA and offers promising insights for solving complex optimization challenges.

Chen et al. [120] introduced an enhanced and adaptive version of the TSA, termed IMATSA. IMATSA addresses four key aspects to enhance TSA's performance: population diversity, local search convergence speed, escaping local optima, and balancing global and local search. The method employs **Tent map and quadratic interpolation** for population initialization to enhance diversity, integrates the **Golden-Sine algorithm** to expedite local search convergence, and adapts **Levy flight and an improved Gauss disturbance method** for global development and local search coordination. Empirical evaluations, including benchmark function experiments, parameter optimization for Support Vector Machine (SVM)

and Gradient Boosting Decision Tree (GBDT), Wilcoxon signed-rank tests, and image multi-threshold segmentation experiments, demonstrate IMATSA's superiority in terms of convergence speed, convergence value, P-value significance level, Peak Signal-to-Noise Ratio (PSNR), and Standard Deviation (STD) compared to TSA and other algorithms.

Zhou et al. [121] proposed a revised algorithm for calibrating the parameters of turbine speed control systems, aiming to address issues related to variable operating conditions, time-varying parameters, and complex nonlinearity. The proposed algorithm introduces **Tent chaotic** initialization to ensure a more even distribution of tunicates in the solution space. Additionally, **the golden sine partition factor** is incorporated to enhance diversity among optimization particles and reduce the likelihood of locally optimal solutions. Moreover, **the nonlinear adaptive weight factor** is introduced to balance development and discovery abilities. Experimental results, which include frequency and load disturbances, demonstrate that the PID control based on the revised TSA improves the dynamic stability characteristics of the system.

Kommula et al. [97] proposed an enhanced DC-DC converter structure coupled with a hybrid control algorithm to mitigate torque ripple in a Brushless DC (BLDC) motor. Initially, the model of the BLDC motor is integrated with an enhanced Cuk converter, where the operation is refined by incorporating a switched inductor. Two control loops, focusing on speed and torque, are implemented to enhance BLDC performance. The Improved TSA (ITSA) is introduced to optimize the control loop operation. ITSA enhances the TSA search behavior through **crossover and mutation operators**. The proposed strategy utilizes the ITSA algorithm to regulate speed and torque errors in the BLDC motor, with optimal gain parameters determined to enhance controller operation. Performance evaluation on the MATLAB/Simulink platform demonstrates torque ripple minimization, showcasing improved performance compared to systems like Particle Swarm Optimization and Bacterial Foraging algorithms.

Chandran et al. [95] introduced the Reinforcement Learning-inspired TSA (RLTSA), which enhances traditional TSA by integrating a **Q-learning approach** to improve convergence accuracy and local search capabilities. The study also implements a **Chaotic Quasi Reflection Based Learning (CQRBL) strategy with multiple chaotic maps** to enhance convergence reliability. By dynamically switching between CQRBL and Reflection-Based Learning (ROBL), RLTSA adapts to varying problem stages. Testing on benchmark functions and engineering design challenges showed that RLTSA outperformed TSA and other metaheuristic algorithms, as confirmed by statistical tests, including Friedman and Wilcoxon rank-sum tests.

Chandran et al. [125] introduced the Quasi-Oppositional Chaotic TSA (QOCTSA) to address limitations in optimization tasks. By integrating **Quasi-Oppositional Based Learning (QOBL)** and **Chaotic Local Search (CLS)**, QOCTSA enhances both exploration and exploitation, improving convergence accuracy while maintaining solution diversity. Extensive tests on CEC2005 and CEC2019 benchmark functions, as well as real-world engineering problems, showed that QOCTSA outperformed the original TSA and other algorithms, making it highly effective for complex engineering optimizations.

4.1.7 Other Modifications

Researchers have introduced other modified versions of the TSA in the literature to balance exploration and exploitation capabilities when tackling intricate optimization problems, as discussed below.

Kavitha et al. [94] proposed the TSA Q-learning-based Collaborative Attacker Detection Algorithm (TSOQCADA) to address vulnerabilities in Mobile Adhoc Networks (MANETs) caused by collaborative and Wormhole Attacks (WHA), Gray Hole Attack (GHA), attacks like Black Hole Attack (BHA). By integrating TSA with **Q-learning**, the algorithm efficiently identifies and prevents collaborative attackers, enhancing routing efficiency. TSOQCADA utilizes node properties feedback to determine optimal packet routing, employing a selective search mechanism and a nonlinear function to balance exploration and exploitation in Q-learning. Simulation results demonstrate superior performance compared to existing algorithms, achieving high Packet Delivery Ratio (PDR), low Packet Loss Rate (PLR), minimal energy consumption, and low End-to-End (E2E) delay, thereby offering robust defense against collaborative attacks in MANETs.

Rizk-Allah, et al. [96] proposed the Enhanced TSA (ETSA) designed to enhance exploration and exploitation capabilities using a **dynamic perturbation strategy**. The study evaluates ETSA on 20 benchmark test functions, demonstrating its robustness and effectiveness compared to other algorithms through statistical measures and Wilcoxon tests. ETSA's scalability is also validated in high dimensions, showing minimal impact on performance. CPU time analysis reveals ETSA's efficiency, outperforming other algorithms for most functions. Moreover, the algorithm's applicability extends to practical optimization tasks such as the Economic Dispatch Problem in electrical applications, further highlighting its utility in real-world scenarios.

Dayana et al. [98] proposed an optimized deep neural network with the **Chronological** TSA (CTSA) for classifying the severity of Diabetic Retinopathy (DR). The study addresses the challenge of accurately classifying the severity level of DR, which is crucial for timely treatment and

prevention of vision impairment. The proposed method involves preprocessing retinal images captured through low-quality fundus photography, then segmentation of the optic disc, blood vasculatures, and lesion areas. Features are then extracted using Gabor filter banks, and the classification is performed using a deep-stacked autoencoder (SAE) jointly optimized with the CTSA. The experimental results demonstrate the effectiveness and robustness of the proposed method, achieving high accuracy, sensitivity, specificity, and F1-Score values for the DIARETDB0 and DIARETDB1 databases.

Yuan et al. [99] proposed a thermal error control system for machine tools integrating the Improved TSA-Gated Recurrent Unit-Attention (ITSA-GRU-A) model within a collaborative framework. The **adaptive weights** are introduced into the ITSA to improve its performance. The authors utilized correlation analysis, VIF, and advanced selection criteria to optimize input variables. The model, enhanced with attention mechanisms, showed superior predictive performance and reduced computation time, significantly improving machining precision.

Srinivas et al. [100] introduced QTSA-EAC, a **Quantum** TSA-based Energy Aware Clustering scheme for Wireless Sensor Networks. Addressing energy efficiency concerns, it optimizes cluster head selection to prolong network lifetime, reduce energy consumption, and minimize delays, outperforming alternative methods.

Ragab et al. [101] proposed a novel method for medical application detection, combining Quantum Computing (QC) and Machine Learning (ML). They used the Quantum Kernel Method (QKM) with the Linear TSA (LTSA) for data prediction. LTSA optimizes the loss function, utilizing a **reference set** for generating random numbers. Testing on various databases, including Lymphography, Dermatology, and Arrhythmia, demonstrates the approach's efficacy in medical application detection.

Fathy et al. [102] introduced the Modified TSA (MTSA) to improve photovoltaic array efficiency during partial shading. MTSA uses **two distinct random numbers** in the tunicate's update process to enhance search-ability and avoid local optima. Validated with the CEC-2017 test suite and practical designs, the method optimally controls the DC-DC boost converter for global power extraction. Comparative analysis and statistical tests show MTSA's superiority in various operating conditions.

Jeyabharathi et al. [103] proposed a novel model, the **Taylor**-TSA-based Generative Adversarial Networks (Taylor-TSA-based GANs), for cancer prediction. The Taylor-TSA enhances prediction efficiency by integrating the Taylor series with the Tunicate Swarm Algorithm (TSA). The Yeo-Johnson (YJ) transformation facilitates data preprocessing, while feature fusion uses a Deep Stacked Autoencoder (Deep SAE). The fused features are input into a GAN trained by

Taylor-TSA for cancer prediction. The model demonstrates effectiveness, achieving promising accuracy (0.9184), False Positive Rate (FPR, 0.1782), and True Positive Rate (TPR, 0.9246) values when utilizing clinical data.

Lathika et al. [104] proposed a stochastic Bayesian method enhanced by the TSA for accurate and early rainfall prediction, focusing on agricultural impacts in countries like India. Traditional prediction methods struggle with computational complexity and weather pattern uncertainty. The study uses a scalable Bayesian approach and improves the exploration stage with TSA. Results show the proposed model, especially with the **crossover**-based TSA (CTSA), achieves better prediction accuracy and efficiency, reducing training loss. This research offers valuable insights for enhancing agricultural practices and economic stability in regions reliant on rainfall.

Jagadeesh et al. [105] proposed a method for facial emotion recognition from video sequences using deep learning. The process involves frame conversion, face detection via the Viola-Jones algorithm, and feature extraction using modified local directional pattern (M-LDP), spatiotemporal features, and scale-invariant feature transforms (SIFT). The **fitness-Distance balance**-based TSA (D-TSA) optimizes feature selection and reduces training complexity. These features are input into a Heuristically Modified Recurrent Neural Network (HM-RNN), where D-TSA optimizes hidden neurons. Experimental results show that the model outperforms existing methods due to the effective use of spatio-temporal features, SIFT, M-LDP, and optimal feature selection.

Althaqafi et al. [122] developed a Hybrid Mutated TSA for Feature Selection and Global Optimization (HMTSA-FSGO) to address challenges in large-scale classification due to irrelevant and redundant data. This approach combines TSA with a **dynamic s-best mutation operator and a directional mutation rule** to improve exploration and exploitation. The HMTSA-FSGO also utilizes a bidirectional long short-term memory (BiLSTM) classifier for feature selection assessment, with hyperparameters fine-tuned by the rat swarm optimizer (RSO). Extensive testing on various datasets demonstrated that HMTSA-FSGO outperformed other models in multiple classification tasks.

Bhimavarapu et al. [123] developed an Improved TSA (ITSA) for the automated detection of diabetic retinopathy (DR) using retinal fundus images. ITSA incorporates **mutation and crossover operations** to enhance genetic diversity and avoid local optima entrapment, utilizing Renyi's entropy for adaptability during different algorithm stages. The study also presents an Improved Hybrid Butterfly Optimization (IHBO) algorithm for feature selection, boosting classification accuracy. Testing on retinal image datasets yielded impressive results, with accuracies of 98.06% and 98.21% on the IDRiD dataset, and 97.95% and 99.96% on the E-Ophtha dataset, demonstrating its potential for early DR detection.

Du et al. [124] developed the Enhanced TSA (ETSA), which integrates a **differential sequencing alteration operator** to optimize the training of feedforward neural networks. This method focuses on reducing classification errors by adjusting connection weights and neuron thresholds based on transmission errors. ETSA addresses the original TSA's limitations in computational accuracy and convergence speed by employing enhanced local search strategies. Tests on seventeen datasets demonstrated ETSA's superior convergence speed, classification accuracy, and stability, making it highly effective for neural network training applications.

4.2 Hybridized Versions of Tunicate Swarm Algorithm

The second type of TSA variant is hybridization. This approach enhances TSA's searching capabilities and performance by integrating components from other methods or approaches with TSA components. Several studies employing the hybridization approach for TSA are summarized in Table 3 and discussed below.

Chouhan et al. [130] introduced the Tunicate Swarm Grey Wolf Optimization (TSGWO) algorithm for multipath routing in IoT-assisted WSNs. TSGWO optimizes routing based on delay, energy, and distance, outperforming other methods in residual energy, link lifetime, PDR, and throughput. It combines features from the FGSA and uses DRINA for route maintenance, enhancing WSN performance.

KI et al. [135] presented a novel strategy for human action recognition and abnormality detection using the Chronological Poor and Rich Tunicate Swarm Algorithm (CPRTSA) combined with a Deep Maxout Network. This approach addresses the challenge of extracting effective features for applications like intelligent video surveillance and human-computer interaction to enhance security. By employing CPRTSA, the method achieves improved accuracy and efficiency in human action recognition. The CPRTSA-based Deep Maxout Network demonstrates promising results, with a maximum accuracy of 0.959, sensitivity of 0.963, and specificity of 0.965, underscoring its effectiveness in human behavior analysis and anomaly detection.

To address the challenges of illegal copying and digital plagiarism, digital watermarking has become crucial for copyright protection. Kumari et al. [136] introduced a robust approach using an optimized DWT for watermark embedding. This optimization combines Simulated Annealing (SA) with the TSA, enhancing the robustness of the watermarking process. Extraction is performed using the RNN-LSTM model, allowing retrieval of the original image. The methodology is evaluated on MATLAB, assessing performance metrics such as PSNR, NC, and SSIM. Comparative analyses show the proposed method's robustness, particularly under

various attacks, validating its effectiveness in digital copyright protection.

Wan et al. [138] developed a Battery Thermal Management System (BTMS) using a Tunicate Swarm Search and Rescue (TSSR) algorithm combined with ANSYS FLUENT. This approach optimizes battery spacing to reduce heat transfer rates, using Computational Fluid Dynamics (CFD) modeling for effective thermal management. Tests show the TSSR algorithm improves cooling performance, addressing safety concerns in Li-ion battery systems.

Houssein et al. [139] introduced TSA-LEO, an enhanced version of the TSA that integrates a Local Escaping Operator (LEO) to improve convergence rate and solution quality. Validation against seven other meta-heuristic algorithms shows significant performance enhancement. TSA-LEO outperforms other algorithms in real-world segmentation tasks, demonstrating its effectiveness in optimization and practical applications.

Chelliah et al. [141] introduced a hybrid optimization model named HTSS to maximize coverage and connectivity in target-based WSNs. Integrating the Salp Swarm Algorithm (SSA) and TSA, HTSS determines optimal sensor node placement positions. TSA enhances SSA's feature exploitation ability through local search operators, improving solution quality. Simulation results demonstrate HTSS's efficacy in solving WSN coverage and connectivity problems across various scenarios, highlighting its outstanding performance in wireless network optimization.

Awad et al. [144] proposed the TSA/Sine Cosine Algorithm (TSA/SCA) for optimizing distributed generation (DG) allocation, crucial for emergency plans and power quality enhancement. The study focused on identifying optimal DG size and location, especially on an IEEE-69 Radial Distribution System (RDS). Evaluation using NEPLAN software showcased the benefits of TSA/SCA in DG allocation for power systems.

Gupta et al. [148] proposed the TSMOA-based BHrEFC+KNN algorithm to enhance product recommendation systems. Integrating TSA and Magnetic Optimization Algorithm (MOA), the method efficiently groups relevant products and recommends similar ones based on user preferences. TSMOA optimizes group matching and sentiment classification using entropy measure and Jaro-Winkler distance. Evaluation metrics demonstrate superiority over existing methods, with improvements in accuracy, TPR, MAPE, and RMSE compared to TSMOA-BHEFC+NN, showcasing its efficacy in generating user-oriented recommendations.

Daniel et al. [150] introduced TSBOA to enhance energy efficiency and path reliability in WSNs. TSBOA optimizes Cluster Head (CH) selection for efficient data transmission among sensor nodes by integrating TSA and Butterfly Optimization Algorithm (BOA). Considerations include inter-cluster and intra-cluster distances, node energy consumption,

Table 3 Summary of the hybridized TSA variants

No.	Hybridized methods or their operators	References	Abbreviations	Category	References
1	Grey Wolf Optimizer	[129]	GWO	Swarm-based	[130] [131] [132] [133]
2	Poor and Rich Optimization	[134]	PRO	Humans-based	[135]
3	Simulated Annealing	[26]	SA	Physics-based	[136]
4	Search and Rescue optimization	[137]	SAR	Humans-based	[138]
5	Gradient-Based Optimizer	[18]	GBO	Mathematics-based	[139]
6	Salp Swarm Algorithm	[140]	SSA	Swarm-based	[141] [142]
7	Sine Cosine Algorithm	[143]	SCA	Mathematics-based	[144] [145, 146]
8	Magnetic Optimization Algorithm	[147]	MOA	Physics-based	[148]
9	Butterfly Optimization Algorithm	[149]	BOA	Swarm-based	[150] [151]
10	Moth Flame Optimization	[152]	MFO	Swarm-based	[153] [154]
11	Genetic Algorithm	[11]	GA	Evolution-based	[155] [156]
12	Flower Pollination Algorithm	[157]	FPA	Swarm-based	[158]
13	Whale Optimization Algorithm	[45]	WOA	Swarm-based	[159] [160]
14	Rat Swarm Optimization	[161]	RSO	Swarm-based	[162]
15	SailFish Optimizer	[163]	SFO	Swarm-based	[164]
16	Naked Mole-Rat Algorithm	[165]	NMRA	Swarm-based	[166] [167]
17	Pattern Search	[168]	PS	Single solution-based	[169]
18	Particle Swarm Optimization	[170]	PSO	Swarm-based	[171] [172]
19	Exponential Weighted Moving Average	[173]	EWMA	Statistical technique	[174] [175]
20	Jaya Optimizer	[176]	JAYA	Swarm-based	[177] [178]
21	Golden Eagle Optimizer	[179]	GEO	Swarm-based	[180]
22	Political Optimizer	[37]	PO	Humans-based	[181]
23	Bacterial Foraging Algorithm	[182]	BFA	Swarm-based	[183]
24	Spotted Hyena Optimization	[184]	SHO	Swarm-based	[185]
25	Harris Hawk Optimization	[186]	HHO	Swarm-based	[187]
26	Grasshopper Optimization Algorithm	[188]	GOA	Swarm-based	[189]
27	Water Cycle Algorithm	[190]	WCA	Physics-based	[191]
28	Invasive Weed Optimization	[192]	IWO	Swarm-based	[193]
29	Beetle Swarm Optimization	[194]	BSO	Swarm-based	[195]
30	Henry Gas Solubility Optimization	[196]	HGSO	Physics-based	[197]
31	Remora Optimization Algorithm	[198]	ROA	Swarm-based	[199]
32	Deer Hunting Optimization	[200]	DHO	Swarm-based	[201] [202]
33	Crow search algorithm	[203]	CSA	Swarm-based	[204]
34	Forest Optimization Algorithm	[205]	FOA	Evolution-based	[206]
35	SunFlower Optimization	[207]	SFO	Swarm-based	[208]
36	Spider Monkey Optimization	[209]	SMO	Swarm-based	[210]
37	Seagull Optimization Algorithm	[211]	SOA	Swarm-based	[212]
38	Black Widow Optimization	[213]	BWO	Swarm-based	[214]
39	Giant Trevally Optimizer	[215]	GTO	Swarm-based	[216]
40	Slime Mould Algorithm	[217]	SMA	Swarm-based	[218]
41	Fire Hawk Optimizer	[219]	FHO	Swarm-based	[220]

predicted energy, link lifetime, and delay. Energy prediction utilizes a Deep, Long, Short Term Memory classifier. TSBOA demonstrated superior performance metrics, with 0.1118J residual energy and 82.101% throughput, offering advancements in network lifespan and data communication efficiency in WSNs.

Renukadevi et al. [153] proposed the MF-TSA crowdsourcing model to address optimization challenges in crowdsourcing systems. Integrating Moth Flame and TSA (MF-TSA) enhances exploitation capabilities and accelerates convergence, optimizing query planning efficiently. Homomorphic encryption techniques ensure data privacy and framework security. The approach optimizes query plan selection while utilizing crowd-controlled administrators for query assessment. Experimental results show superior performance to existing algorithms, including sequential, parallel, and CrowdOp approaches.

Diaz et al. [155] proposed an integrated approach using TSGA with DRN for feature selection and weighting. TSGA combines TSA and Genetic Algorithm (GA) to enhance classifier performance. Wrapper-based techniques optimize feature selection and weighting, reducing computation time and complexity. The method's effectiveness is evaluated against TSA, CS-GA, and PSO-GA, while DRN's performance is compared with KNN, C4.5, and RF classifiers. Results show promising improvements in classification accuracy and efficiency.

Boobalan et al. [142] introduced the SCES-AOMDV routing protocol to enable secure communication with efficient energy consumption in WSNs. SCES-AOMDV employs an adaptive security-aware routing mechanism using cross-layering to overcome traditional security scheme limitations. It utilizes OTP verification to secure against DoS attacks, maximizing Network Lifetime (NL). Additionally, SCES-AOMDV incorporates a Hybrid Tunicate Weighted Salp Swarm algorithm (HyTWSSA) for effective sensor node localization. Simulation results show that SCES-AOMDV outperforms conventional methods, reducing the impact of DoS attacks and maximizing network lifetime.

Yu et al. [158] introduced TSA-DVFPA to enhance the Flower Pollination Algorithm (FPA) in terms of solution accuracy, convergence speed, and stability. TSA-DVFPA incorporates a simplified TSA and a random selection strategy into FPA's cross-pollination process. Additionally, a differential variation strategy enhances local search, increasing population diversity. Experimentation on 16 benchmark functions demonstrates TSA-DVFPA's improved convergence speed and optimization accuracy compared to similar algorithms.

Singh et al. [159] proposed a novel routing technique utilizing the Whale-based TSA (WTSA) for cluster head (CH) selection and AO for inter-cluster routing in WSNs.

WTSA efficiently identifies CHs based on factors like residual energy, node degree, distance from the base station (BS), and intra-cluster distance, while AO optimizes inter-cluster routing by cultivating optimal routes between CHs. Performance evaluation against existing techniques demonstrates significant improvements, including an 8.3% reduction in average energy consumption compared to WTS, aiming for a delay of 0.121 seconds for 200 nodes.

Mohana et al. [162] proposed TRSWOAMF, a hybrid approach for medical image denoising, particularly in blood cell images. TRSWOAMF combines the median filter with the Tunicate Rat Swarm Optimization Algorithm (TRSWOA) to detect and remove noise while preserving image quality. The method demonstrates promising results in producing denoised medical images with reduced error rates, addressing the challenge of preserving crucial data in low-contrast medical images.

Muthu et al. [164] proposed a heart disease prediction model using Wireless Body Area Network (WBAN) technology, structured in three stages. The first stage involves data aggregation and scheduling using Time Division Multiple Access. In the second stage, a hybrid metaheuristic algorithm called the Tunicate Swarm-Sail Fish Optimization (TS-SFO) algorithm is employed for channel selection, addressing multi-objective optimization. The final stage focuses on heart disease prediction, incorporating feature extraction and prediction processes. Test results demonstrate high prediction rates, showcasing the potential of flexible RNN hyper-parameter design and tuning for accurate heart disease prediction.

Singh et al. [166] proposed TSNMRA, a novel optimization approach combining TSA and Naked Mole-Rat Algorithm (NMRA) characteristics. TSNMRA enhances NMRA's exploration abilities, introducing self-adaptive parameters and SA mutation operators. Evaluation on CEC 2019 test problems shows TSNMRA outperforms TSA and NMRA. TSNMRA exhibits superior performance in image segmentation compared to MTEMO, PSO, GA, and BF optimization algorithms.

Khajehzadeh et al. [169] proposed CTSA-PS, a sequential hybrid optimization algorithm for seismic slope stability analysis. CTSA-PS combines TSA's global search capability with Pattern Search's local search ability to address complex optimization problems in slope stability evaluation under earthquake loading. Numerical investigations and comparisons with standard TSA and other methods demonstrate CTSA-PS's effectiveness in providing better optimal seismic slope stability analysis solutions, outperforming previous methodologies.

Sharma et al. [171] proposed a hybrid TSA-PSO algorithm for maximizing power extraction from PV systems under partial shading conditions (PSCs). By combining TSA with PSO, the approach enhances TSA's exploitation

capability. Comparative analysis against various MPPT algorithms demonstrated the superior performance of TSA-PSO in swiftly and efficiently locating the maximum power point, achieving a PV tracking efficiency of 97.64%. Validation through non-parametric tests further affirmed the efficacy of the proposed TSA-PSO MPPT method.

Divya et al. [174] proposed a hybrid optimization algorithm-based deep learning classifier for automatic tumor detection in multimodal brain MRI images. The approach involves preprocessing, segmentation using a modified Deep-Joint model, and Deep CNN classification trained by the TEWMA algorithm integrating TSA and Exponential Weighted Moving Average (TEWMA). Subsequently, a GAN trained by PS-TEWMA, integrating PSO with TSA and EWMA, computes volume difference and change percentage, demonstrating superior performance in tumor detection and change analysis with lower MSE and RMSE.

Singh et al. [160] introduced WTSAs, a fusion of TSA and whale Optimization Algorithm (WOA), to optimize cluster head selection in WSNs for multipath routing. WTSAs selects cluster heads based on various criteria and improves network performance metrics such as delay and throughput. Results show significant enhancements, with a reduction in delay to 0.140 seconds for 100 nodes and an increase in throughput to 69,641 kbps.

Kumar et al. [177] proposed a novel approach for brain tumor segmentation and classification, integrating AFACFM for segmentation enhanced by the hybrid Jaya-Tunica Swarm Algorithm (J-TSA), followed by CNN combined with a Fuzzy classifier for classification. The study demonstrates the efficacy of deep learning in MRI images for automated tumor segmentation and classification, achieving significantly enhanced accuracy compared to conventional methods. Comparative analysis showed substantial improvement in accuracy over SVM, NN, DBN, CNN, Fuzzy, and CNN-Fuzzy approaches, showcasing its potential for accurate brain tumor diagnosis.

James et al. [180] proposed a scheme to enhance security in LNG facilities by detecting failure patterns and minimizing risks. Their approach involves a hybrid technique combining Golden Eagle Optimizer (GEO) with TSA and ANFIS. The integration of GEO-TSA offers improved leak detection accuracy compared to other methods. This hybrid method provides a fresh perspective on identifying leaks, hazards, and dangers associated with LNG accidents. Additionally, ANFIS aids in risk identification, determining SIL rates, and designing safety zones. Implemented on MATLAB/Simulink, the approach demonstrates comparability with PSO with fuzzy logic and WOA with fuzzy logic, showcasing its potential effectiveness in LNG risk assessment and management.

Sangeetha et al. [181] proposed a novel technique for secure communication within UAV networks (UAVNs) using

the TSPO algorithm, which combines TSA and Political Optimizer (PO). TSPO optimizes routing paths to address mobility and unstable links in UAVNs. The method involves simulating UAVNs, establishing data transmission routes, and utilizing a DRN for malicious detection. The DRN, trained using TSPO, considers parameters like round trip time, signal strength, and packet delivery. Upon classification, a defensive agent mitigates attacks, ensuring enhanced network performance with minimal delay, high detection rates, and improved packet delivery ratios.

Sharma et al. [156] introduced T-GA, which combines TSA and Genetic Algorithm (GA) to address energy consumption challenges. T-GA is used to select Cluster Heads (CHs) and Relay Head (RH) nodes, optimizing overall energy preservation and facilitating multi-hop communication. Experimental results demonstrate T-GA's superiority over existing algorithms, highlighting its potential for diverse WBAN applications.

Doraiswami et al. [178] proposed Jaya-TSA with GAN for early COVID-19 infection prediction. The method involves lung lobe segmentation using Bayesian fuzzy clustering, feature extraction, and prediction via GAN. Training the GAN with Jaya-TSA yields optimal solutions, and feature dimensionality reduction enhances training speed. The approach demonstrates remarkable effectiveness, achieving high specificity, accuracy, and sensitivity, with values of 0.8857, 0.8727, and 0.85, respectively, when varying training data, addressing the pressing need for early COVID-19 detection.

Guan et al. [183] proposed a novel path-tracking control approach for robotic roller technology in earth-rock dams. Their TSABFA-PID controller integrates TSA and Bacterial Foraging Algorithm (BFA) and a modified kinematic model to dynamically self-tune hyperparameters. This enables efficient adaptation to varying construction conditions. Comparative assessments in simulation and on-site tests showed superior performance compared to existing methods. Future enhancements may involve integrating deep reinforcement learning and human-computer interaction techniques to enhance compaction performance.

Das et al. [185] proposed a novel clustering protocol for energy-efficient IoT sensor networks, termed Adaptive Spotted Hyena Tunica Swarm Optimization (ASHTSO). This method combines Spotted Hyena Optimization (SHO) with the TSA to optimize clustering effectively. By considering multiple factors such as distance, energy, delay, security, and quality of service (QoS), ASHTSO achieves superior performance compared to existing algorithms. Simulation results underscore its potential for enhancing energy efficiency in IoT sensor networks.

Divya et al. [175] introduced a novel MRI classification approach, termed TEWMA-deep CNN, to bridge the semantic gap between low-level optical information and high-level

clinical interpretation. The method integrates preprocessing for artifact elimination, modified deep-joint segmentation for tumor region segmentation, and classification using deep CNN tuned by TEWMA. TEWMA combines TSA and EWMA for optimization. Experimental validation across three datasets demonstrates high specificity (99%), accuracy (98.76%), sensitivity (98.88%), precision (94.76%), F1-measure (98.46%), and minimal processing time (7.24 s) using dataset-1. The approach shows promising performance across metrics and datasets, indicating its potential for MRI classification tasks.

Manoj et al. [151] proposed a 3D MRI brain tumor segmentation method using A-3D-U-Net combined with Butterfly Optimization Algorithm (BOA) and TSA, forming B-TSA. Multi-objective optimization achieved optimal segmentation. Numerical features were extracted, and malignancy detection was performed using HDNN with parameter optimization by B-TSA. Experimental results showed effectiveness comparable to conventional methods.

Barshandeh et al. [187] proposed a hybrid approach for object localization in IoT, combining TSA with the Harris Hawk Optimization (HHO) and integrating it with DV-Hop. Experiments showed significant accuracy improvements compared to basic DV-Hop and previous methods, demonstrating TSA's potential in enhancing localization techniques in IoT environments.

Kumar et al. [154] proposed a secure map reduce scheduling method for cloud-dependent systems managing big data. They introduced TCMFA, a hybrid algorithm combining Moth Flame Optimization (MFO) and TSA, to optimize task scheduling for minimized makespan, resource utilization, and enhanced security. TCMFA exhibited superior performance, achieving optimal execution time and reduced error rates compared to conventional methods, emphasizing its efficiency and security in map-reduce scheduling for big data in cloud environments.

Shang et al. [172] introduced a novel approach to optimizing Selective Harmonic Elimination Pulse Width Modulation (SHEPWM) for power electronics applications. Their method utilizes TSA-PSO, integrating TSA with Particle Swarm Optimization (PSO), to enhance convergence speed and accuracy while minimizing the risk of local optima. Experimental results showcased superior performance in accuracy and total harmonic distortion rate, effectively optimizing the modulation of the seven-level SHEPWM inverter.

Sameera et al. [145] proposed an IoT-based method for automating the detection of foliar diseases in apple trees. Their approach uses a hybrid classifier combining Deep Residual Network (DRN) and Deep Q Network (DQN), optimized by the Adaptive Tunicate Swarm Sine-Cosine Algorithm (TSSCA). Results showed high accuracy (98.36%), sensitivity (98.58%), specificity (96.32%), and low energy consumption (0.413 J), highlighting its effectiveness.

Antony et al. [189] proposed the MFRCNN-HGTS approach for liver disease prediction using ultrasound liver images. This model combines a Modified Faster Region-Based Convolutional Neural Network (MFRCNN) with the Hybrid Grasshopper Tunicate Swarm (HGTS) algorithm for optimizing weight factors and enhancing classification accuracy. Experimental results in MATLAB R2016a showed a notable accuracy of 98.45%, surpassing traditional liver disease prediction methods.

Krishnan et al. [191] proposed a novel method for viral detection using gene expression data and a deep residual network (DRN) optimized with the Water Cycle Tunicate Swarm Algorithm (WCTSA), integrating the Water Cycle Algorithm (WCA) and TSA. The approach involves feature selection, data transformation, and virus detection, achieving high accuracy (91.4%), sensitivity (92.6%), and specificity (90.7%). This method demonstrates the promising potential for accurate virus detection leveraging optimized deep learning architectures and gene expression data.

Shobana et al. [131] proposed a novel method for ultrasound image quality management and fetal heart chamber segmentation and classification. The approach utilizes a hybrid optimization algorithm combining TSA and GWO. It automates quality assessment through data preprocessing, feature extraction, SRDCF segmentation, and classification with MLSTM Network. The method significantly enhances PSNR and classification accuracy compared to existing techniques, demonstrating its effectiveness in medical applications.

Singh et al. [193] introduced a novel approach for text classification utilizing incremental learning and hybrid optimization algorithms. Their method, the Henry Fuzzy Competitive Multi-verse Optimizer (HFCVO)-based Deep Maxout Network (DMN), aims to enhance accuracy in text classification. The hybrid optimization algorithm, IWTSO, combines Invasive Weed Optimization (IWO) and TSA for feature selection. The DMN, the classifier, is trained using HFCVO, integrating Henry Gas Solubility Optimization (HGSO) and Competitive Multi-verse Optimizer (CMVO) with fuzzy theory. The proposed approach achieved impressive results with high precision, accuracy, True Positive Rate (TPR), and True Negative Rate (TNR), showcasing its effectiveness in handling large-scale text data and improving classification accuracy.

Kumar et al. [195] proposed a model for enhancing energy efficiency and security in WSN through multi-hop routing. Their model involves clustering and transmission phases, where energy-efficient cluster heads are selected based on various criteria. Trustworthiness in routing is ensured through trust score calculation. To optimize cluster head selection, they introduced a hybrid optimization model called BITA, which combines Beetle Swarm Optimization Algorithm (BSO) and TSA. This approach aims to enhance

the security and energy efficiency of WSNs by facilitating reliable multi-hop routing.

Arumugasamy et al. [197] introduced a novel technique for fruit ripening classification using deep learning models. They employed THGSO, a hybrid optimization algorithm combining TSA and Henry Gas Solubility Optimization (HGSO), to train DCNN and DRN for ripening classification. Their approach achieved elevated accuracy, sensitivity, and specificity, showcasing promising results for fruit ripening assessment.

Gupta et al. [199] introduced ROTEE, a novel energy-efficient routing approach for EH-enabled WSNs, employing ROATSA, a hybrid optimization algorithm combining Remora Optimization Algorithm (ROA) and TSA. By strategically placing EH-enabled nodes and optimizing CH selection, ROTEE outperformed recent clustering techniques, enhancing WSN efficiency and longevity.

Jeyshri et al. [132] proposed a cervical cancer diagnosis method using adaptive fuzzy-region growing fusion for abnormality segmentation. They enhanced it with a hybridized optimization algorithm called the Gray Wolf-Tunicate Swarm Algorithm (GW-TSA). Their ensemble classification approach, utilizing Improved CNN with ANFIS, optimized by GW-TSA, demonstrated high accuracy in diagnosis.

Roshan et al. [201] proposed a hybrid meta-heuristic-based multi-objective cluster head selection model for advancing smart city development in India. Utilizing the Deer Hunting-Tunicate Swarm Optimization (DH-TSO) algorithm, their approach optimizes variables such as distance, delay, energy, load, and temperature of IoT devices to enhance efficiency and sustainability. Comparative analysis validates the model's efficacy, particularly regarding the number of alive nodes and normalized energy consumption, ensuring prolonged network lifetime and improved performance in IoT-enabled smart city environments.

Kiran et al. [204] proposed a novel hybrid approach to enhance energy-efficient communication in mobile relay networks, particularly in Fifth Generation (5G) networks. They introduced a multi-objective energy-efficient relay selection method using the Best Fitness-derived Crow Tunicate Swarm Optimization (BF-CTS) algorithm to minimize the number of hops while considering factors like link reliability, energy consumption, and transmission delay. Their approach showed superior performance over traditional methods, promising optimized relay selection and improved efficiency in cooperative communication networks.

Ravikumar et al. [206] proposed a cost-efficient technique for hybrid precoding in mm-wave massive MIMO systems, employing an Adaptive Deep CNN for channel estimation and reconstruction, enhanced by a hybrid meta-heuristic algorithm combining Forest Optimization Algorithm (FOA)

and TSA. The O-RNN-based hybrid precoder design outperforms existing methods, showcasing TSA's effectiveness in optimizing channel estimation and hybrid precoding for mm-wave massive MIMO systems.

Singh et al. [167] introduced a hybrid Tunicate Swarm Naked Mole-Rat Algorithm (TSNMRA) for enhancing wireless sensor network (WSN) localization. This method addresses the need for accurate event positioning by combining TSNMRA with static anchor nodes and virtual anchors to determine precise locations. The study demonstrates that TSNMRA significantly improves the accuracy and efficiency of WSN localization, outperforming other location optimization strategies in terms of the number of localized nodes and localization error.

Disney et al. [208] introduced TSA for enhancing Non-Orthogonal Multiple Access (NOMA) performance in Heterogeneous Networks (HetNets) with non-uniform small cell deployment. The study employs power domain multiplexing to improve key metrics like energy efficiency and coverage probability. It utilizes a Sunflower-based Tunicate Swarm Optimization (SF-TSO) algorithm for optimal base station placement and fuzzy logic for cell dimensioning. Simulations reveal NOMA's superiority over Orthogonal Multiple Access (OMA) in HetNets, highlighting TSA's effectiveness in optimizing complex network scenarios.

Dayana et al. [210] developed an advanced method for grading diabetic retinopathy severity involving pre-processing, segmentation, and feature extraction of retinal images. They used a refined deep residual network (RDRN) enhanced by the Tunicate Swarm Spider Monkey Optimization (TSSMO) algorithm for classification. This approach, tested on DIARETDB1 and DIARETDB0 datasets, significantly improves classification accuracy in medical image analysis.

Iniyavan et al. [202] developed a novel channel estimation technique for broadband wireless communication systems by integrating LS and MMSE methods with evolutionary programming. They introduced the Hybrid Heuristic-based ISS-ZA-NLMS (HH-ISS-NLMS) method, enhanced with the Tunicate Swarm-Deer Hunting Optimization (TS-DHO) algorithm. This approach minimizes Mean Square Error (MSE) and improves performance compared to traditional methods, showcasing the effectiveness of TSA in optimizing channel estimation for wireless communication systems.

Kumari et al. [146] introduced a robust digital image watermarking technique using Discrete Wavelet Transform (DWT) and Singular Value Decomposition (SVD). They optimized image block selection with an Enhanced TSA combined with the Sine Cosine Algorithm (SCA). The watermark is secured through Arnold scrambling and Tent Map chaotic encryption. This method shows superior robustness and accuracy against geometric attacks, demonstrating its

effectiveness in digital image watermarking for content protection.

Ramasamy et al. [133] proposed a novel hybrid energy-efficient and secure QoS-based multipath routing protocol for MANETs. This approach combines a modified Crow Search Algorithm with the Tunicate Swarm Butterfly Optimization Algorithm (TSBO) and uses a density-based clustering technique for selecting cluster heads. The protocol employs a Collaborative Trust-Based Approach (CTBA) for secure data transmission and integrates MO-GWO with the Fruit Fly Algorithm for secure multipath routing. Simulations indicate a 4% improvement in packet delivery ratio, reduced energy consumption, and shorter delays, outperforming existing models regarding end-to-end delay, energy efficiency, PDR, and throughput.

Balaji et al. [212] introduced a novel approach for early detection of Alzheimer's disease (AD) and Parkinson's disease (PD) using the Hybrid Seagull and Tunicate Swarm (Hyb-SGTS) optimization technique with a DSDCNN. This method improves feature selection efficiency for enhanced classification accuracy. Experimental results show superior performance to traditional methods, promising better early detection and personalized treatment strategies for neurodegenerative disorders.

Pahuja et al. [214] introduced BWO-TSA to optimize wireless cooperative communication networks (WCCNs). By leveraging Black-widow optimization (BWO) and TSA, BWO-TSA achieves optimal solutions with reduced computational complexity. Comparative analysis with the Branch and Bound (BB) algorithm demonstrates its superiority in schedule length reduction and performance improvement, enhancing energy-efficient wireless communication technologies.

Zhao et al. [216] proposed a novel approach for predicting unconfined compressive strength (UCS) of soil-stabilizer combinations using the K-nearest neighbors (KNN) model. The study integrates the Giant Trevally Optimizer (GTO) and TSA to enhance prediction accuracy. Three distinct models are introduced: KNGT, KNTS, and an independent KNN model. The KNGT model outperforms others with high R² and low RMSE values, showcasing its accuracy and reliability. This innovative approach improves UCS prediction accuracy and offers insights for future research and practical applications in civil engineering, addressing data challenges by integrating GTO and TSA algorithms.

Mishra et al. [218] proposed a novel methodology for predicting heart disease using IoT-enabled ECG devices. It integrates DL algorithms for ECG signal analysis with feature extraction and selection. Feature selection employs a hybrid optimization model combining the TSA and Slime Mould Algorithm (SMA). Heart disease detection uses a three-layer DL framework. Implemented in MATLAB, the

approach shows promise for accurate heart disease prediction, improving healthcare diagnostics with IoT-based ECG devices.

By integrating fog computing, Minu et al. [220] proposed a privacy preservation and security scheme for Vehicular Ad-Hoc Networks (VANETs). The scheme addresses user privacy and authentication issues and comprises node authentication, privacy preservation, and message verification. Node authentication employs an Adaptive Deep Bayesian network (ADBN) tuned by Integrated Fire Hawk with TSA (IFHTSA). Hybrid Attribute-Based Advanced Encryption Standard (HABAES) encryption ensures privacy, while fog nodes replace Road-Side Units (RSUs) for analysis, reducing latency. Experimental results show the scheme's efficacy, achieving high accuracy and precision with reduced computation and communication overhead compared to traditional techniques.

4.3 Multi-Objective Tunicate Swarm Algorithm

Multi-objective optimization differs significantly from traditional single-objective optimization as it simultaneously balances multiple goals. This often requires trade-offs between conflicting objectives, which complicates finding optimal solutions. Achieving an ideal solution in such contexts becomes difficult, necessitating collaborative efforts to achieve the best possible outcomes. As a result, addressing problems with numerous objectives presents a significant challenge within the optimization field. Given TSA's expertise in optimizing single objectives, researchers have focused on enhancing its capabilities to handle multi-objective scenarios through various improvements.

Sharma et al. [221] introduced MOTSA, a multi-objective extension of TSA. MOTSA integrates an external archive for non-dominated solutions and uses a roulette wheel mechanism for their selection. Experimental results show MOTSA outperforming four established multi-objective optimization algorithms across various benchmark tests, highlighting its effectiveness in tackling multi-objective optimization problems.

El-Sehiemy et al. [222] introduced TSA to solve the optimal power flow (OPF) problem in modern power systems. TSA addresses economic, technical, and environmental objectives such as generation cost minimization, power loss reduction, and voltage stability enhancement. Single and multi-objective frameworks were developed, leveraging Pareto optimization and fuzzy set theory for solution extraction. Evaluation across 19 case studies on standard systems demonstrated TSA's effectiveness and robustness, outperforming other algorithms in the literature regarding statistical indices, standard deviation, and error metrics.

Rizk-Allah et al. [223] introduced CMOTSA, a chaos-enhanced multi-objective TSA tailored to solve thermal

plants' combined economic-emission dispatch (CEED) problem. CMOTSA integrates an exponential strategy based on a chaotic logistic map (ESCL) to enhance exploration and exploitation abilities, effectively addressing the CEED problem's multimodality and non-convex nature influenced by valve ripple effects. Evaluation against multi-objective benchmarking functions demonstrates CMOTSA's robustness and efficiency in producing high-quality solutions with shorter computational time than other algorithms. Application to practical CEED problems, including those with valve ripples in different system configurations, validates CMOTSA's effectiveness, achieving competitive results in large-scale cases such as the 118-bus system.

Al-Wesabi et al. [224] proposed the Multi-Objective Quantum Tunicate Swarm Optimization with Deep Learning (MOQTSO-DL), a novel approach for diagnosing dystrophinopathies using muscle MRI images. The model integrates optimized region growing for ROI detection via MOQTSO, Capsule Network for feature extraction and an Extreme Learning Machine (ELM) classifier for label assignment. Experimental analysis showcases MOQTSO-DL's superior classification performance compared to other methods, highlighting its novelty and effectiveness in medical image diagnosis.

Liu et al. [225] tackled uncertainty in new energy generation, proposing the Hybrid Dynamic Economic Emission Model (HDEED) with a penalty mechanism and introducing the Multi-objective TSA (MTSA) for optimization. MTSA enhances Pareto front distribution and diversity compared to existing algorithms, addressing challenges in system scheduling caused by sources like solar and wind power. The application of HDEED and MTSA in a modified test system elucidates the impacts of clean energy on system stability, economics, and environmental benefits, emphasizing the importance of addressing uncertainty for promoting sustainable energy systems.

5 Applications of Tunicate Swarm Algorithm

Numerous publications have documented TSA's applications to real-world and benchmark optimization problems. Many also compare TSA's performance with that of other optimization algorithms. The following subsections provide a detailed discussion of various domains where TSA has been applied, including power and energy, the Internet of Things, cyber security, computer science selection, engineering, medical fields, and environmental modeling. These application domains are concisely summarized in Table 4 and their distribution in Fig. 8. As depicted in the figure, power and energy are the most prominent domains for utilizing TSA, accounting for 34%. The second most significant

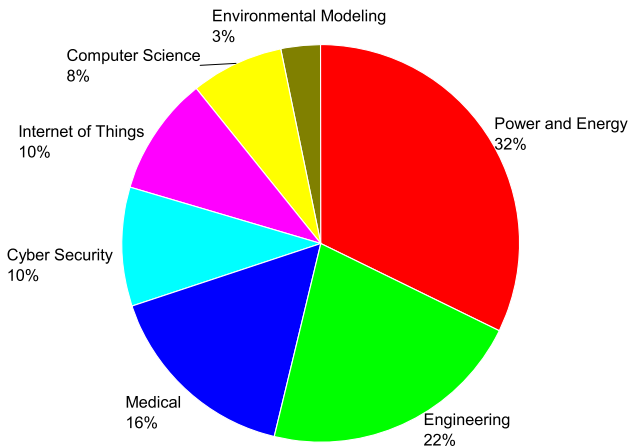


Fig. 8 The distribution of TSA applications in various domains

area for applying TSA is engineering, with 23%, followed by the medical field, which ranks third at 17%.

5.1 Power and Energy

Menesy et al. [226] employed TSA to optimize parameters of Proton Exchange Membrane Fuel Cell (PEMFC) mathematical models, crucial for understanding fuel cell performance. The study focused on three PEMFC stack types and validated TSA's effectiveness in optimization. Statistical analyses confirmed TSA's reliability in parameter extraction. Comparative simulations against other meta-heuristic algorithms highlighted TSA's stability and precision in identifying PEMFC parameters under varying conditions, showcasing its utility in optimizing PEMFC performance.

Sàingh et al. [227] addressed proper sizing in Hybrid Renewable Energy Systems (HES) due to the intermittent nature of renewable sources. They developed a bi-objective model using TSA to minimize the levelized cost of energy while maximizing emission curtailment. Comparative tests showed grid-connected configurations' economic and reliability advantages. TSA's performance was compared with other meta-heuristic methods and traditional solvers, demonstrating its effectiveness in optimizing HES sizing.

Ajayi et al. [231] proposed two novel methods based on MPA and TSA to solve the economic dispatch problem in electric power systems. The objective is to minimize fuel costs while meeting load demand and operational constraints. Comparative analysis with other methods demonstrates the competitive performance of MPA and TSA, affirming their effectiveness in power system optimization.

Nguyen et al. [229] introduced a novel method for reducing power loss in distribution power networks by combining local and distribution line compensation. The authors apply PSO, PPA, and TSA to optimize capacitor placement. TSA demonstrates superior effectiveness, achieving significant

Table 4 Overview of TSA applications

Domain	Optimization problem	Year	References
Power and energy	Optimization of PEMFC parameters	2021	Menesy et al. [226]
	Sizing of Hybrid Renewable Energy Systems	2021	Singh et al. [227]
	Energy Management in Data Centers	2022	Ajai et al. [228]
	Reducing power loss in distribution power networks	2021	Nguyen et al. [229]
	Maximum Power Point Tracking for Wind Energy Conversion Systems	2021	Rajesh et al. [230]
	Economic dispatch problem in electric power systems	2021	Ajai et al. [231]
	Power quality enhancement in distribution systems	2021	Sathish et al. [232]
	Configuration optimization of stand-alone hybrid microgrids	2021	Abd El-Sattar et al. [233]
	Parameter extraction in solar PV cells	2021	Sharma et al. [234]
	Optimization of feed-forward neural network for power system stabilizers	2021	Aribowo et al. [235]
	Economic Load Dispatch problem in thermal power plants	2021	Nguyen et al. [236]
	Optimization of PV systems and maximum power tracking	2021	Ganti et al. [237]
	Maximum Power Point Tracking (MPPT) strategy for PV systems under partial shading (PS) conditions	2021	Mansoor et al. [238]
	Solar PV power prediction in microgrid energy management systems	2022	Tayab et al. [239]
	Optimizing the size of components in island microgrids	2022	Ge et al. [240]
	Placement and sizing of distributed generation systems	2022	Patnaik et al. [241]
	Optimization of Electric Vehicles performance, particularly focusing on Permanent Magnet Synchronous Motors	2022	Vishal et al. [242]
	Designing Power System Stabilizers for multi-machine power system networks	2022	Tayeb et al. [243]
	Optimizing parameters of power system stabilizers in a Single Machine Infinite Bus network integrated with a Unified Power Flow Controller	2022	Hossen et al. [244]
	Economic Load Dispatch problem focusing on cooperation between thermal power plants and wind farms in the modified ELD scenario	2022	Hien et al. [245]
	Dynamic Combined Economic Environmental Dispatch problems considering variable real transmission losses and valve-point loading effects	2022	Larouci et al. [246]
	Optimal adaptive intelligent energy management strategy for a DC microgrid incorporating FC, PV, and battery bank	2022	Fathy et al. [247]
	Short-term commercial load forecasting model	2022	Zhou et al. [248]
	Hybrid control scheme for enhancing power system reliability in Hybrid Renewable Energy Source	2022	Krishnakumar et al. [249]
Internet of Things	Maximum Power Point Tracking technique for PV systems	2022	Sholikhah et al. [250]
	Forecasting crude oil prices	2022	Li et al. [251]
	Load frequency control in interconnected hybrid power systems	2023	Memon et al. [252]
	Optimal distributed generation installation in electrical distribution systems, particularly focusing on integrating renewable-based DG sources	2023	Madupu et al. [253]
	Size optimization of hybrid renewable energy systems	2023	Sharma et al. [254]
	Automatic Generation Control in multi-area power systems under a restructured environment	2024	Saha et al. [255]
	Energy management for multi-microgrid systems	2024	Rashidi et al. [256]
Internet of Things	Sizing hybrid energy systems	2024	Anand et al. [257]
	Designing power system stabilizers	2024	Islam et al. [258]
	Limited energy resources concern in IoT-based WSNs for Wildfire Detection	2020	Verma et al. [259]

Table 4 (continued)

Domain	Optimization problem	Year	References
Cyber security	Energy constraints in WSNs for Intelligent Transportation Systems	2020	Verma et al. [260]
	Limited battery constraints of sensor nodes in Wireless Body Area Networks	2021	Sharma et al. [261]
	Limited energy resources of sensor nodes in IoT networks	2021	Dogra et al. [262]
	Hot-spot problems in WSN-based IoT	2022	Avdhesh et al. [263]
	Enhanced data collection efficiency in healthcare IoT networks	2022	Khan et al. [264]
	Enhancing energy efficiency in IoT-supported WSNs	2022	Subramani et al. [265]
	Energy hole mitigation in the Internet of Underwater Things	2022	Gupta et al. [266]
	Load balancing in RPL models	2024	Raj et al. [267]
	Enhancing intrusion detection efficiency in IoT networks	2022	Taher et al. [268]
	Secure image steganography	2022	Chaudhary et al. [269]
	Text classification	2022	Singh et al. [270]
	DDoS attack classification in 5G networks	2023	Aljebreen et al. [271]
	Text differentiation between human and ChatGPT-generated text	2023	Katib et al. [272]
Feature selection	Sentiment analysis	2023	Seth et al. [273]
	Security challenges in WSNs and the IoT	2023	Krishnasamy et al. [274]
	Detecting violent crowd behavior in computer vision systems	2023	[275]
	Early detection of cyberattacks in cyber-physical systems	2023	Alrurban et al. [276]
	Enhancing security and accuracy of a multi-modal biometric system combining fingerprint and retina traits	2024	Sasikala et al. [277]
	Scalability in sentiment analysis of online product reviews	2021	Daniel et al. [278]
	Compare meta-heuristic optimization algorithms for feature selection and weighting	2022	Diaz et al. [279]
Engineering	Supply chain risk management	2024	Gupta et al. [280]
	Predicting customer churn	2024	PS et al. [281]
	Optimizing the operation of the Halilrood multi-reservoir system to minimize total deficit	2021	Sharifi et al. [282]
	Coordinating distance and direction overcurrent relays in a protection system to improve the adaptive protection scheme's effectiveness	2022	Abdelhamid et al. [283]
	Improving short-term traffic flow prediction accuracy in intelligent transportation systems (ITS) by integrating weather conditions for weather and periodicity analysis	2022	Al Duhayyim et al. [284]
	Enhancing intruder detection accuracy in underwater environments to improve intruder position accuracy and reduce overhead in UASN	2023	Kammula et al. [285]
	Optimizing power allocation in CCNs to efficiently improve system parameters such as symbol error rate, outage probability, and bit error rate	2023	Pahuja et al. [286]
	Improving the estimation of undrained shear strength of soil	2023	Qiang et al. [287]
	Accurate small-signal model parameter extraction in Gallium Nitride High Electron Mobility Transistors to enhance efficiency and reliability in parameter extraction	2023	Husain et al. [288]
	Trajectory tracking control of a Tricopter Unmanned Aerial Vehicle	2023	Hasan et al. [289]
	Optimizing a PID controller based on a BP neural network for self-driving bicycles	2023	Li et al. [290]
	Designing high-stability and highly reliable DNA sequences for DNA computing, meeting various thermodynamic and logical constraints	2023	Guo et al. [291]
	Enhance classification performance of Deep Variational Autoencoder model for digitally-modulated signal recognition	2023	Alnfiai et al. [292]

Table 4 (continued)

Domain	Optimization problem	Year	References
Networks	Enhance accuracy and efficiency of fabric wrinkle evaluation	2023	Zhou et al. [293]
	Optimize transistor sizing of CMOS differential amplifiers	2023	Kamalkumar et al. [294]
	Optimize the Random Forest model for predicting overbreak in tunnel blasting	2023	He et al. [295]
	Predicting ETR of aseismic concrete material	2023	Mei et al. [296]
	Optimizing CPVC component manufacturing	2023	Barua et al. [297]
	Predicting compressive strength and slump of High-performance concrete	2023	Liu et al. [298]
	Selective Harmonic Elimination in Multilevel Inverters	2024	Kala et al. [299]
	Estimating Compressive Strength of High-performance Concrete	2024	Wang et al. [300]
	Optimization of 3D-printed Fiber-reinforced Concrete composition for enhanced Compressive Strength	2024	Alyami et al. [301]
	Predicting remaining useful life of lithium-ion batteries	2024	Zhai et al. [302]
	Cost evaluation in the plastic injection industry	2024	Kengpol et al. [303]
	Estimating displacement amplitude in geo-structures	2024	Jeyanthi et al. [304]
	Adaptive channel equalization in wireless communication	2024	Shwetha et al. [305]
	Optimizing routing decisions and energy consumption in Mobile Ad Hoc Networks (MANETs) to improve network lifetime and energy efficiency	2022	Sudha et al. [306]
Medical	Optimizing routing decisions in MANETs to mitigate local optima traps and improve efficiency	2022	Inamdar et al. [307]
	Selecting cluster heads in underwater sensor networks to enhance energy efficiency and prolong network operation	2023	Khan et al. [308]
	Optimizing cluster head selection and routing paths to enhance energy efficiency and prolong network lifetime in WSNs for IoT applications	2023	Saad et al. [309]
	Optimizing parameters for minimizing Energy Consumption and maximizing PDR in underwater IoT networks to improve efficiency and reliability	2024	Simon et al. [310]
	Optimization of weighted coefficients for cluster centers in Black Hole Entropic Fuzzy Clustering for COVID-19 data clustering	2020	Chander et al. [311]
	Optimization of keys for the Simon cipher to enhance security and energy efficiency in an IoHT system	2020	Nguyen et al. [312]
	Hyperparameter tuning using TSA for enhancing the performance of 3D dental image segmentation and classification using deep learning models	2022	Awari et al. [313]
	Biomedical image segmentation, particularly vessel segmentation	2022	Çetinkaya et al. [314]
	Optimizing the ensemble deep learning model for accurate prediction of heart disease	2022	Wankhede et al. [315]
	Optimization of weight parameters for early prediction and classification of breast cancer	2022	Srikanth et al. [316]
	Optimization of hyperparameters using TSA to analyze the impact of instructional approaches on mental well-being	2023	Sun et al. [317]
	Hyperparameter optimization using TSA for disease classification in lung cancer diagnosis	2023	Mahaveerakannan et al. [318]
	Optimal feature selection using TSA to improve classification accuracy in Parkinson's disease detection	2023	Akram et al. [319]
	Hyperparameter fine-tuning using TSA to improve colorectal cancer classification accuracy	2023	Abdullah et al. [320]
	Tuning hyperparameters of the gated recurrent unit using TSA for brain tumor classification	2023	Poonguzhaliet al. [321]

Table 4 (continued)

Domain	Optimization problem	Year	References
Environmental Modeling	Optimization of parameters for contrast enhancement using TSA to improve automated breast cancer detection systems	2023	Laishram et al. [322]
	Hyperparameter tuning using TSA to improve pancreatic cancer classification performance in CT scans	2023	Gandikota et al. [323]
	Hyperparameter optimization using TSA to improve early detection of pancreatic ductal adenocarcinoma in contrast-enhanced computed tomography images	2024	Laxminarayananma et al. [324]
	Tailoring filter parameters using TSA to preserve waveform characteristics in ECG signals for cardiac arrhythmia detection	2024	Digumarthi et al. [325]
	Early detection of Alzheimer's Disease using MRI	2024	Ganesan et al. [326]
	Risk assessment for predicting COVID-19	2024	Kengpol et al. [327]
	Bone Age Assessment using deep learning	2024	Palaniswamy et al. [328]
	Hyperparameter optimization using TSA of a Deep Belief Network for land cover classification	2023	Lavanya et al. [329]
	Optimization of the parameters of a fuzzy-based Convolutional Neural Network for classifying banana ripeness.	2023	Saranya et al. [330]
	Parameter optimization of neuro-fuzzy models for water quality forecasting	2024	Kumar et al. [331]
	Photocatalytic degradation rates of airborne pollutants	2024	Javed et al. [332]

loss reduction across various distribution systems compared to PSO and PPA. The study underscores TSA's potential as a powerful tool for minimizing power loss in distribution systems, highlighting its practical relevance and applicability.

Rajesh et al. [230] proposed a hybrid method combining TSA with a Radial Basis Function Neural Network to enhance Maximum Power Point Tracking (MPPT) in Wind Energy Conversion Systems (WECS). TSA improves fault power reduction, generating a training dataset for the Radial Basis Function. Implemented in MATLAB/Simulink, the approach was more effective than Particle Swarm Optimization and hill climb searching. This study underscores TSA's potential in optimizing WECS MPPT performance, contributing to renewable energy optimization.

Sathish et al. [232] introduced a hybrid RBFNN-TSA approach to enhance power quality in distribution systems. Combining the Radial Basis Function Neural Network (RBFNN) with TSA mitigates power quality issues, losses, and harmonic distortion. RBFNN trains on input data to optimize demand outcomes, and then TSA optimizes RBFNN parameters for best neuron configuration. Comparative evaluations across different test cases show superior performance in maximizing distribution system benefits and ensuring desired output power levels under various load conditions.

Abd El-Sattar et al. [233] proposed optimizing stand-alone hybrid microgrid configurations using TSA. Their study, conducted in a southwest Egypt oasis, aimed to minimize energy production costs while ensuring high reliability. Results demonstrated the profitability and viability of the

proposed hybrid microgrid system for regional electrification.

Sharma et al. [234] applied TSA for parameter extraction in solar photovoltaic (PV) cells, achieving superior performance compared to other optimization algorithms. Their study focused on optimizing parameters under standard temperature conditions, demonstrating TSA's higher precision and robustness through statistical analyses.

Aribowo et al. [235] proposed using TSA to optimize a feed-forward neural network (FFNN) for power system stabilizers. Comparative analysis with other methods showed TSA's superior performance, reducing speed overshoot by 35.17% and rotor angle undershoot by 15.36%.

Nguyen et al. [236] applied TSA to solve the Economic Load Dispatch (ELD) problem in thermal power plants (TPPs). The objective is to minimize power generation costs, which is crucial due to high TPP fuel expenses. TSA was implemented across various test systems with different unit numbers and constraints. Comparative analysis against prior methods showed TSA's capability to achieve equal or lower costs, affirming its effectiveness in addressing the ELD problem.

Ganti et al. [237] proposed the TSA-RBFNN hybrid approach to optimize photovoltaic (PV) systems' performance and maximum power tracking. This method combines TSA with Radial Basis Function Neural Network (RBFNN) to optimize tilt angles and consider environmental factors. MATLAB/Simulink simulations showed their efficiency compared to existing techniques, including ANN, GBDT,

SSA, and SSA-GBDT, regarding dependability, sensitivity, accuracy, and computation time.

Mansoor et al. [238] introduced a novel Maximum Power Point Tracking (MPPT) strategy based on TSA to address partial shading (PS) issues in photovoltaic (PV) systems. Their TSA model, employing a Search and Skipping (SAS) scheme, simplifies the MPPT process, reducing tracking time and search area by discarding voltage ranges lacking the global maximum power point (GMPP). Rigorous evaluations against existing techniques like Incremental Conductance (InC), IPSO, GWO, and CSA, including practical hardware validation, demonstrated TSA's superior performance and real-world applicability.

Ajayi et al. [228] introduced TSA for energy management in data centers (DCs). TSA demonstrated superior performance in prediction accuracy by training artificial neural network models to predict DC energy demand using historical data from a Cape Town, South Africa, DC operator. Ambient temperature was found to impact energy demand significantly. The study highlights TSA's versatility beyond DCs and offers insights for optimizing cooling systems and reducing energy costs.

Tayab et al. [239] proposed an ensemble forecasting strategy for solar PV power prediction in microgrid energy management systems (M-EMS). Their approach combines four methods, including TSA-based models and WOA-based models, aggregated using Bayesian model averaging (BMA). Simulations showed a significant reduction in root mean square error compared to other strategies, demonstrating its effectiveness in solar PV power forecasting for M-EMS.

Ge et al. [240] proposed TSA to optimize component sizes in island microgrids, aiming to minimize energy cost while considering constraints like energy surplus rate and CO₂ emissions. Simulation results showed that a hybrid storage system combining hydrogen and ice storage outperformed other configurations regarding economy, reliability, and environmental impact.

Patnaik et al. [241] proposed a method using TSA to address placement and sizing issues of distributed generation (DG) systems, focusing on wind turbine generators (WTG) and solar PV generators. They optimized the deployment of DGs within the IEEE 33-bus radial distribution system. Simulation results showed significant improvements, including enhanced voltage profiles, increased minimum security margin by 7.8%, reduced network losses by 22.7%, and deferred feeder investment by at least 13 years for distribution feeder up-gradation.

Vishal et al. [242] proposed employing TSA to optimize Electric Vehicles (EVs) performance, contributing to environmental preservation efforts. With EVs being a solution to reduce pollution from conventional vehicles, improving their performance is crucial. The study focuses on optimizing time domain parameters, crucial for electrical

machine performance, particularly Permanent Magnet Synchronous Motors (PMSMs), using TSA in a PID controller. Comparative analysis against PSO and conventional PID controllers demonstrated TSA's efficacy in enhancing PMSM performance, suggesting its superiority as a biological meta-heuristic technique.

Tayeb et al. [243] proposed utilizing TSA to design Power System Stabilizers (PSSs) for multi-machine power system networks, aiming to address system instability caused by low-frequency oscillations. They introduced a damping ratio-based objective function and adopted a traditional lead-lag type PSS structure to enhance system damping. The effectiveness of the TSA-based PSS architecture was demonstrated on both four-machine and ten-machine systems through various performance tests. The study also compared the results with those obtained using PSO, providing additional credibility to the proposed method's effectiveness and robustness in this domain.

Hossen et al. [244] proposed using TSA to optimize power system stabilizer (PSS) parameters in a Single Machine Infinite Bus (SMIB) network with a Unified Power Flow Controller (UPFC). Their aim was to improve system damping by minimizing a damping ratio-based objective function using a lead-lag compensator-type PSS structure. Simulation analyses demonstrated the algorithm's robustness in converging the PSS model effectively and improving system stability during three-phase faults. Comparative analysis with the Backtracking Search Algorithm (BSA) validated the efficacy of the proposed TSA method.

Hien et al. [245] proposed a novel approach for economic load dispatch (ELD), focusing on cooperation between thermal power plants (TPPs) and wind farms (WFs) in modified ELD scenarios. The authors introduced the TSA as a robust method, comparing it with PSO and SSD. TSO showed effectiveness, especially in WF-TPP coordination scenarios, highlighting wind power's role in cost reduction.

Larouci et al. [246] proposed meta-heuristic techniques like SOA, CSA, TSA, and FFA for solving dynamic combined economic environmental dispatch problems (DCEED). CSA, tailored for various objectives, showed efficiency and robustness in MATLAB simulations, offering advantages for DCEED problems.

Fathy et al. [247] proposed an optimal adaptive intelligent energy management strategy for a DC microgrid integrating a fuel cell system (FC), photovoltaic array (PV), and battery bank to enhance power saving. Their approach involves designing an optimal adaptive FC-based energy management strategy (EMS) where fuzzy membership functions are updated based on energy from the fuel cell and the main grid. Various meta-heuristic optimization strategies, including PSO, SSA, AOA, MPA, AEO, EO, PO, and TSA, are utilized to optimize the EMS. Comparative analysis in Matlab

Simulink showed that the PO outperformed others, achieving 7.7% power saving with a tracking efficiency of 99.571%. Statistical analysis using ANOVA is proposed to validate the strategy's performance.

Zhou et al. [248] proposed a TSA-ELM model for short-term commercial load forecasting, combining TSA with an Extreme Learning Machine (ELM). Analyzing daily load characteristics in a Romanian shopping mall, the model identified peak and valley loads within 24-hour periods. Historical load data underwent MIC analysis, with features having MIC ≥ 0.8 integrated into TSA-ELM for short-term load forecasting. Comparative analysis showed superior prediction accuracy of the PV-TSA-ELM model over others, significantly reducing error metrics compared to traditional ELM, validated with industrial data.

Krishnakumar et al. [249] proposed a hybrid control scheme for enhancing power system reliability in hybrid renewable energy sources (HRES). Leveraging TSA, the scheme optimizes cost functions to improve system reliability across scenarios involving solar photovoltaic wind energy and hybrid fuel cells. Implemented in MATLAB/Simulink, the scheme outperformed existing methods like MA-RBFNN, exhibiting an efficiency rate of 97.83099%, compared to DE, NSGA-II, NSGA-III, and MA-RBFNN, which recorded 82.136%, 77.26588%, 80.7532%, and 97.52470% efficiency, respectively.

Sholikhah et al. [250] proposed TSA-MPPT, a novel Maximum Power Point Tracking technique for Photovoltaic systems. Evaluated through simulation experiments, TSA-MPPT showcased 99% accuracy and outperformed conventional methods like P&O-MPPT and PSO-MPPT, suggesting its potential as an effective alternative in PV system MPPT applications.

Li et al. [251] proposed a novel model for crude oil price forecasting based on improving variational mode decomposition by TSA (TVMD). The model outperformed nine other forecasting models in terms of accuracy, demonstrating its potential for predicting crude oil prices.

Memon et al. [252] proposed a novel approach for load frequency control (LFC) in interconnected hybrid power systems using a classical PID controller optimized by the TSA. The study simplified the system by applying TSA to optimize PID parameters and achieved results within acceptable ranges. TSA was utilized across various areas of hybrid power systems, and performance evaluation demonstrated its robustness through sensitivity analysis across load variations. Comparative analysis with other optimization algorithms revealed TSA's superiority in overshooting, undershooting, and settling time, highlighting its effectiveness in enhancing LFC performance.

Madupu et al. [253] proposed TSA for optimal distributed generation (DG) integration in electrical distribution systems, focusing on renewable-based sources. They addressed

realistic load modeling's importance and aimed to enhance system efficiency by optimizing DG installation. Simulations on an IEEE 33 bus system validated TSA's superiority over existing algorithms, showing improvements in voltage profile, network losses, and voltage stability.

Sharma et al. [254] proposed an innovative approach for size optimization of hybrid renewable energy systems (HRES) to meet increasing energy demand and address fossil fuel costs. They focused on improving size optimization accuracy by hourly forecasting of weather parameters using machine learning techniques, with Gaussian process regression (GPR) being the most effective forecasting method. To further optimize HRES sizing, the authors compared CPA, TSA, and AO. TSA outperformed CPA and AO, resulting in a significant reduction in the per-unit cost of energy. These findings highlight TSA's potential for enhancing the efficiency and cost-effectiveness of grid-connected HRES, particularly in remote areas like India's Haryana province.

Saha et al. [255] introduced a novel approach to automatic generation control (AGC) in multi-area power systems, combining proportional-derivative with filter (PDN) and fractional-order proportional-integral (FOPI) controllers. Their method, optimized using TSA, showed superior performance over traditional controllers, effectively managing diverse power sources in different areas and enhancing power system control and performance optimization.

Rashidi et al. [256] developed an innovative energy management strategy for multi-microgrid (MMG) systems using TSA at the tertiary level control (TLC). The TSA optimized the connection and operation of individual microgrids to minimize operational costs while ensuring stability. By incorporating Information Gap Decision Theory (IGDT), the model effectively addressed uncertainties in power generation and consumption. TSA showed superior performance in balancing energy supply and managing operational constraints, validated through multiple case studies.

Islam et al. [258] utilized TSA with the Jellyfish Search Algorithm (JSA) to design power system stabilizers (PSS) for mitigating low-frequency oscillations (LFO) in electrical networks. The TSA and JSA optimized conventional lead-lag PSS parameters to enhance system damping. Testing on various systems showed significant improvements over traditional methods like Particle Swarm Optimization. The TSA-tuned PSS achieved a minimum damping ratio 2.55 times greater than conventional approaches, demonstrating its effectiveness in enhancing stability.

Anand et al. [257] introduced an innovative approach to sizing hybrid energy systems (HES) by integrating meteorological forecasts with TSA. They identified Gaussian Process Regression (GPR) as the most effective method for hourly meteorological data forecasting. The TSA optimized HES sizing to meet energy demands in remote regions of Uttar Pradesh, India, outperforming Particle Swarm Optimization

and Harmony Search. The study achieved a 0.33% reduction in the per-unit cost of energy, highlighting TSA's efficacy in optimizing energy systems and its potential for sustainable energy solutions.

5.2 Internet of Things

Verma et al. [260] proposed DOCAT, a Dual sink-based Optimized Clustering Architecture using the TSA, for energy-efficient WSNs in Intelligent Transportation Systems (ITS). DOCAT integrates novel fitness parameters for Cluster Head (CH) selection, optimizing traffic monitoring and accident detection tasks. It outperforms similar algorithms in network reliability, lifetime, throughput, and energy efficiency, making it suitable for accident-prone areas transmitting critical information to healthcare venues via IoT platforms.

Sharma et al. [261] proposed I-Raw, an algorithm for Wireless Body Area Networks (WBANs), which addresses sensor node battery constraints. I-Raw utilizes two sinks for data collection, optimizing cluster head selection with the TSA. Simulation results demonstrate that I-Raw significantly improves network stability and operational period compared to existing protocols.

Dogra et al. [262] introduced TORM, a routing mechanism for IoT networks, utilizing the TSA to optimize energy efficiency. By prioritizing cluster head node selection based on key fitness parameters, TORM extends network lifetime and enhances overall performance metrics, surpassing existing algorithms according to simulation results.

Verma et al. [259] introduced SEOF, a Sleep scheduling-based Energy Optimized Framework for IoT-based Wireless Sensor Networks (WSNs) in Wildfire Detection (WD). SEOF utilizes TSA for energy-efficient Cluster Head (CH) selection and sleep scheduling to reduce data transmissions. MATLAB simulations show SEOF's effectiveness in improving network stability period and scalability compared to conventional methods, promising enhanced wildfire detection while addressing energy constraints in WSNs.

Avdhes et al. [263] introduced NORTH, a novel routing technique for WSN-based IoT, to mitigate hot-spot issues in multi-hop routing architectures. Using the TSA, NORTH optimizes cluster-based routing by selecting cluster heads (CH) based on parameters such as energy status, distance from sink, load balancing, and node proximity. Simulation results showcase NORTH's effectiveness in prolonging network longevity, stability duration, and throughput and conserving remaining energy, surpassing existing algorithms.

Khan et al. [264] proposed an optimized AI system for healthcare IoT applications, enhancing data collection efficiency from biosensor networks. They introduced an optimized TSA to optimize data routes between patients and doctors, considering parameters like distance, energy, and

node proximity. Evaluation metrics such as stability period, lifetime, throughput, and clusters per round showcased the efficacy of their approach in healthcare IoT networks compared to existing methods.

Subramani et al. [265] introduced the Energy Aware Clustering and Multi-hop Routing Protocol with mobile sink (EACMRP-MS) for IoT-supported WSNs, aiming to enhance energy efficiency. The authors utilized the TSA for cluster head selection and Type-II fuzzy logic (T2FL) for optimal multi-hop route selection. Additionally, a mobile sink with a route adjustment scheme was introduced to adapt routes based on the sink's trajectory, further enhancing energy efficiency. Through comprehensive experimental analysis, EACMRP-MS showcased superior performance compared to contemporary methods across various evaluation metrics, highlighting its potential for IoT applications.

Gupta et al. [266] proposed EOCSR for energy-efficient routing in the Internet of Underwater Things (IoUT), leveraging the TSA for optimized Cluster Head selection and strategic routing. Simulation results showed a 16.8% increase in network stability and a 17.7% improvement in lifetime compared to a recent method, indicating its effectiveness in addressing energy challenges in IoUT deployments.

Raj et al. [267] proposed an enhanced Routing Protocol for Low Power and Lossy Networks (RPL) in IoT environments by addressing congestion and security issues. They introduced the Kullback Leibler Divergence-based TSA (KLD-TSA) for effective load balancing in RPL models. The KLD-TSA was integrated with an Exponential Poisson Distribution-Fuzzy (EPD-Fuzzy) model to predict congestion and ensure secure communication through hash-based verification. This approach improved packet delivery rates and minimized latency, demonstrating TSA's potential in optimizing IoT networks.

5.3 Cyber Security

Taher et al. [268] proposed a novel approach for enhancing intrusion detection in IoT networks by combining TSA with LSTM-RNN. This hybrid model preprocesses input data to identify IoT attacks efficiently. TSA optimizes LSTM-RNN hyperparameters to improve convergence speed and performance. Benchmark tests show the superiority of TSA-LSTM-RNN in accuracy, recall, and precision compared to related models, offering promising results for IoT intrusion detection.

Aljebreen et al. [271] introduced MEOADL-ADC for DDoS attack classification in 5G networks. The method combines feature selection, LSTM classification, and TSA hyperparameter tuning. Experimental results show that MEOADL-ADC achieves a maximum accuracy of 97.60%, outperforming current methods.

Chaudhary et al. [269] introduced a secure image steganography technique employing TSA. The method combines chaotic map-based image scrambling and graph signal processing with a Meyer wavelet filter. TSA optimizes alpha blending for efficient data hiding. Experimental results show superior imperceptibility and robustness compared to existing methods, evaluated using PSNR, MSE, and SSIM.

Singh et al. [270] introduced TSA-HAN, a novel text classification approach combining TSA and HAN. TSA optimizes the algorithm, leveraging jet propulsion and Swarm Intelligence. Evaluation on various parameters and datasets, including Reuters and 20-Newsgroup, shows TSA-HAN exhibits slightly superior performance compared to ISCA.

Katib et al. [272] introduced TSA-LSTM-RNN for identifying human and ChatGPT-generated text. The model employs TF-IDF, word embedding, and count vectorizers for feature extraction, with classification performed by LSTM-RNN. TSA enhances parameter selection. Evaluation on benchmark datasets shows TSA-LSTM-RNN achieves a maximum accuracy of 93.17% and 93.83% on human- and ChatGPT-generated datasets, respectively.

Seth et al. [273] introduced a hybrid approach to sentiment analysis addressing existing limitations. Data from Twitter was collected using the Twitter API, and an n-gram representation model was employed. The study proposed TSA to enhance scalability and reduce computation time. Additionally, a hybrid HHO algorithm was custom-built to mitigate local optima problems. The model achieved a feature size reduction of up to 64% and an accuracy of 96.37%, outperforming state-of-the-art algorithms in sentiment analysis of Twitter feedback.

Krishnasamy et al. [274] introduced EFDPN, a robust cyber-physical system addressing security challenges in WSNs and IoT. EFDPN incorporates F3S to mitigate computational complexity in attack identification. Leveraging DPN for intrusion classification, TSA enhances the sigmoid transformation function for improved prediction accuracy. Validated using cyber-attack datasets, EFDPN outperforms traditional methods, particularly in achieving higher F1-score values. Integrating F3S enhances prediction accuracy by eliminating irrelevant features, promising enhanced security in WSN-IoT networks.

Singh et al. [275] introduced CA-TSA-based GAN for detecting violent crowd behavior in computer vision systems. The model combines Conditional Autoregressive Value at Risk with TSA to model crowd behavior. Feature extraction includes Tanimoto-based Violence Flows descriptor, Local Ternary patterns, and Gray level co-occurrence matrix. Evaluation on the ASLAN challenge dataset shows promising performance metrics, with accuracy, sensitivity, and specificity values of 93.688%, 94.261%, and 94.051%, respectively.

Alrurban et al. [276] introduced CTOASDL-CD, a novel approach for early detection of cyberattacks in cyber-physical systems (CPS). The method utilizes TSA for hyperparameter selection in the SDBN model, enhancing cyberattack detection in Industrial CPS platforms. Combining feature selection with hyperparameter-tuned deep learning models, CTOASDL-CD addresses high dimensionality issues and improves security outcomes in CPS environments.

Sasikala et al. [277] introduced a multi-modal biometric system combining fingerprint and retina traits, leveraging deep learning and hashing methods to enhance template security. The methodology includes pre-processing, feature extraction using ConvGRUSA, and chaos-based hashing for template generation. TSA optimizes ConvGRUSA parameters for efficient feature correlation detection. Implementation on MATLAB achieves high accuracy (99.93%) and low FAR, FRR, and EER, demonstrating improved biometric security and accuracy.

5.4 Computer Science

5.4.1 Feature Selection

Daniel et al. [278] proposed a hybrid sentiment analysis framework integrating TSA for feature reduction in online product reviews. The framework addresses scalability issues by combining lexicton-based methods and machine-learning techniques. TSA reduces feature set size by 43% while maintaining 93% accuracy, outperforming existing techniques like particle swarm optimization and genetic algorithm. Evaluation metrics validate the approach's effectiveness in automatic sentiment analysis.

Diaz et al. [279] compared meta-heuristic optimization algorithms for feature selection and weighting in ANNs. Evaluated algorithms include ChOA, TSA, BSSA, ALO, and modified ALO. Experimental results on five datasets show these algorithms enhance classification by reducing features and improving accuracy. TSA and chimp optimization exhibit superior performance, highlighting their efficacy in machine learning tasks.

5.4.2 Networks

Sudha et al. [306] introduced the Energy Centric Tunicate Swarm Algorithm (ECTSA) for addressing energy efficiency and network lifetime in MANETs. ECTSA adopts cross-layer routing, considering factors like residual energy and mobility. It employs ACW adjustment to minimize energy consumption. Performance evaluation shows that ECTSA outperforms existing techniques like CEELBRP and EECRP-PSO, achieving lower energy consumption (7.1

joules) and extending network lifetime to 1603 seconds for 50 nodes.

Inamdar et al. [307] introduced a directional routing approach for MANETs using TSA. The paper proposes CLI to exchange network density parameters across layers and adaptations in directional antenna-enabled MANETs for efficiency. Simulation results show TSA and CLI-based routing outperform competing proposals, demonstrating their effectiveness in MANETs.

Khan et al. [308] introduced a bio-inspired autonomous surveillance system for enhancing energy efficiency in underwater sensor networks. Their approach utilizes TSA for selecting cluster heads based on energy, distance, and density parameters. Comparative analysis shows the proposed protocol extends the network's lifespan by improving energy balance through intelligent cluster head selection.

Saad et al. [309] introduced an energy-efficient clustering-based routing algorithm for WSNs, which is crucial for IoT applications. Based on TSA, their algorithm optimizes cluster head selection considering factors like energy, distance to the base station, and load balancing. It establishes paths from cluster heads to the base station through relay nodes, prolonging network lifetime and conserving energy, thus enhancing WSN performance in IoT environments.

Simon et al. [310] introduced the IGOR protocol to enhance efficiency in underwater IoT networks by reducing void hole occurrence and improving Packet Delivery Ratio (PDR). Meta-heuristic optimization using TSA optimizes parameters to minimize Energy Consumption (EC) and maximize PDR. The evaluation shows the proposed protocols outperform benchmark protocols by 80–81% in PDR and reduce void holes by around 30%, contributing to improved efficiency and reliability in underwater IoT networks.

5.5 Engineering

Sharifi et al. [282] compared TSA with other evolutionary algorithms in optimizing the Halilrood multi-reservoir system operation. The study evaluated reliability, resilience, vulnerability, and sustainability criteria over 223 months. Results showed the MSA outperformed others, followed by HHO. TSA demonstrated competitive performance, surpassing GA and PSO but falling below MSA and HHO. MSA's superior sustainability index suggests water resources managers adopt it for improved operations.

Abdelhamid et al. [283] introduced an adaptive protection scheme based on the TSA. This novel approach coordinates distance and direction over current relays in the protection system. Evaluation on the IEEE 8-bus test system demonstrates its effectiveness, comparing favorably with other well-known algorithms.

Al Duhayyim et al. [284] introduced the AITFP-WC model for short-term Traffic Flow Prediction (TFP) in intelligent transportation systems, considering weather conditions. This model integrates the Elman Neural Network (ENN) for traffic flow prediction and employs TSA with Feed Forward Neural Networks (TSA-FFNN) for weather analysis. Simulation analysis showed improved predictive performance compared to state-of-the-art methods, highlighting its potential for mitigating traffic congestion in smart cities.

Kammula et al. [285] introduced an energy-efficient surveillance scheme for underwater acoustic sensor networks (UASN) to enhance intruder detection accuracy. This scheme utilizes a single beacon node and Boolean perception probability for intrusion detection, considering factors like energy constraints and network overhead. A rapid convergent TSA is applied to improve intruder position accuracy. Simulations show reduced overhead and enhanced accuracy compared to existing schemes.

Pahuja et al. [286] proposed optimizing power allocation in Cooperative Communication Networks (CCNs) to enhance system efficiency. The authors utilized TSA to optimize system parameters like SER, outage probability, and BER. Evaluation of relaying protocols and combining schemes showed the effectiveness of the proposed algorithm compared to other metaheuristic algorithms like PSO and BWO, as well as the traditional EPA method.

Qiang et al. [287] proposed a study to enhance undrained shear strength (USS) estimation of soil using innovative machine learning techniques. The authors employed least square support vector regression (LSSVR) and metaheuristic optimization techniques like TSA, EO, and TFWO to optimize input variables. The LSTS model achieved the highest R-squared value of 0.998 and the lowest root mean square error (RMSE) of 34.28 compared to other models, showcasing its efficacy in USS estimation.

Husain et al. [288] introduced MPA, POA, and TSA for precise parameter extraction in Gallium Nitride (GaN) HEMTs. These, combined with direct methods, improved efficiency. Comparison favored OA-based hybrid modeling for its physical relevance despite both approaches showing excellent agreement up to 40 GHz.

Hasan et al. [289] introduced an Active Disturbance Rejection Control (ADRC) system for trajectory tracking of a Tricopter UAV, emphasizing the extended state observer (ESO). Three types of ESOs were explored: fractional order (FOESO), nonlinear (NESO), and super-twisting (STESO), comparing their robustness and disturbance rejection. The TSA optimized ADRC parameters for enhanced dynamic performance. Numerical simulations assessed the ADRC system's effectiveness, particularly the FOESO variant, under uncertainties and external disturbances for robust trajectory tracking.

Li et al. [290] proposed a novel approach using the TSA to optimize a PID controller based on a Backpropagation (BP) neural network for self-driving bicycles. The controller dynamically adjusts PID parameters in real time, improving robustness and reliability. TSA optimizes the initial neural network weights, addressing convergence issues. Simulation results show significant improvements in dynamic performance and robustness, effectively managing environmental changes. This controller design offers an effective solution to the balancing problem of self-driving bicycles, with broad application potential.

Guo et al. [291] proposed an approach for designing high-stability and reliable DNA sequences for DNA computing in search applications. The method incorporates epsilon constraints to address the multi-objective nature of sequence design, encompassing thermodynamic and logical constraints. Two meta-heuristic algorithms, the TSA and GOA, are employed at different stages based on their features and applicability. Results show that integrating epsilon constraints with these algorithms leads to superior DNA sequence sets compared to previous methods.

Alnfiai et al. [292] proposed the DLIMR-CS technique for Intelligent Modulation Recognition of Communication Signals (CS), addressing the need for fast and reliable wireless networks, especially in emerging 5G contexts. Using Deep Learning, it employs a Deep Variational Autoencoder (DVAE) model with Sevcik Fractal Dimension (SFD) features for signal classification. The TSA fine-tunes hyperparameters, enhancing the DVAE model's performance. Simulations demonstrate superior recognition rates compared to existing methods, highlighting its efficacy for next-gen networks.

Zhou et al. [293] introduced the R18-COTSA-RVFL model to improve fabric wrinkle evaluation. This model combines ResNet18 with an enhanced RVFL, using TSA for classification. The model's parameters are optimized for accuracy and stability, outperforming other methods in classification accuracy.

Kamalkumar et al. [294] introduced a method for optimizing transistor sizing in CMOS differential amplifiers using the TSA. By leveraging TSA, they improved various circuit specifications, including circuit area, power dissipation, and MOS transistor size, while meeting design criteria. The fitness function of TSA was tailored to the design objectives of CMOS differential amplifiers. Implemented in MATLAB, their CMOS-DA-TSA method demonstrated significant enhancements compared to existing methods like CMOS-ACD-SOA, CMOS-PAI-FOPSO, and CMOS-PSO-MOL.

He et al. [295] investigated overbreak prediction in tunnel blasting, a crucial construction concern. They enhanced the Random Forest (RF) model using three meta-heuristic

algorithms, including TSA. Results showed RF-TSA outperforming other models in accuracy, emphasizing TSA's effectiveness in optimizing RF hyperparameters. This study highlights TSA's potential for improving predictive modeling in construction projects.

Mei et al. [296] investigated the prediction of energy absorption in a novel aseismic concrete material using the Split-Hopkinson Pressure Bar (SHPB) device. They employed six metaheuristic optimization algorithms, including TSA and a Random Forest (RF) model. Results showed that the TSA-RF model outperformed others, with cement being the most influential parameter. This study demonstrates the potential of artificial intelligence in predicting energy absorption and contributes insights for aseismic materials in tunnel engineering.

Barua et al. [297] utilized the TSA to optimize the manufacturing process of CPVC components for electrical wire casing. They focused on injection moulding parameters to reduce the weight of CPVC elbow components, conducting 27 tests using Response Surface Method-based Box-Behnken Design. The study highlighted the significant impact of mould pressure on weight reduction, showcasing the effectiveness of the TSA in optimizing CPVC component manufacturing. This research provides valuable insights into enhancing production efficiency while minimizing waste in fire-retardant electrical wire casing components.

Liu et al. [298] used machine learning to predict the compressive strength (CS) and slump (SL) of High-performance concrete (HPC). They combined models like LGBM and DT with meta-heuristic algorithms such as Zebra Optimization and TSA to enhance accuracy. The LGZO model showed promising results with low RMSE values for CS and SL, suggesting that these methods offer efficient alternatives to traditional testing, reducing costs and time in concrete strength prediction.

Kala et al. [299] proposed an enhanced method for solving the selective harmonic elimination (SHE) problem in multilevel inverters (MLI). The authors utilized TSA to obtain an initial solution, which was refined iteratively. TSA demonstrated superior convergence efficiency compared to other optimization algorithms like grey wolf and whale optimization. Further optimization using the Newton-Raphson method resulted in the TSANR approach, which showed improved convergence speed and accuracy. This method effectively controlled fundamental and detrimental harmonics in dynamic modulation index scenarios, as confirmed by simulations and experiments.

Wang et al. [300] proposed hybrid methods for estimating the compressive strength of high-performance concrete by combining support vector regression models with optimization algorithms like MAVO, AVOA, and TSA. The evaluation showed SVMiA's superior performance in achieving higher

accuracy and lower error values than other hybrids, improving CS estimation while simplifying modeling.

Alyami et al. [301] utilized metaheuristic algorithms, including the TSA, to optimize the composition of 3D-printed fiber-reinforced concrete (3DPFRC) for improved compressive strength (CS). Among the models developed, TSA-RF showed the best performance, demonstrating high correlation and low error values. They also used Shapley Additive exPlanation (SHAP) interpretability to gain insights into feature relationships, aiding in optimizing 3DPFRC mixtures for construction applications.

Kengpol et al. [303] introduced a hybrid deep learning approach that combines TSA with an ANN for cost evaluation in the plastic injection industry. TSA optimizes the initial weights of the ANN, enhancing the accuracy and speed of cost assessments for complex surface products. The TSA-ANN model achieved prediction accuracies of 96.66% for part costs and 93.75% for mold costs. This model significantly outperformed traditional ANN methods in evaluating costs for plastic injection molding.

Shwetha et al. [305] developed a method for adaptive channel equalization in wireless communication systems using TSA to optimize equalizer coefficients. This approach effectively reduces mean square error and mitigates inter-symbol interference. Implemented in MATLAB, it was evaluated against metrics like bit error rate and convergence rate. Comparative analysis showed that the TSA-based technique outperformed other methods, including the Bat Algorithm and Slime Mould Algorithm, enhancing signal quality.

Jeyanthi et al. [304] introduced a hybrid model, NFC-TSA, combining a neuro-fuzzy controller with TSA to estimate displacement amplitude in geo-structures under vibrational loads. The model is trained using data from extensive field vibration experiments, considering factors like foundation bed and dynamic excitation. Compared to existing methods such as ANN-EHO and RNN, NFC-TSA demonstrated superior prediction accuracy in geo-structural applications. This innovative approach enhances the reliability of displacement amplitude estimates.

5.6 Medical

Chander et al. [311] proposed the TSA-based Black-hole Entropic Fuzzy Clustering (BHEFC) for clustering COVID-19 data. The TSA optimizes the weighted coefficients for cluster centers in BHEFC. Data preprocessing involves log transformation, and significant features are selected using the Pearson Correlation coefficient. The TSA-based BHEFC achieves high accuracy (95.061%), Jaccard coefficient (90.852%), and Dice coefficient (90.420%), outperforming other clustering methods for COVID-19 data.

Nguyen et al. [312] proposed an energy-efficient fog-based Internet of Health Things (IoHT) system using a lightweight Simon cipher optimized by the TSA algorithm. This framework enhances energy efficiency and security for medical data stored in the cloud. TSA optimizes key selection for the Simon cipher, preserving image quality as measured by the peak signal-to-noise ratio (PSNR). A lightweight encryption step in the fog layer reduces the computational burden on the cloud server. Experimental results show that the TSA-Simon model achieves a high PSNR of 61.37 dB and a pixel change rate of 95.31%, ensuring accurate medical report generation from IoHT devices.

Awarei et al. [313] proposed 3DDISC-DLTS, a novel approach for 3D dental image segmentation and classification using deep learning and the TSA. This system automates tooth segmentation and classification into seven types within CAD models, which is crucial for dental treatment planning. The methodology includes image preprocessing, U-Net segmentation, and feature extraction with DenseNet-169, followed by TSA-based hyperparameter tuning. Experimental results show that the 3DDISC-DLTS model achieves high accuracy, with 96.67% on dataset-1 and 97.48% on dataset-3, outperforming modern models.

Çetinkaya et al. [314] proposed the TSA for enhancing biomedical image analysis, particularly vessel segmentation. TSA offers global optimum convergence, rapid convergence rates, and minimal control parameters. The study adapts TSA and other metaheuristic algorithms, like JS, MPA, and MA, for clustering-based vessel segmentation. These algorithms are compared based on convergence rates, error values, CPU time, sensitivity, specificity, and accuracy. Comparative analyses against PSO, GWO, and DE demonstrate TSA's efficacy, highlighting its potential for precise biomedical image segmentation.

Wankhede et al. [315] introduced a Hybrid TSA and Ensemble Deep Learning (TSA-EDL) for accurate heart disease prediction. The model integrates data mining techniques, including pre-processing, clustering with DBSCAN, and classification using a hybrid classifier. Implemented in Python, the approach is evaluated on the University of California Irvine (UCI) and Cardiovascular Disease (CVD) datasets, achieving a high accuracy of 98.33% for CVD and 97.5% for UCI datasets. Results surpass previous algorithms, demonstrating the efficacy of TSA-EDL in heart disease prediction.

Srikanth et al. [316] proposed a method for early prediction and classification of breast cancer using data mining techniques and meta-heuristic optimization. The approach combines an improved fractional rough fuzzy K-means clustering strategy for disease prediction with the TSA for optimizing weight parameters. A labeled ensemble classifier (LEC) is then employed for classification. Comparative analysis against existing approaches shows a remarkable 99.3%

accuracy on breast cancer Wisconsin dataset (diagnosis), highlighting the potential of the proposed method for highly accurate early diagnosis and classification of breast cancer.

Sun et al. [317] proposed the TSOADBN model to evaluate the impact of instructional approaches in arts education on college student's mental well-being. TSOADBN outperformed alternative models in identifying patterns related to mental health conditions. By leveraging DBN classification and TSA for hyperparameter optimization, it offers valuable insights into the domain, addressing the relationship between mental and physical health.

Mahaveerakannan et al. [318] proposed a methodology for patient monitoring in the healthcare system, focusing on lung cancer diagnosis using IoT. Machine learning techniques address computational challenges, including SMOTE for data preprocessing and BGWOA for feature selection. TSA optimizes hyperparameters, and XGBoost performs classification. Experimental results demonstrate improved accuracy and recall values, indicating the efficacy of the proposed model.

Akram et al. [319] proposed a deep-learning mechanism to improve Parkinson's disease detection accuracy. Their approach involves pre-processing with Gabor filtering, feature extraction using EWT and DT-CWT, optimal feature selection with TSA, and classification with FBLstmNet. Experimental results in Python show superior performance in accuracy (99.5%), precision (99.54%), recall (99.52%), specificity (99.57%), and F-measure (99.56%) compared to existing methods.

Abdullah et al. [320] proposed MDCNN-C3HI, a meta-heuristic technique combined with deep convolutional neural networks for colorectal cancer (CRC) classification. The approach involves noise removal, feature vector extraction using an enhanced capsule network, and classification with a modified deep-learning neural network classifier. Hyperparameter fine-tuning is achieved through TSA. Experimental results show superior performance with a maximum accuracy, sensitivity, and specificity of 99.45%, demonstrating promising potential for accurate CRC classification.

Poonguzhali et al. [321] proposed ADRU-SCM, an Automated Deep Residual U-Net Segmentation with a Classification model for Brain Tumor Diagnosis. The model includes preprocessing with wiener filtering, deep residual U-Net segmentation, and feature extraction with VGG-19. TSA with GRU optimizes classification. Evaluation on the FigShare dataset shows superior performance compared to recent methods, demonstrating potential for streamlining brain tumor diagnosis.

Laishram et al. [322] proposed a computer-aided detection scheme for breast cancer utilizing contrast enhancement for mammograms. They introduced a hyperbolic tangent function for contrast enhancement, optimized by TSA. Additionally, they used the median robust extended local binary

pattern for texture-based analysis to minimize false positives. Evaluation on standard databases showed high sensitivities of 95.3% and 94.1% with low false positives per image. This study demonstrates TSA's potential in optimizing parameters for enhancing mammogram images and improving automated breast cancer detection systems.

Gandikota et al. [323] proposed TSADL-PCSC for pancreatic cancer (PC) classification in CT scans. This technique employs W-Net segmentation, GhostNet feature extraction, and DESN for classification. TSA optimizes hyperparameters. Experimental results on a benchmark CT scan database demonstrate the superiority of TSADL-PCSC in PC classification.

Laxminarayananma et al. [324] introduced IDRCNN for early pancreatic ductal adenocarcinoma (PDAC) detection using CE-CT images. TSA optimizes IDRCNN hyperparameters. The method improves PDAC diagnosis accuracy by segmenting surrounding anatomical structures. Three IDR-CNN variants were trained: lesion detection, tumor and pancreas segmentation, and pancreatic duct segmentation. Evaluation on a CT image dataset shows superior performance, enhancing early PDAC detection in clinical settings.

Digumarthi et al. [325] introduced SANN CAD for detecting arrhythmias in ECG signals. The model incorporates an OS-G digital filter optimized by TSA and PLASSVR for feature extraction. Classification is performed using a Siamese neural network based on GAN. GOA adjusts hyperparameters. Evaluated on the MIT-BIH Arrhythmia Database, SANN CAD achieves high classification accuracy, outperforming traditional classifiers with maximum accuracies of 99.74% and 98.23%, respectively.

Ganesan et al. [326] developed an automated framework for early Alzheimer's Disease detection using structural MRI and machine learning. TSA optimizes the segmentation threshold in the Otsu method, enhancing Region of Interest identification. Feature extraction utilizes Local Binary Pattern and Local Directional Pattern variance, followed by classification with Deep Belief Networks. The model achieved impressive accuracies of 99.80% and 99.92% on the ADNI and AIBL datasets, respectively.

Palaniswamy et al. [328] introduced ODL-BAAM, a Deep Learning model for Bone Age Assessment (BAA) that improves the efficiency and accuracy of hand X-ray analysis. Addressing the limitations of traditional methods, ODL-BAAM employs advanced preprocessing and a feature extraction process using Faster R-CNN and MobileNet. The integration of TSA for hyperparameter optimization significantly enhances performance, resulting in an impressive accuracy of 96.5%. This advancement sets a new benchmark in medical image analysis for BAA.

5.7 Environmental Modeling

Lavanya et al. [329] proposed TSADL-LULCCD for Land Use and Land Cover Change Detection (LULCCD) in the Nallamalla Forest, India. The method combines the TSA with deep learning, using LANDSAT images and an EfficientNet model for feature extraction. TSA optimizes the hyperparameters of a Deep Belief Network (DBN) for classification. Experimental results show that TSADL-LULCCD outperforms existing models in accurately detecting land use changes due to deforestation.

Saranya et al. [330] proposed a method for automatically categorizing banana ripeness, which is crucial for agriculture and sales. Traditional manual methods for assessing ripeness are time-consuming and error-prone. Leveraging computer vision and machine learning, the study uses a CNN to classify banana ripeness into four stages: unripe, mid-ripe, ripe, and overripe. The approach integrates a fuzzy-based CNN with the TSA. Experimental results show the model achieves an overall accuracy of 96.9%, surpassing contemporary computer vision algorithms in accurately classifying banana ripeness.

Kumar et al. [331] enhance water quality forecasting by optimizing neuro-fuzzy models using the TSA. This study addresses the challenges in parameter optimization for complex models, highlighting the importance of accurate water quality estimates for environmental management. By integrating TSA into the optimization process, the research improves model performance. TSA effectively balances exploration and exploitation in the parameter space. Experimental results show the proposed approach outperforms traditional techniques, offering a promising environmental forecasting and decision-making tool.

6 Evaluation and Analysis of the TSA Algorithm

This section analyzes the optimization performance of TSA in standard CEC2017, CEC2020, and CEC2022 benchmark functions. Section 6.1 details the experimental environments and implementation. Section 6.2 provides the parameters of competitor algorithms and TSA. Section 6.3 summarizes the experimental results and analyzes the performance of TSA.

6.1 Experimental Environments and Implementation

We conducted numerical experiments on a Lenovo Legion R9000P running Windows 10, powered by an AMD R9 7945HX CPU, 16GB of DDR5 RAM, and an NVIDIA GeForce RTX 4060 GPU. These specific experimental settings are provided to ensure reproducibility.

Table 5 Parameters of optimizers

MAs	Parameters	Value
GA	Selection scheme	Tournament
	Crossover rate	0.8
	Mutation rate	0.01
DE	Mutation strategy	DE/cur-to-rand/1/bin
	Scaling factor F	0.9
	Crossover rate Cr	0.7
CMA-ES	σ	1.3
GWO	Parameter-free	
MFO	Parameter-free	
SCA	Constant A	2
WOA	Constant b	1
GJO	Parameter-free	
FOX	Jumping probabilities c_1 and c_2	0.18 and 0.82
POA	Parameter-free	
jSO	N_{max} and N_{min}	$12 \times D$ and 4
	p_{max} and p_{min}	0.25 and 0.125
	M_F	0.3
L-SHADE-cnEpSin	N_{max} and N_{min}	$18 \times D$ and 4
	μ_F and μ_{Cr}	0.5 and 0.5
	σ_F and σ_{Cr}	0.1 and 0.1
	H	5
	ps and pc	0.5 and 0.4
TSA	Parameter-free	

6.2 Competitor Algorithms and Parameters

This section details the competitor algorithms and their parameters. We select three categories of optimizers as follows, and the detailed parameters are summarized in Table 5.

- Classic MAs: Genetic Algorithm (GA) [333], Differential Evolution (DE) [334], and Covariance Matrix Adaptation Evolution Strategy (CMA-ES) [335].
- Highly-cited MAs: Grey Wolf Optimizer (GWO) [129], Moth Flame Optimizer (MFO) [152], Sine Cosine Algorithm (SCA) [143], and Whale Optimization Algorithm (WOA) [45].
- Latest MAs: Golden Jackal Optimizer (GJO) [336], FOX Optimizer (FOX) [337], and Pelican Optimization Algorithm (POA) [338].
- State-of-the-art MAs: jSO [339] and L-SHADE-cnEpSin [340].

Table 6 Summarized statistical analysis in CEC benchmarks

Bench	Dim.	Metric	GA	DE	CMA-ES	GWO	MFO	SCA	WOA	GJO	FOX	POA	jSO	L-SHADE-cnEpsSin	TSA
CEC2017	10	+≈/-	22/6/1	20/5/4	19/6/4	11/18/0	28/1/0	19/9/1	23/5/1	20/9/0	27/2/0	13/10/6	2/9/18	8/8/13	—
		Avg. ranks	8.7	8.4	6.2	5.5	12.5	6.4	9.7	7.7	11.4	5.9	1.4	2.8	4.4
	30	+≈/-;	29/0/0	28/0/1	22/1/6	8/16/5	29/0/0	25/2/2	26/3/0	27/2/0	24/2/3	24/3/2	6/9/14	15/4/10	—
		Avg. ranks:	10.5	10.3	6.2	3.6	12.5	6.6	9.4	8.1	7.6	7.0	2.3	3.7	3.1
CEC2020	50	+≈/-;	29/0/0	29/0/0	22/2/5	13/12/4	29/0/0	26/3/0	26/3/0	29/0/0	22/3/4	25/3/1	13/5/11	20/5/4	—
		Avg. ranks:	11.0	10.9	6.0	3.5	12.4	6.7	8.9	8.7	6.3	7.3	3.0	3.8	2.4
	100	+≈/-;	29/0/0	29/0/0	23/1/5	17/8/4	29/0/0	28/1/0	26/1/2	28/1/0	21/2/6	25/2/2	21/1/7	23/2/4	—
		Avg. ranks:	11.4	10.6	6.1	3.3	12.2	6.8	8.4	9.4	5.3	7.5	3.6	4.2	2.3
CEC2022	10	+≈/-;	10/0/0	6/2/2	6/1/3	7/3/0	10/0/0	9/1/0	8/2/0	10/0/0	9/1/0	6/3/1	0/2/8	0/5/5	—
		Avg. ranks:	11.1	5.2	6.0	5.2	12.9	7.5	9.7	10.1	8.7	6.7	1.1	2.7	4.1
	20	+≈/-;	10/0/0	7/2/1	7/0/3	6/4/0	10/0/0	9/1/0	10/0/0	10/0/0	7/3/0	9/1/0	5/2/3	6/1/3	—
		Avg. ranks:	11.6	4.3	5.9	5.6	12.9	7.2	9.3	10.7	5.4	8.8	2.8	4.2	2.3
CEC2022	10	+≈/-;	9/2/1	5/3/4	7/4/1	6/6/0	12/0/0	7/2/3	10/2/0	10/2/0	11/1/0	6/4/2	1/1/10	2/3/7	—
		Avg. ranks:	9.9	5.7	6.7	6.3	12.8	6.4	9.8	9.7	9.5	5.4	1.3	3.1	4.5
	20	+≈/-;	11/1/0	9/2/1	7/4/1	7/4/1	11/1/0	10/1/1	10/2/0	12/0/0	8/3/1	9/2/1	6/1/5	6/1/5	—
		Avg. ranks:	10.8	6.8	6.8	5.3	12.6	6.2	9.8	9.6	6.0	7.3	2.7	3.7	3.5

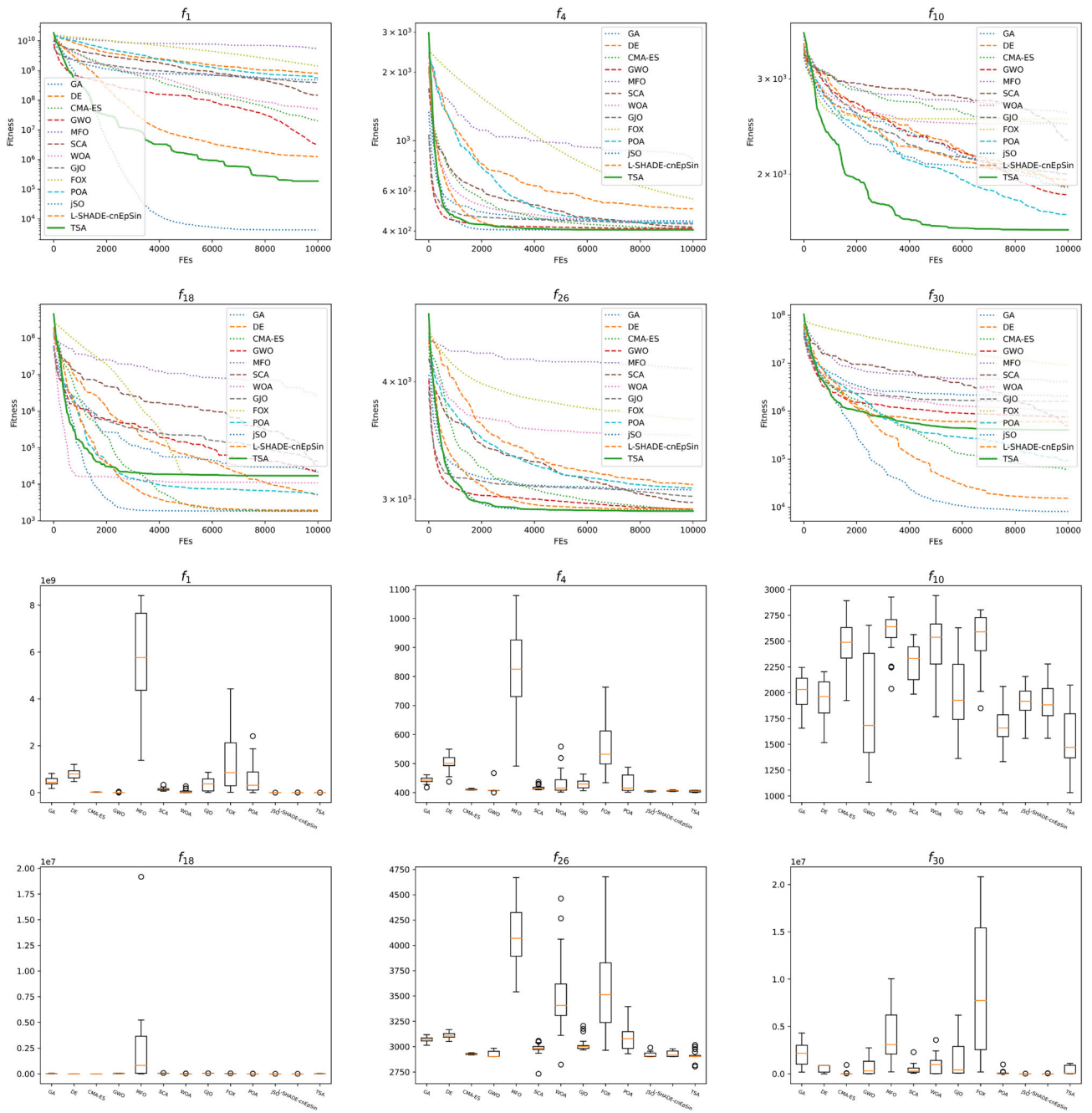


Fig. 9 Convergence curves and boxplots of optimizers in 10-D CEC2017 functions

The common parameters among competitor algorithms include a fixed population size of 50, a maximum fitness evaluation (FE) of $1000 \times$ dimension size, and 30 trial runs.

6.3 Experimental Results and Analysis

This section presents the experimental results in CEC2017, CEC2020, and CEC2022 benchmarks. Additionally, we

applied the Mann-Whitney U test to identify the statistical significance between every pair of optimizers, and the p-values obtained from the Mann-Whitney U are corrected using the Holm multiple comparison test. Symbols +, ≈, and – indicate that TSA is significantly better, statistically equivalent, or significantly worse than the specific competitor optimizer. Furthermore, we calculated the average rank for each algorithm, with the best fitness values highlighted in bold. Table 6 summarizes the statistical analysis and results

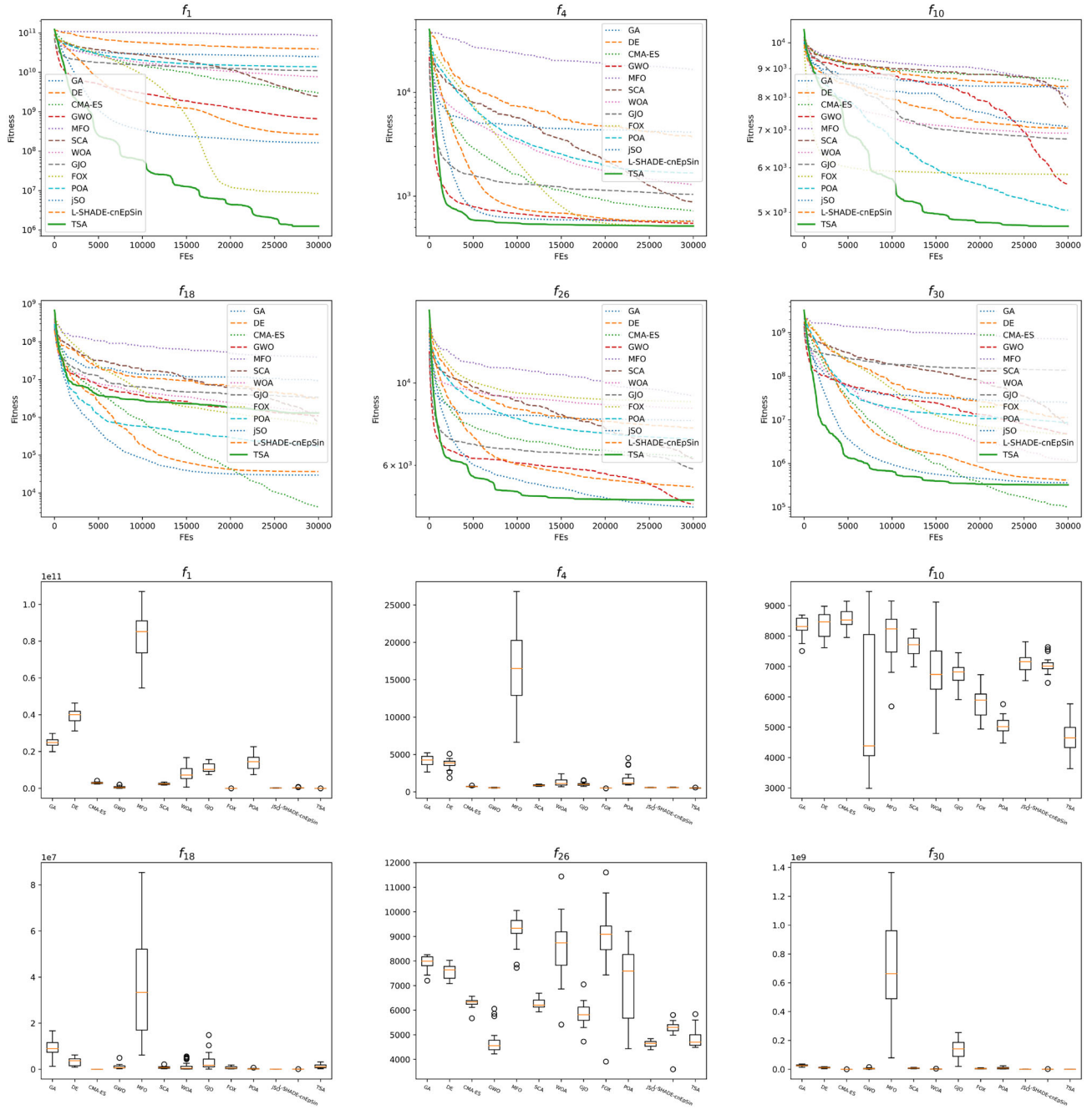


Fig. 10 Convergence curves and boxplots of optimizers in 30-D CEC2017 functions

of the Friedman test in CEC benchmarks, while the detailed experimental results in CEC2017, CEC2020, and CEC2022 are listed in Appendices Appendix A, Appendix B, and Appendix C, respectively. Figs. 9, 10, 11, 12, 13, and 14 present the convergence curves and boxplots of optimizers in CEC benchmarks.

In the low-dimensional CEC benchmarks, the winner algorithms of the CEC competition, jSO and L-SHADE-cnEpSin, have demonstrated remarkable performance, significantly outperforming TSA and other optimizers. Specifically, jSO achieves average ranks of 1.4 and 2.3 in 10-D and 30-D CEC2017, 1.1 and 2.8 in 10-D and 20-D CEC2020,

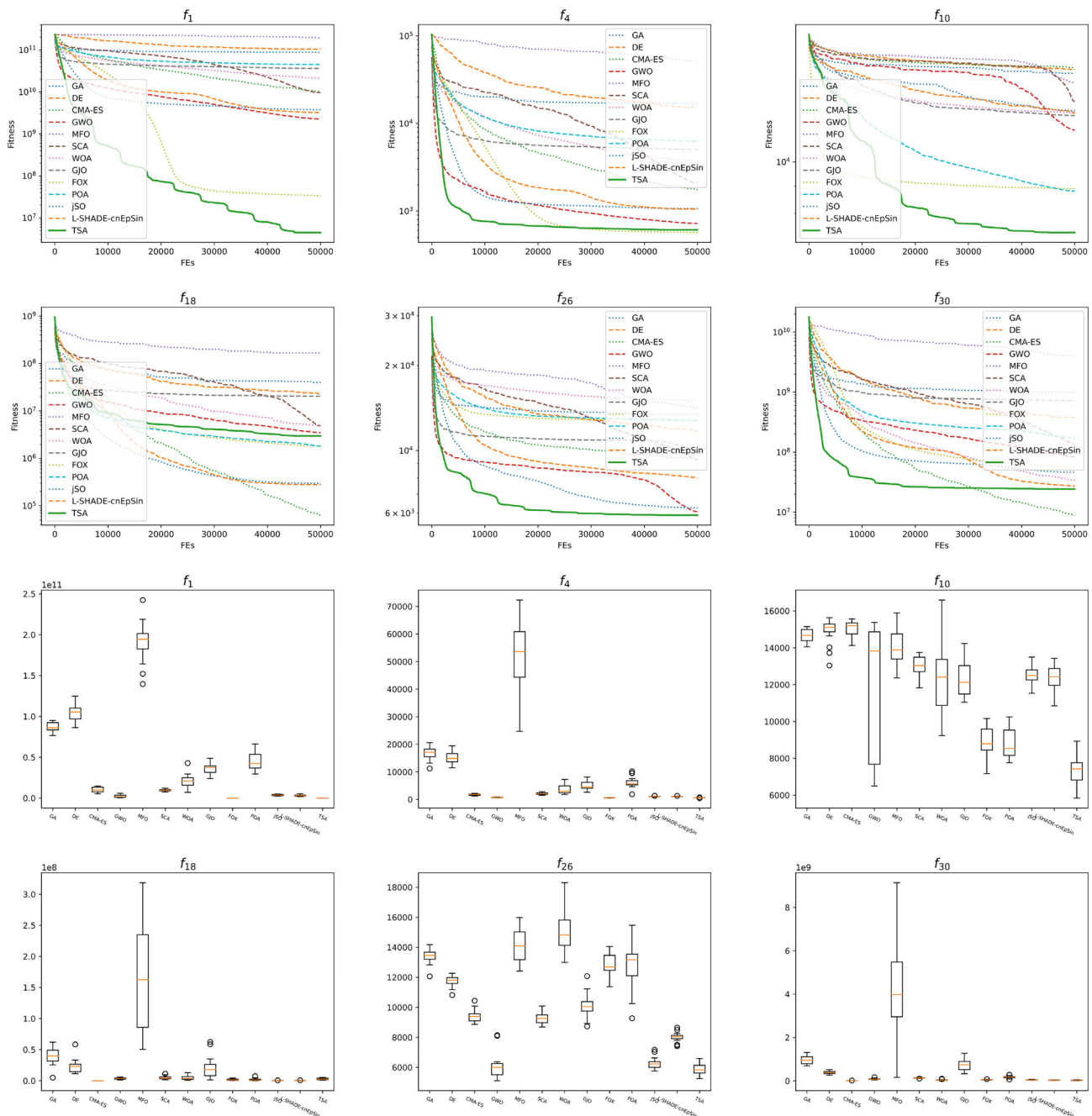


Fig. 11 Convergence curves and boxplots of optimizers in 50-D CEC2017 functions

and 1.3 and 2.7 in 10-D and 20-D CEC2022, respectively. Similarly, L-SHADE-cnEpSin attains average ranks of 2.8 and 3.7 in 10-D and 30-D CEC2017, 2.7 and 4.2 in 10-D and 20-D CEC2020, and 3.1 and 3.7 in 10-D and 20-D CEC2022, respectively. These results highlight the robust performance of jSO and L-SHADE-cnEpSin across various dimensions and benchmarks. The statistical analyses conducted using the Holm multiple comparison test and the Friedman test further

validate the superior efficacy of jSO and L-SHADE-cnEpSin in low-dimensional search spaces.

However, as the dimensionality of the problem increases, the competitiveness of TSA becomes increasingly pronounced. This remarkable performance can be attributed to the unique simulation of tunicate individuals, which effectively captures the dynamic behaviors and interactions of these marine organisms. By leveraging these biological inspirations, TSA demonstrates an improved ability to explore

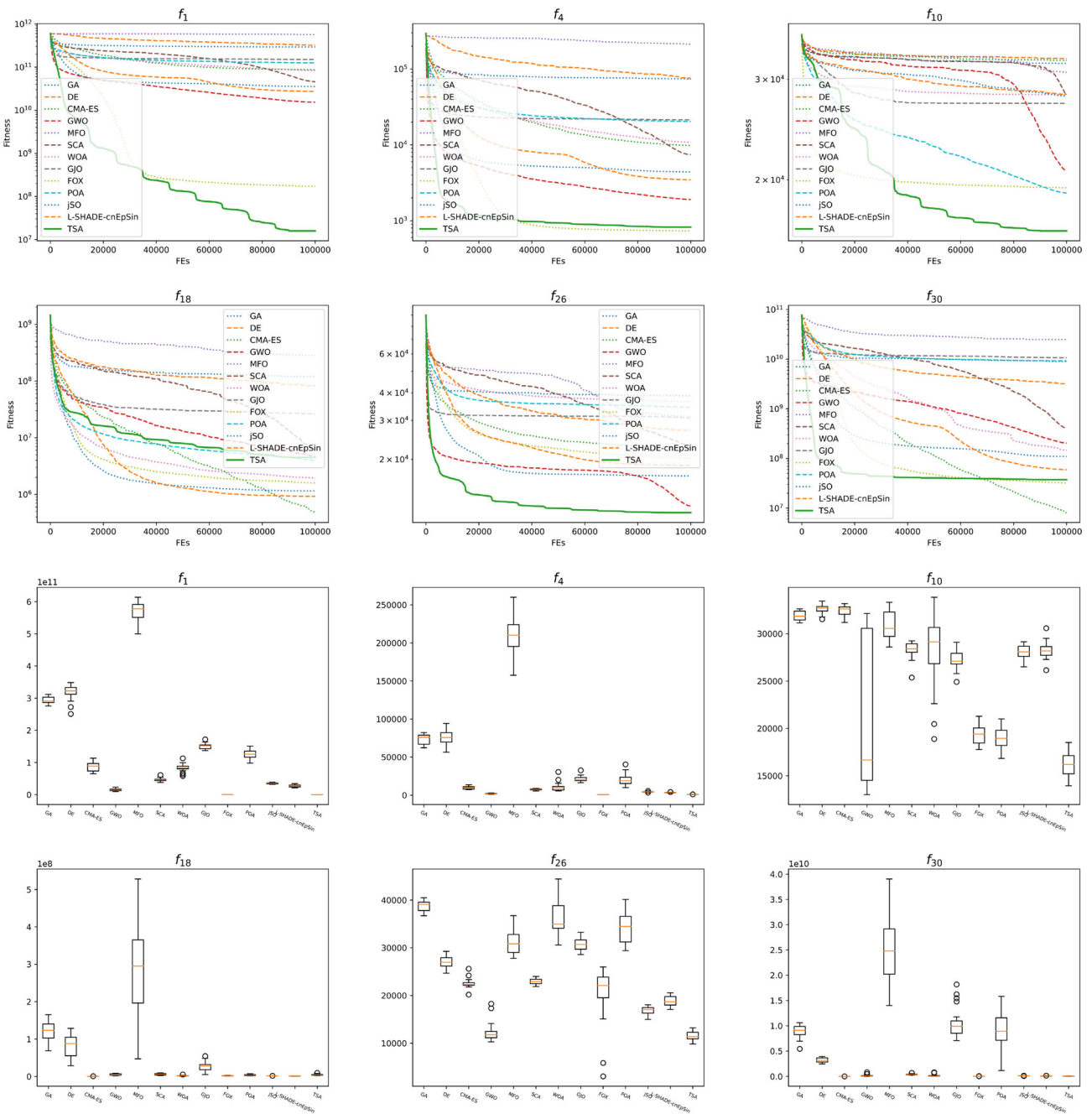


Fig. 12 Convergence curves and boxplots of optimizers in 100-D CEC2017 functions

and exploit the high-dimensional search space, enabling it to adapt and excel in more complex optimization scenarios.

7 Discussion and Further Work

The TSA algorithm has gained significant recognition for its ability to effectively tackle a wide range of optimization problems since its introduction. This success can be

attributed to its simple design, minimal control parameters, and flexible exploration capabilities. However, as a stochastic optimization algorithm, it is not without its limitations and shortcomings, which can hinder its overall efficiency (Figs. 15, 16).

The primary limitation arises from the No-Free-Lunch (NFL) theorem [341], which asserts that no single optimization algorithm can effectively solve all optimization

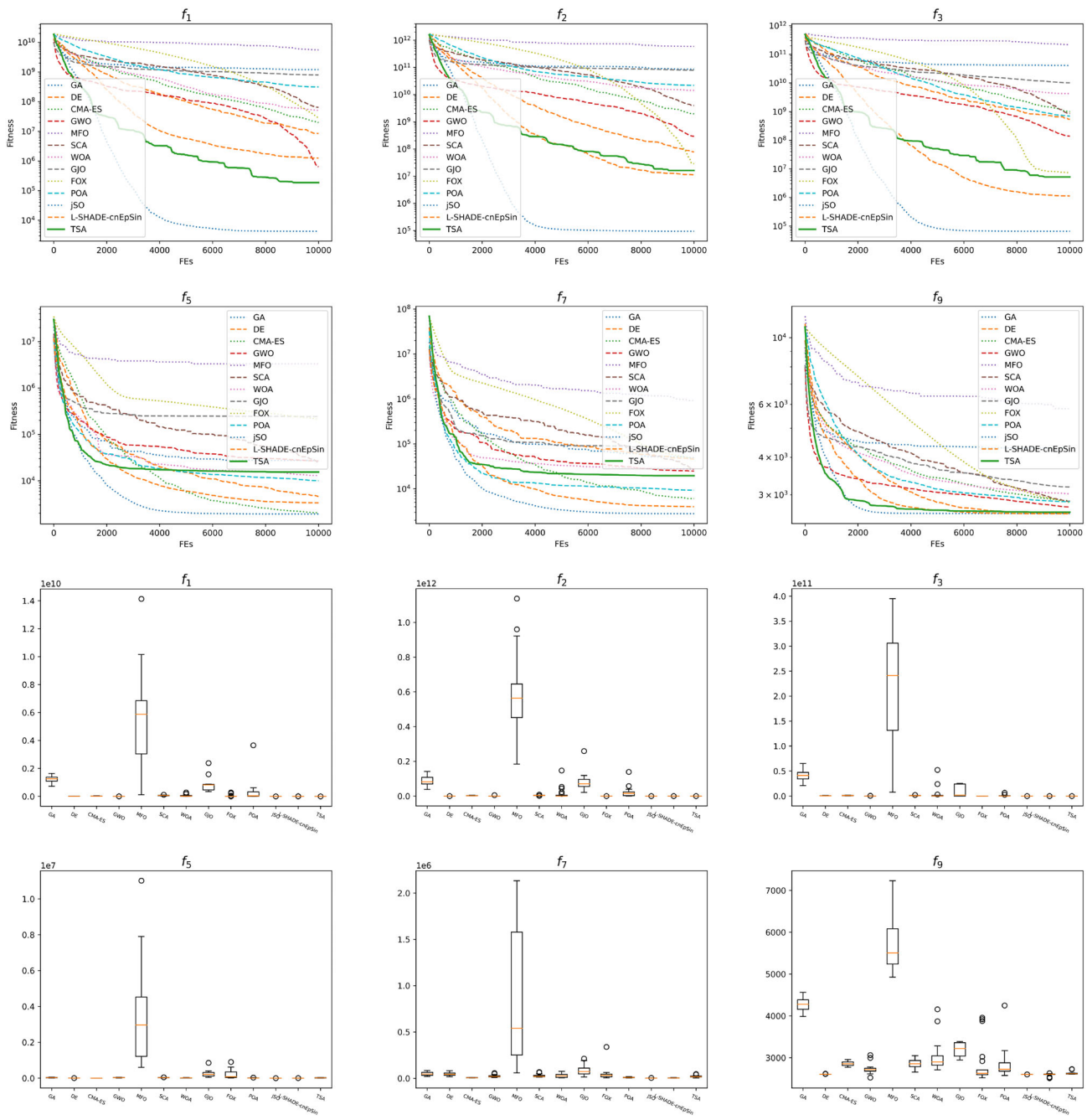


Fig. 13 Convergence curves and boxplots of optimizers in 10-D CEC2020 functions

problems. This implies that TSA may necessitate adaptations when applied to specific real-world scenarios.

Another limitation is that TSA, originally designed for single-objective, unconstrained, and continuous optimization problems, requires adaptations to address a broader spectrum of real-world challenges. Practical optimization problems frequently involve multiple objectives, discrete decision variables, and constraints, necessitating modifications

to the conventional TSA framework. To effectively tackle the diverse optimization challenges encountered in various fields, including multi-objective, discrete, binary, combinatorial, and dynamic scenarios, TSA requires enhancements to broaden its applicability and augment its problem-solving capabilities.

TSA's search process heavily relies on inherited values from its operators, predominantly concentrating on specific

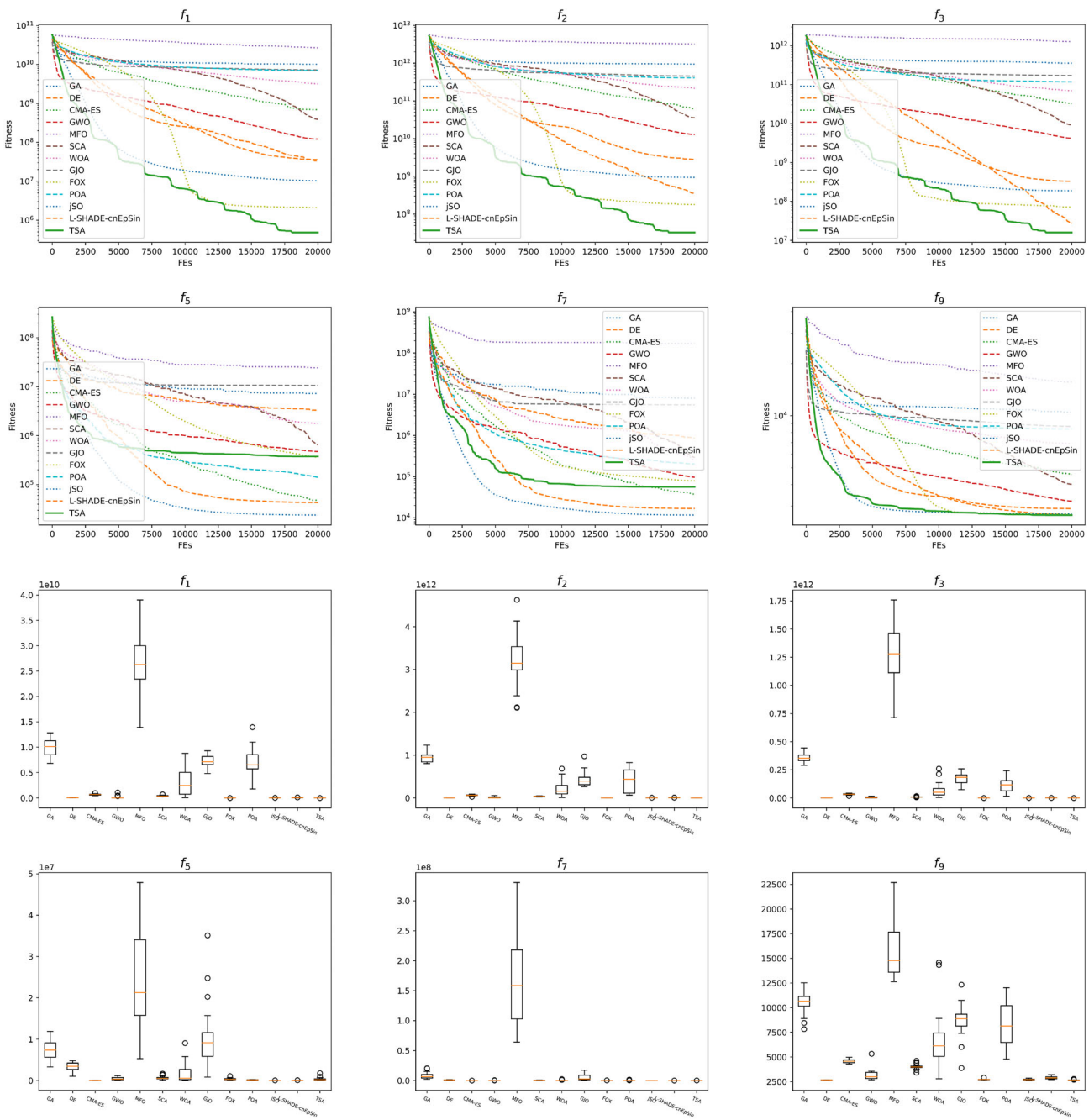


Fig. 14 Convergence curves and boxplots of optimizers in 20-D CEC2020 functions

regions within the search space. This limitation impedes its exploitation capabilities, making it less effective in addressing problems characterized by complex, multi-modal landscapes.

Finally, the performance of the TSA algorithm shows a significant degradation as the dimensionality of the problem increases. This decline may be attributed to the initial population becoming trapped in local optima when dealing with problems of higher complexity.

The inherent limitations of TSA have motivated researchers to refine the base algorithm from various perspectives, broadening its applicability to a diverse range of real-world optimization problems. These efforts have highlighted TSA's substantial research value and its promising potential for practical applications.

While enhanced variants of the TSA algorithm have introduced notable advancements, opportunities for further

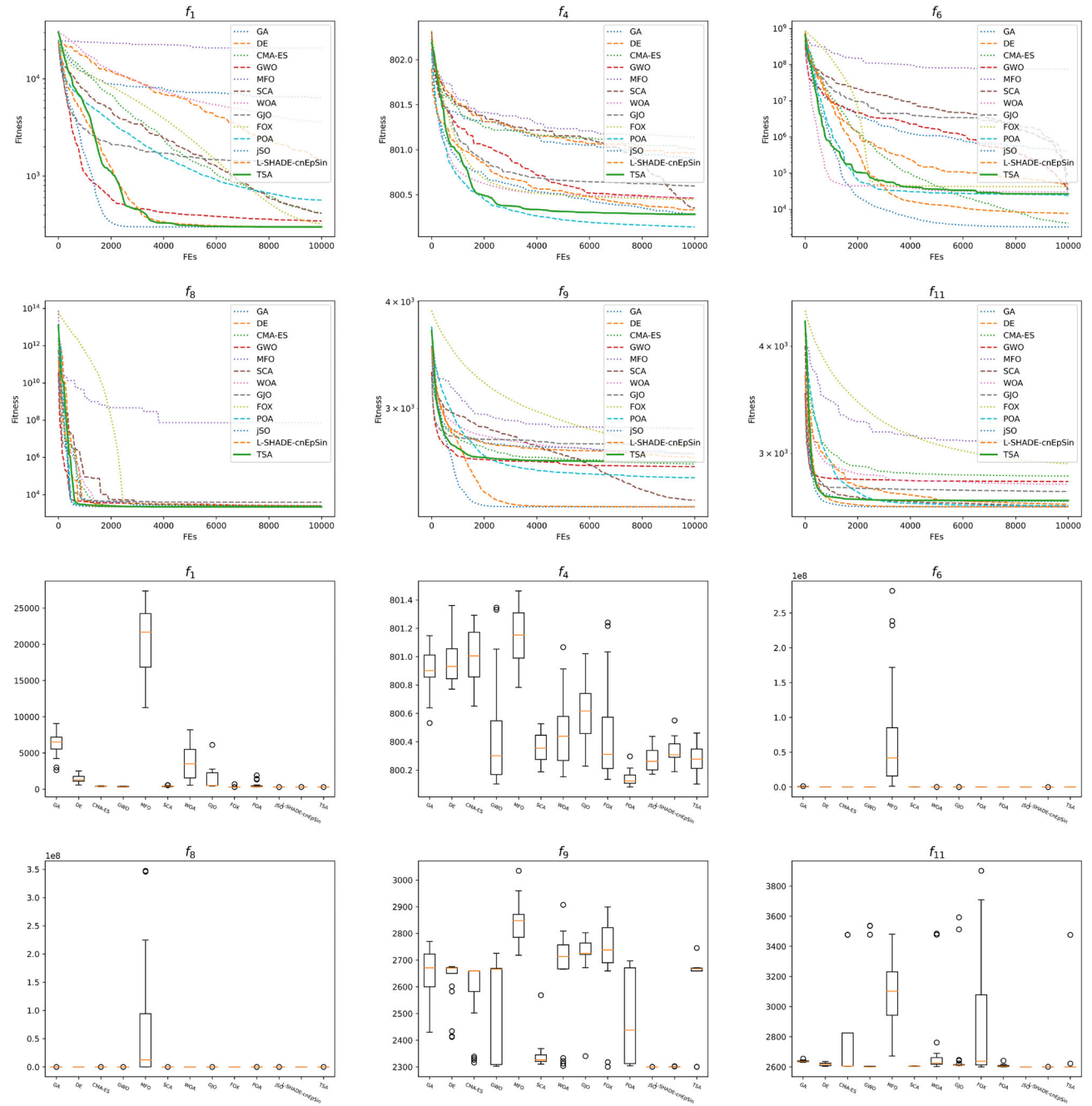


Fig. 15 Convergence curves and boxplots of optimizers in 10-D CEC2022 functions

refinement to improve its effectiveness persist. The following recommendations outline specific areas for future research:

- Despite significant advancements, untapped opportunities exist to integrate valuable concepts into TSA. Investigating novel TSA variants that incorporate techniques such as wavelet mutation and orthogonal learning presents an exciting avenue for future research.

- Future research efforts should focus on developing multi-objective and discrete variants of TSA. Limited research in these areas hampers TSA's application to a wider range of practical problems. Given TSA's inherent strengths in handling discrete problems, expanding into multi-objective and discrete realms holds significant promise.
- The hybridization of TSA with various swarm-based meta-heuristic algorithms has proven effective. Exploring integration with human-based, mathematics-based,

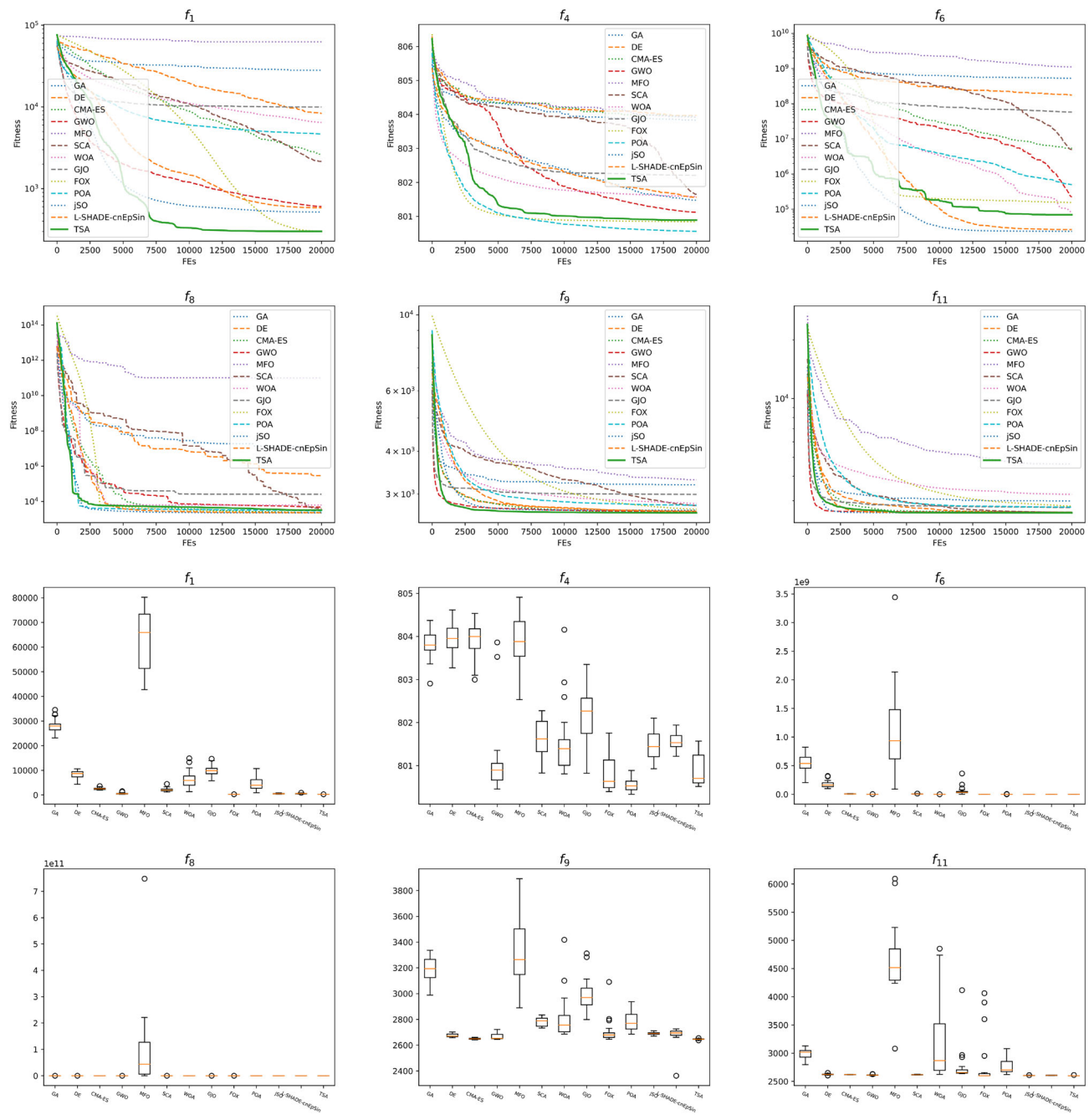


Fig. 16 Convergence curves and boxplots of optimizers in 20-D CEC2022 functions

- and physics-based meta-heuristic algorithms can enhance TSA's computational efficiency and generate high-quality solutions across a broader range of optimization problems.
- Developing a comprehensive framework for selecting suitable TSA versions for specific optimization scenarios poses a formidable challenge. This may involve proposing a typology to classify TSA variants based on application domains, limitations, and applicability criteria, coupled with theoretical, axiomatic, and pragmatic comparisons.
 - Exploring the integration of machine learning techniques to augment TSA's optimization capabilities presents a promising research direction. While previous studies have utilized TSA for parameter optimization or feature selection in machine learning models, exploring the reciprocal relationship remains largely unexplored.
 - Despite notable success in addressing global optimization problems, TSA holds immense potential for expansion into diverse problem domains. Researchers can explore its application to intricate optimization problems across various fields by adapting and tailoring TSA to the specific characteristics of different problem classes.
 - Tackling the challenge of local optima in problems with a large number of variables requires the integration of mechanisms that can slow down convergence speed and exploitation. Adaptive mechanisms, dynamically adjusting convergence speed based on the number of iterations or the quality of the best solution obtained, hold promise in this regard.

8 Conclusion

In summary, the Tunicate Swarm Algorithm (TSA) has emerged as a promising metaheuristic due to its simplicity, adaptability, and effectiveness in addressing various optimization challenges. Its unique structure, inspired by tunicate behaviors and jet propulsion, provides flexibility and

robustness in navigating search spaces. Despite its strengths, TSA shares common limitations with other metaheuristic algorithms, which require further investigation and enhancement to improve performance. This review has explored TSA's foundational principles, analyzed its strengths and weaknesses, and examined proposed modifications aimed at aligning its search mechanisms with real-world optimization problems. Moving forward, there are significant opportunities for further refining TSA by addressing its inherent challenges and expanding its application across more complex and diverse optimization tasks. This will likely contribute to the algorithm's continued growth and effectiveness in the broader field of optimization.

Appendix A

Comparison Experiments in CEC2017

Tables 7, 8, 9, and 10 summarize the detailed experimental results and statistical analysis of TSA against competitor algorithms in CEC2017.

Appendix B

Comparison Experiments in CEC2020

See Tables 11, 12.

Appendix C

Comparison Experiments in CEC2022

See Tables 13, 14

Table 7 Experimental results and statistical analyses on 10-D CEC2017

Function	GA	DE	CMA-ES	GWO	MFO	SCA	WOA	GJO	FOX	POA	jSO	L-SHADE-cmEpSim	TSA
f_1	4.833e+08 +	7.945e+08	1.975e+07	3.274e+06	5.541e+09	1.468e+08	5.127e+07	3.967e+08	1.395e+09	5.673e+08	4.267e+03	1.254e+06 +	1.869e+05
f_3	1.272e+04 +	2.456e+04	7.833e+02	4.188e+02	3.811e+04	4.284e+03	6.314e-03	4.598e+03	2.084e+04	2.484e+03	3.118e+02	4.558e+02 +	3.159e+02
f_4	4.426e+02 +	5.016e+02	4.104e+02	4.103e+02	8.213e+02	4.168e+02	4.355e+02	4.303e+02	5.540e+02	4.333e+02	4.050e+02	4.062e+02 \approx	4.048e+02
f_5	5.369e+02 +	5.600e+02	5.465e+02	5.205e+02	5.745e+02	5.361e+02	5.620e+02	5.320e+02	5.740e+02	5.414e+02	5.151e+02	5.245e+02 +	5.171e+02
f_6	6.091e+02 +	6.303e+02	6.146e+02	6.007e+02	6.510e+02	6.095e+02	6.431e+02	6.058e+02	6.537e+02	6.225e+02	6.000e+02	6.010e+02 +	6.005e+02
f_7	7.849e+02 +	8.593e+02	7.804e+02	7.414e+02	9.989e+02	7.549e+02	8.038e+02	7.484e+02	7.956e+02	7.620e+02	7.249e+02	7.332e+02 +	7.273e+02
f_8	8.361e+02 +	8.684e+02	8.490e+02	8.175e+02	8.997e+02	8.332e+02	8.412e+02	8.295e+02	8.316e+02	8.199e+02	8.144e+02	8.197e+02 \approx	8.195e+02
f_9	1.059e+03 +	2.165e+03	1.084e+03	9.025e+02	3.067e+03	9.334e+02	1.651e+03	9.713e+02	1.802e+03	1.069e+03	9.000e+02	9.003e+02 -	9.006e+02
f_{10}	2.007e+03 +	1.942e+03	2.475e+03	1.834e+03	2.588e+03	2.312e+03	2.477e+03	2.001e+03	2.529e+03	1.685e+03	1.894e+03 +	1.900e+03 +	1.578e+03
f_{11}	1.217e+03 +	1.198e+03	1.128e+03	1.122e+03	2.978e+03	1.165e+03	1.214e+03	1.184e+03	1.833e+03	1.141e+03	1.106e+03	1.112e+03 -	1.117e+03
f_{12}	5.427e+06 +	1.140e+07	2.421e+04	1.059e+06	1.650e+08	1.349e+06	9.700e+05	1.424e+06	1.496e+06	2.586e+05	4.991e+03	1.042e+04 -	5.243e+05
f_{13}	1.537e+04 +	1.991e+03	1.350e+03	1.400e+04	1.759e+06	1.091e+04	9.141e+03	9.547e+03	1.526e+04	2.569e+03	1.347e+03	1.469e+03 -	1.053e+04
f_{14}	8.469e+03	1.439e+03	1.518e+03	4.071e+03	3.322e+04	5.216e+03	1.681e+03	1.536e+03	4.121e+03	9.062e+03	1.444e+03	1.417e+03	1.430e+03 \approx
f_{15}	1.022e+04	1.587e+03	1.430e+03	2.842e+03	5.216e+03	2.526e+03	2.253e+03	1.110e+04	5.027e+04	1.700e+03	1.505e+03	1.521e+03 -	6.110e+03
f_{16}	1.710e+03	1.722e+03	1.765e+03	1.715e+03	2.090e+03	1.703e+03	1.987e+03	1.754e+03	2.127e+03	1.780e+03	1.610e+03	1.659e+03 \approx	1.729e+03
f_{17}	1.756e+03	1.799e+03	1.822e+03	1.764e+03	2.070e+03	1.764e+03	1.848e+03	1.778e+03	1.924e+03	1.752e+03	1.737e+03	1.747e+03 \approx	1.748e+03
f_{18}	2.111e+04	5.135e+03	1.836e+03	2.188e+04	2.587e+06	3.259e+04	1.088e+04	4.326e+04	1.751e+04	5.226e+03	1.836e+03	1.946e+03 -	1.715e+04
f_{19}	8.349e+03 +	1.941e+03	1.909e+03	6.266e+03	1.156e+05	3.298e+03	1.793e+04	2.308e+04	1.313e+04	1.940e+03	1.903e+03	1.905e+03 -	6.778e+03

Table 7 (continued)

Function	GA	DE	CMA-ES	GWO	MFO	SCA	WOA	GJO	FOX	POA	jSO	L-SHADE-cmEpSim	TSA
f_{20}	2.027e+03	2.088e+03	2.186e+03	2.086e+03	2.270e+03	2.074e+03	2.197e+03	2.134e+03	2.234e+03	2.071e+03	2.031e+03	2.043e+03	2.029e+03
f_{21}	—	+	+	+	+	+	+	+	+	+	+	+	2.285e+03
f_{22}	2.329e+03 +	2.322e+03	2.348e+03	2.289e+03	2.359e+03	2.220e+03	2.325e+03	2.319e+03	2.303e+03	2.241e+03	2.213e+03	2.206e+03	—
f_{23}	2.366e+03 +	2.452e+03	2.316e+03	2.309e+03	3.287e+03	2.320e+03	2.375e+03	2.352e+03	2.536e+03	2.349e+03	2.302e+03	2.302e+03	2.306e+03
f_{24}	2.653e+03 +	2.649e+03	2.642e+03	2.625e+03	2.673e+03	2.627e+03	2.680e+03	2.636e+03	2.731e+03	2.639e+03	2.579e+03	2.617e+03	2.621e+03
f_{25}	2.782e+03 +	2.779e+03	2.773e+03	2.762e+03	2.800e+03	2.698e+03	2.803e+03	2.760e+03	2.846e+03	2.654e+03	2.673e+03	2.603e+03	2.731e+03
f_{26}	2.976e+03 +	2.990e+03	2.928e+03	2.941e+03	3.248e+03	2.937e+03	2.987e+03	2.940e+03	2.985e+03	2.931e+03	2.913e+03	2.916e+03	2.903e+03
f_{27}	3.108e+03 +	3.096e+03	3.095e+03	3.096e+03	3.126e+03	3.113e+03	3.184e+03	3.099e+03	3.203e+03	3.102e+03	3.095e+03	3.096e+03	3.101e+03
f_{28}	3.319e+03	3.222e+03	3.306e+03	3.357e+03	3.542e+03	3.207e+03	3.207e+03	3.399e+03	3.388e+03	3.506e+03	3.262e+03	3.190e+03	3.169e+03
f_{29}	3.250e+03 +	3.235e+03	3.228e+03	3.212e+03	3.377e+03	3.220e+03	3.409e+03	3.213e+03	3.506e+03	3.212e+03	3.181e+03	3.198e+03	3.227e+03
f_{30}	2.062e+06 +	6.060e+05	6.168e+04	7.575e+05	4.049e+06	5.025e+05	9.965e+05	1.590e+06	9.067e+06	9.287e+04	8.159e+03	1.534e+04	4.087e+05
+/-/-	22/6/1	20/5/4	19/6/4	11/18/0	28/1/0	19/9/1	23/5/1	20/9/0	27/2/0	13/10/6	2/9/18	8/8/13	—
Avg. ranks	8.7	8.4	6.2	5.5	12.5	6.4	9.7	7.7	11.4	5.9	1.4	2.8	4.4

f_1 : Unimodal function; $f_3 - f_9$: Multimodal functions; $f_{10} - f_{19}$: Hybrid functions; $f_{20} - f_{30}$: Composite functions

Table 8 Experimental results and statistical analyses on 30-D CEC2017

Function	GA	DE	CMA-ES	GWO	MFO	SCA	WOA	GJO	FOX	POA	jSO	L-SHADE-crEpsIn	TSA
f_1	2.521e+10	3.929e+10	2.992e+09	6.648e+08	8.301e+10	2.470e+09	7.704e+09	1.099e+10	8.460e+06	1.383e+10	1.641e+08	2.654e+08	1.244e+06
f_3	+ 1.324e+05	+ 2.444e+05	+ 9.323e+04	2.088e+04 ≈	2.771e+05	8.000e+04	9.846e+04	7.578e+04	5.930e+04	4.488e+04	2.215e+04	2.950e+04	1.962e+04
f_4	4.128e+03	3.740e+03	7.214e+02	5.485e+02	1.643e+04	8.832e+02	1.287e+03	1.041e+03	5.133e+02	1.678e+03	5.783e+02	5.717e+02	5.165e+02
f_5	8.243e+02	8.888e+02	7.663e+02	6.451e+02 ≈	1.010e+03	7.086e+02	8.324e+02	7.539e+02	7.744e+02	7.650e+02	6.293e+02	6.628e+02	5.849e+02
f_6	6.531e+02	6.762e+02	6.398e+02	6.043e+02	7.027e+02	6.293e+02	6.697e+02	6.389e+02	6.745e+02	6.607e+02	6.017e+02	6.106e+02	6.076e+02
f_7	1.617e+03	2.479e+03	1.151e+03	8.921e+02 ≈	3.074e+03	1.000e+03	1.337e+03	1.046e+03	1.324e+03	1.232e+03	8.494e+02	8.809e+02	8.387e+02
f_8	1.113e+03	1.188e+03	1.069e+03	8.921e+02	1.300e+03	9.922e+02	1.043e+03	9.922e+02	9.833e+02	9.974e+02	9.089e+02	9.444e+02	8.998e+02
f_9	9.351e+03	1.677e+04	4.923e+03	1.343e+03 —	2.720e+04	2.899e+03	9.294e+03	4.570e+03	8.436e+03	5.274e+03	9.184e+02	1.179e+03	1.801e+03
f_{10}	8.306e+03	8.366e+03	8.577e+03	5.616e+03 ≈	8.030e+03	7.696e+03	6.910e+03	6.747e+03	5.841e+03	5.045e+03	7.100e+03	7.055e+03	4.724e+03
f_{11}	4.215e+03	3.205e+03	1.359e+03	1.300e+03 ≈	2.621e+04	1.973e+03	4.015e+03	4.040e+03	1.368e+03	2.260e+03	1.242e+03	1.251e+03	1.315e+03
f_{12}	2.176e+09	1.711e+09	2.450e+07	2.900e+07	6.928e+09	1.290e+08	5.142e+07	1.218e+09	1.236e+07	6.884e+08	3.313e+06	3.896e+06	1.567e+07
f_{13}	3.057e+08	1.034e+08	7.090e+03	1.764e+05 ≈	3.926e+09	1.694e+07	3.879e+06	4.791e+08	4.724e+05	1.621e+07	2.323e+04	2.615e+04	1.549e+05
f_{14}	8.732e+05	1.289e+04	1.506e+03	7.240e+04 ≈	+ 1.251e+05	+ 1.110e+09	3.917e+05	3.600e+04	1.669e+07	8.667e+04	5.726e+03	1.511e+03	1.551e+03
f_{15}	1.194e+06	5.313e+05	1.835e+03	2.024e+03 —	+ —	+ —	+ —	+ —	+ —	+ —	+ —	+ —	5.228e+04
f_{16}	3.730e+03	3.870e+03	3.517e+03	2.565e+03	4.820e+03	3.080e+03	3.803e+03	3.549e+03	3.608e+03	2.998e+03	2.689e+03	2.994e+03	2.584e+03
f_{17}	2.635e+03	2.683e+03	2.619e+03	2.024e+03	3.490e+03	2.092e+03	2.934e+03	2.491e+03	2.813e+03	2.149e+03	1.889e+03	2.042e+03	2.164e+03
f_{18}	9.311e+06	3.241e+06	4.196e+03	1.097e+06 ≈	3.781e+07	7.862e+05	1.373e+06	3.424e+06	6.584e+05	1.710e+05	2.962e+04	3.680e+04	1.299e+06
f_{19}	1.103e+07	8.253e+06	2.155e+03	5.247e+05 —	1.115e+09	1.504e+06	6.760e+06	1.317e+07	1.309e+06	1.060e+06	4.436e+03	6.164e+03	1.049e+04

Table 8 (continued)

Function	GA	DE	CMA-ES	GWO	MFO	SCA	WOA	GJO	FOX	POA	jSO	L-SHADE- cnePSim	TSA
f_{20}	2.521e+03	2.586e+03	2.893e+03	2.428e+03	3.097e+03	2.471e+03	3.007e+03	2.752e+03	3.030e+03	2.368e+03	2.345e+03	2.484e+03 \approx	2.410e+03
f_{21}	2.599e+03	2.656e+03	2.559e+03	2.385e+03	2.750e+03	2.500e+03	2.586e+03	2.504e+03	2.624e+03	2.535e+03	2.413e+03	+ \approx	2.453e+03 +
f_{22}	5.149e+03	9.848e+03	9.728e+03	4.614e+03	9.361e+03	2.747e+03	7.577e+03	3.619e+03	7.283e+03	3.882e+03	2.340e+03	2.350e+03 -	3.985e+03
f_{23}	3.037e+03	2.988e+03	2.918e+03	2.750e+03	3.072e+03	2.926e+03	3.273e+03	2.899e+03	3.407e+03	3.024e+03	2.754e+03	+ \approx	2.818e+03 +
f_{24}	3.195e+03	3.120e+03	3.077e+03	2.956e+03	3.185e+03	3.085e+03	3.381e+03	3.052e+03	3.623e+03	3.189e+03	2.889e+03	2.975e+03 +	2.926e+03
f_{25}	4.456e+03	6.369e+03	3.144e+03	2.942e+03	1.316e+04	3.052e+03	3.151e+03	3.175e+03	2.942e+03	3.229e+03	2.980e+03	+ \approx	-
f_{26}	7.920e+03	7.569e+03	6.306e+03	4.725e+03	9.238e+03	6.260e+03	8.554e+03	5.875e+03	8.905e+03	7.073e+03	4.631e+03	5.243e+03 +	4.841e+03
f_{27}	3.501e+03	3.287e+03	3.243e+03	3.233e+03	3.478e+03	3.412e+03	3.717e+03	3.380e+03	3.923e+03	3.336e+03	3.231e+03	3.267e+03 +	3.236e+03
f_{28}	4.726e+03	4.743e+03	3.438e+03	3.328e+03	7.575e+03	3.527e+03	3.742e+03	3.795e+03	3.266e+03	3.922e+03	3.352e+03	3.354e+03 +	3.300e+03
f_{29}	4.982e+03	4.232e+03	4.445e+03	3.784e+03	6.194e+03	4.188e+03	5.551e+03	4.501e+03	5.183e+03	4.344e+03	3.805e+03	4.015e+03 \approx	3.990e+03
f_{30}	2.493e+07	1.136e+07	9.981e+04	4.796e+06	6.989e+08	7.939e+06	1.185e+06	1.381e+08	4.643e+06	8.640e+06	3.623e+05	\approx \approx	4.196e+05 \approx
+/-/-	29/0/0	28/0/1	22/1/6	8/16/5	29/0/0	25/2/2	26/3/0	27/2/0	24/2/3	24/3/2	6/9/14	15/4/10	-
Avg. ranks	10.5	10.3	6.2	3.6	12.5	6.6	9.4	8.1	7.6	7.0	2.3	3.7	3.1

Table 9 Experimental results and statistical analyses on 50-D CEC2017

Function	GA	DE	CMA-ES	GWO	MFO	SCA	WOA	GIO	FOX	POA	jSO	L-SHADE- cnfpSim	TSA
f_1	8.719e+10	1.042e+11	1.026e+10	2.275e+09	1.923e+11	9.620e+09	2.132e+10	3.628e+10	3.344e+07	4.500e+10	3.776e+09	3.212e+09 +	4.463e+06
f_3	+ 2.736e+05	+ 4.515e+05	+ 2.623e+05	5.640e+04	+ 4.544e+05	+ 1.811e+05	+ 1.276e+05	+ 1.792e+05	+ 1.307e+05	9.947e+04	7.599e+04	9.408e+04 ≈	8.705e+04
f_4	1.666e+04	1.516e+04	1.755e+03	7.227e+02	5.082e+04	2.113e+03	3.748e+03	5.057e+03	5.691e+02	6.302e+03	1.068e+03	1.052e+03 +	6.107e+02
f_5	1.177e+03	1.270e+03	1.011e+03	7.120e+02	1.566e+03	9.069e+02	1.016e+03	1.007e+03	8.715e+02	9.250e+02	7.665e+02	8.336e+02 +	7.083e+02
f_6	6.778e+02	6.960e+02	6.532e+02	6.097e+02	7.288e+02	6.436e+02	6.810e+02	6.688e+02	6.784e+02	6.678e+02	6.067e+02	6.208e+02 +	6.127e+02
f_7	3.021e+03	4.836e+03	1.508e+03	1.051e+03	5.919e+03	1.307e+03	1.801e+03	1.445e+03	1.866e+03	1.760e+03	1.028e+03	1.098e+03 +	9.872e+02
f_8	1.479e+03	1.580e+03	1.310e+03	1.012e+03	1.845e+03	1.238e+03	1.316e+03	1.336e+03	1.189e+03	1.239e+03	1.071e+03	1.139e+03 +	9.835e+02
f_9	3.351e+04	4.886e+04	1.347e+04	5.203e+03	7.253e+04	1.335e+04	1.964e+04	2.231e+04	3.076e+04	1.774e+04	1.752e+03	4.844e+03 ≈	5.679e+03
f_{10}	1.467e+04	1.494e+04	1.506e+04	1.148e+04	1.404e+04	1.301e+04	1.240e+04	1.223e+04	8.908e+03	8.810e+03	1.247e+04	1.236e+04 +	7.363e+03
f_{11}	2.033e+04	2.081e+04	1.653e+03	1.683e+03	6.328e+04	5.700e+03	4.363e+03	1.150e+04	1.522e+03	6.304e+03	1.752e+03	1.814e+03 +	1.586e+03
f_{12}	1.897e+10	1.459e+10	2.623e+08	1.527e+08	5.021e+10	1.037e+09	1.195e+09	1.048e+10	3.330e+07	9.715e+09	1.211e+08	1.106e+08 +	6.799e+07
f_{13}	4.834e+09	2.024e+09	2.074e+05	3.797e+07	+ 2.222e+10	+ 1.394e+08	+ 3.448e+07	+ 1.930e+09	+ 2.331e+06	+ 7.349e+08	7.926e+04	8.708e+04 –	2.154e+05
f_{14}	3.997e+06	1.464e+06	1.617e+03	5.702e+05	2.876e+07	5.897e+05	1.280e+06	3.029e+06	1.114e+05	2.943e+05	9.536e+06	1.372e+04 –	2.722e+05
f_{15}	5.744e+08	3.944e+07	3.486e+03	9.432e+05	+ 8.529e+09	+ 1.152e+07	+ 2.623e+06	+ 3.157e+08	+ 6.522e+05	+ 2.943e+05	+ 9.610e+03	1.023e+04 –	4.449e+04
f_{16}	5.962e+03	6.195e+03	5.362e+03	3.535e+03	7.627e+03	4.211e+03	5.642e+03	4.541e+03	4.742e+03	4.252e+03	3.142e+03	3.813e+03 +	3.417e+03
f_{17}	4.725e+03	5.066e+03	4.144e+03	3.110e+03	1.119e+05	3.302e+03	4.894e+03	4.151e+03	3.831e+03	3.394e+03	2.878e+03	3.288e+03 ≈	3.317e+03
f_{18}	3.973e+07	2.278e+07	6.333e+04	3.482e+06	1.669e+08	4.846e+06	4.995e+06	2.049e+07	1.764e+06	1.815e+06	2.972e+05	2.781e+05 –	2.977e+06
f_{19}	2.434e+08	5.416e+07	5.747e+03	1.900e+06	3.470e+09	5.749e+06	1.328e+05	4.330e+08	3.102e+06	1.400e+07	5.632e+04	5.346e+04 ≈	5.167e+04

Table 9 (continued)

Function	GA	DE	CMA-ES	GWO	MFO	SCA	WOA	GIO	FOX	POA	jSO	L-SHADE- cnfpSim	TSA
f_{20}	4.062e+03	4.356e+03	4.179e+03	3.290e+03	4.506e+03	3.346e+03	3.962e+03	3.737e+03	3.896e+03	2.982e+03	3.100e+03	3.466e+03 +	3.185e+03
f_{21}	+ 2.974e+03	+ 3.071e+03	+ 2.811e+03	2.480e+03	+ 3.280e+03	≈ 2.715e+03	2.978e+03	2.801e+03	3.044e+03	- 2.768e+03	≈ 2.547e+03	2.624e+03 +	2.486e+03
f_{22}	1.651e+04	1.675e+04	1.664e+04	1.111e+04	1.585e+04	1.208e+04	1.415e+04	1.186e+04	1.139e+04	1.104e+04	6.574e+03	1.105e+04 +	9.439e+03
f_{23}	3.612e+03	3.492e+03	3.317e+03	2.917e+03	3.727e+03	3.319e+03	4.075e+03	3.327e+03	4.245e+03	3.526e+03	2.961e+03	3.114e+03 +	2.945e+03
f_{24}	3.795e+03	3.557e+03	3.479e+03	3.131e+03	3.659e+03	3.489e+03	4.140e+03	3.556e+03	4.369e+03	3.643e+03	3.064e+03	3.231e+03 +	3.093e+03
f_{25}	1.419e+04	1.941e+04	4.071e+03	3.243e+03	4.579e+04	4.098e+03	5.188e+03	5.803e+03	3.104e+03	6.217e+03	3.582e+03	3.497e+03 +	3.102e+03
f_{26}	1.342e+04	1.175e+04	9.383e+03	6.075e+03	1.414e+04	9.262e+03	1.504e+04	1.008e+04	1.282e+04	1.276e+04	6.263e+03	8.012e+03 +	5.903e+03
f_{27}	4.770e+03	3.663e+03	3.518e+03	3.480e+03	4.369e+03	4.215e+03	5.893e+03	4.435e+03	5.591e+03	4.077e+03	3.524e+03	3.619e+03 +	3.490e+03
f_{28}	1.019e+04	8.775e+03	4.500e+03	3.779e+03	1.140e+04	4.730e+03	5.529e+03	5.973e+03	3.347e+03	6.507e+03	4.273e+03	4.117e+03 +	3.362e+03
f_{29}	8.460e+03	6.926e+03	5.801e+03	4.319e+03	1.893e+04	5.421e+03	1.007e+04	7.303e+03	6.406e+03	6.528e+03	4.505e+03	5.076e+03 +	4.629e+03
f_{30}	9.668e+08	3.824e+08	8.927e+06	8.350e+07	4.001e+09	1.384e+08	3.419e+07	7.231e+08	5.560e+07	1.733e+08	4.603e+07	2.727e+07 ≈	2.433e+07
+/-/-	29/0/0	29/0/0	22/2/5	13/12/4	29/0/0	26/3/0	29/0/0	22/3/4	25/3/1	13/5/11	20/5/4	-	-
Avg. ranks	11.0	10.9	6.0	3.5	12.4	6.7	8.9	8.7	7.3	3.0	3.8	2.4	

Table 10 Experimental results and statistical analyses on 100-D CEC2017

Function	GA	DE	CMA-ES	GWO	MFO	SCA	WOA	GIO	FOX	POA	jSO	L-SHADE- cnfpSim	TSA
f_1	2.936e+11	3.192e+11	8.679e+10	1.533e+10	5.690e+11	4.605e+10	8.344e+10	1.506e+11	1.714e+08	1.260e+11	3.542e+10	2.738e+10 +	1.591e+07
f_3	6.554e+05	1.123e+06	6.708e+05	2.226e+05	1.076e+06	4.473e+05	3.098e+05	3.429e+05	4.093e+05	2.382e+05	2.304e+05	2.866e+05 -	3.783e+05
f_4	7.356e+04	7.553e+04	9.776e+03	1.904e+03	2.119e+05	7.437e+03	1.075e+04	2.141e+04	7.334e+02	2.035e+04	4.395e+03	3.466e+03 +	8.233e+02
f_5	2.223e+03	2.320e+03	1.695e+03	1.109e+03	2.958e+03	1.559e+03	1.603e+03	1.769e+03	1.412e+03	1.556e+03	1.231e+03	1.390e+03 +	9.779e+02
f_6	7.058e+02	7.203e+02	6.718e+02	6.241e+02	7.580e+02	6.607e+02	6.843e+02	6.912e+02	6.800e+02	6.774e+02	6.194e+02	6.404e+02 +	6.252e+02
f_7	7.821e+03	1.140e+04	2.731e+03	1.623e+03	1.303e+04	2.407e+03	3.487e+03	3.088e+03	3.628e+03	3.370e+03	1.715e+03	1.928e+03 +	1.514e+03
f_8	2.578e+03	2.658e+03	2.017e+03	1.290e+03	3.328e+03	1.868e+03	2.100e+03	2.135e+03	1.911e+03	2.005e+03	1.536e+03	1.739e+03 +	1.250e+03
f_9	1.095e+05	1.360e+05	4.593e+04	2.872e+04	2.091e+05	4.737e+04	4.468e+04	6.063e+04	6.864e+04	3.570e+04	1.088e+04	2.200e+04 ≈	2.002e+04
f_{10}	3.193e+04	3.262e+04	3.237e+04	2.077e+04	3.086e+04	2.827e+04	2.819e+04	2.722e+04	1.937e+04	1.897e+04	-	-	1.628e+04
f_{11}	2.527e+05	4.290e+05	1.372e+04	1.274e+04	5.130e+05	1.022e+05	5.497e+04	1.510e+05	3.586e+03	5.426e+04	3.265e+04	3.343e+04 +	4.195e+03
f_{12}	1.047e+11	8.568e+10	3.922e+09	2.195e+09	2.059e+11	6.751e+09	1.363e+10	5.576e+10	2.796e+08	5.393e+10	3.374e+09	2.295e+09 +	4.942e+08
f_{13}	1.789e+10	9.405e+09	9.149e+06	1.387e+08	4.633e+10	3.702e+08	6.800e+08	1.121e+10	6.738e+06	1.090e+10	3.483e+07	2.010e+07 +	1.354e+05
f_{14}	6.691e+07	2.237e+07	2.680e+03	4.301e+06	1.757e+08	5.197e+06	2.968e+06	2.517e+07	1.073e+06	3.571e+06	1.615e+06	8.339e+05 +	2.537e+06
f_{15}	4.928e+09	1.347e+09	4.353e+04	3.536e+07	1.917e+10	5.731e+07	2.892e+06	3.102e+09	2.405e+06	2.774e+09	4.721e+04	6.461e+04 -	1.058e+05
f_{16}	1.424e+04	1.327e+04	1.114e+04	5.877e+03	1.815e+04	8.805e+03	1.331e+04	1.155e+04	7.555e+03	1.003e+04	7.152e+03	8.391e+03 +	6.097e+03
f_{17}	2.235e+04	1.248e+04	7.745e+03	4.365e+03	2.879e+06	6.126e+03	1.450e+04	2.478e+04	6.494e+03	1.401e+04	4.606e+03	5.426e+03 ≈	5.334e+03
f_{18}	1.201e+08	8.331e+07	4.769e+05	4.713e+06	2.868e+08	6.062e+06	1.954e+06	2.659e+07	1.587e+06	4.009e+06	1.152e+06	9.255e+05 -	4.495e+06
f_{19}	4.874e+09	1.919e+09	3.609e+05	3.831e+07	1.795e+10	7.011e+07	1.562e+07	2.868e+09	5.356e+06	1.990e+09	5.578e+05	4.706e+05 -	2.581e+06

Table 10 (continued)

Function	GA	DE	CMA-ES	GWO	MFO	SCA	WOA	GIO	FOX	POA	jSO	L-SHADE- cnfpSim	TSA
f_{20}	7.523e+03	7.967e+03	7.620e+03	5.717e+03	8.371e+03	6.030e+03	6.858e+03	6.777e+03	6.241e+03	5.057e+03	5.904e+03	6.565e+03 +	5.489e+03
f_{21}	4.159e+03	4.268e+03	3.649e+03	2.823e+03	4.824e+03	3.430e+03	4.073e+03	3.753e+03	4.344e+03	3.702e+03	2.933e+03	3.222e+03 +	2.828e+03
f_{22}	3.433e+04	3.443e+04	3.415e+04	2.199e+04	3.276e+04	3.079e+04	3.131e+04	2.739e+04	2.194e+04	2.400e+04	3.071e+04	3.095e+04 +	1.853e+04
f_{23}	5.033e+03	4.501e+03	4.348e+03	3.332e+03	4.781e+03	4.343e+03	5.777e+03	4.831e+03	5.908e+03	4.578e+03	3.313e+03	3.815e+03 +	3.315e+03
f_{24}	6.942e+03	5.334e+03	5.142e+03	3.932e+03	5.701e+03	5.414e+03	8.080e+03	6.539e+03	6.598e+03	5.809e+03	4.178e+03	4.482e+03 +	3.784e+03
f_{25}	4.447e+04	6.738e+04	8.675e+03	4.693e+03	1.284e+05	7.234e+03	8.756e+03	1.196e+04	3.381e+03	1.250e+04	6.003e+03	5.490e+03 +	3.521e+03
f_{26}	3.875e+04	2.696e+04	2.252e+04	1.231e+04	3.131e+04	2.294e+04	3.649e+04	3.078e+04	2.024e+04	3.444e+04	1.683e+04	1.878e+04 +	1.148e+04
f_{27}	7.794e+03	4.594e+03	3.812e+03	3.755e+03	5.591e+03	5.193e+03	9.169e+03	7.063e+03	5.628e+03	5.482e+03	4.140e+03	4.294e+03 +	3.751e+03
f_{28}	3.425e+04	2.393e+04	1.128e+04	5.327e+03	2.741e+04	9.690e+03	9.986e+03	1.666e+04	3.469e+03	1.528e+04	8.998e+03	7.965e+03 +	3.597e+03
f_{29}	2.801e+04	2.318e+04	1.083e+04	6.918e+03	1.656e+06	1.006e+04	2.042e+04	2.291e+04	1.037e+04	1.425e+04	8.436e+03	1.005e+04 +	7.800e+03
f_{30}	8.960e+09	3.215e+09	8.111e+06	2.036e+08	2.472e+10	4.102e+08	1.467e+08	1.065e+10	3.187e+07	9.219e+09	1.097e+08	5.931e+07 +	3.748e+07
+/-/-	29/0/0	29/0/0	23/1/5	17/8/4	29/0/0	281/0	261/2	281/0	21/2/6	25/2/2	21/1/7	23/2/4	-
Avg. ranks	11.4	10.6	6.1	3.3	12.2	6.8	8.4	9.4	5.3	7.5	3.6	4.2	2.3

Table 11 Experimental results and statistical analyses on 10-D CEC2020. f_1 : Unimodal function; $f_2 - f_4$: Multimodal functions; $f_5 - f_7$: Hybrid functions; $f_8 - f_{10}$: Composite functions

Function	GA	DE	CMA-ES	GWO	MFO	SCA	WOA	GIO	FOX	POA	jSO	L-SHADE-cnEpSin	TSA
f_1	Mean	1.208e+09	8.404e+06	1.975e+07	6.376e+05	5.588e+09	6.523e+07	5.127e+07	7.957e+08	2.808e+07	3.165e+08	4.267e+03	1.254e+06 \approx
	Std	2.262e+08	2.553e+06	7.320e+06	9.911e+05	3.348e+09	2.168e+07	7.367e+07	4.628e+08	7.576e+07	7.891e+08	1.056e+04	2.573e+06
f_2	Mean	8.660e+10	7.840e+07	1.956e+09	2.943e+08	5.905e+11	3.964e+09	1.436e+10	7.966e+10	2.873e+07	2.184e+10	9.458e+04	1.144e+07 $-$
	Std	2.732e+10	2.957e+07	8.726e+08	1.223e+09	2.279e+11	1.701e+09	3.385e+10	4.791e+10	1.352e+07	3.081e+10	1.831e+05	3.623e+07
f_3	Mean	4.042e+10	5.393e+08	9.874e+08	1.389e+08	2.138e+11	8.718e+08	4.250e+09	1.019e+10	7.224e+06	6.944e+08	6.610e+04	1.128e+06 $-$
	Std	1.034e+10	1.635e+08	3.854e+08	1.463e+08	1.175e+11	4.094e+08	1.219e+10	1.132e+10	2.375e+06	1.453e+09	6.283e+04	1.984e+06
f_4	Mean	1.935e+03	1.904e+03	1.905e+03	1.903e+03	2.423e+04	1.904e+03	2.119e+03	1.914e+03	1.923e+03	1.903e+03	1.902e+03	1.902e+03 \approx
	Std	2.576e+01	5.716e-01	5.841e-01	5.881e-01	3.732e+04	7.233e-01	2.214e+02	2.455e+01	8.370e+00	3.139e+00	3.362e-01	6.203e-01
f_5	Mean	2.700e+04	4.574e+03	2.036e+03	2.676e+04	3.329e+06	2.522e+04	1.300e+04	2.435e+05	2.134e+05	1.007e+04	1.924e+03	3.362e+03 $-$
	Std	1.432e+04	6.721e+02	1.041e+02	1.157e+04	2.617e+06	9.803e+03	6.187e+03	7.171e+05	2.444e+05	7.839e+03	2.089e+02	1.290e+03
f_6	Mean	6.152e+03	2.824e+03	1.905e+03	3.412e+03	1.477e+05	2.778e+03	9.662e+03	4.356e+03	1.177e+04	2.232e+03	1.648e+03	1.842e+03 \approx
	Std	3.662e+03	4.703e+02	1.344e+02	1.540e+03	1.702e+05	4.431e+02	7.365e+03	1.375e+03	7.709e+03	5.397e+02	3.948e+01	1.791e+02
f_7	Mean	4.936e+04	4.542e+04	6.078e+03	2.485e+04	9.251e+05	2.741e+04	2.770e+04	8.601e+04	4.748e+04	9.296e+03	2.805e+03	4.022e+03 $-$
	Std	1.738e+04	1.569e+04	1.366e+03	1.398e+04	7.532e+05	1.531e+04	1.940e+04	5.688e+04	6.875e+04	3.829e+03	5.857e+02	1.248e+03
f_8	Mean	2.320e+03	2.305e+03	2.311e+03	2.305e+03	2.346e+03	2.310e+03	2.327e+03	2.308e+03	2.406e+03	2.301e+03	2.303e+03 \approx	
	Std	2.044e+00	8.960e-01	7.834e-01	3.601e+00	8.177e+00	1.015e+00	1.187e+01	4.143e+00	5.065e+01	8.663e+00	8.332e-01	1.527e+00
f_9	Mean	4.270e+03	2.607e+03	2.860e+03	2.734e+03	5.802e+03	2.857e+03	3.025e+03	3.185e+03	2.829e+03	2.846e+03	2.601e+03	2.597e+03
	Std	1.603e+02	4.355e+00	5.111e+01	1.146e+02	7.588e+02	1.039e+02	3.668e+02	1.690e+02	4.744e+02	3.540e+02	1.162e+00	3.228e+01
f_{10}	Mean	3.100e+03	2.994e+03	2.996e+03	3.413e+03	3.017e+03	3.144e+03	3.024e+03	3.070e+03	3.021e+03	2.987e+03	2.996e+03 \approx	
	Std	2.177e+01	5.577e+00	5.324e+00	1.045e+01	2.049e+02	1.173e+01	8.283e+01	1.769e+01	6.141e+01	3.859e+01	1.118e+01	1.227e+01
+/-	Avg. ranks	10/0/0	6/2/2	6/1/3	7/3/0	10/0/0	9/1/0	8/2/0	10/0/0	9/1/0	6/3/1	0/2/8	0/5/5
	Avg. ranks	11.1	5.2	6.0	5.2	12.9	7.5	9.7	10.1	8.7	6.7	1.1	2.7

Table 12 Experimental results and statistical analyses on 20-D CEC2020

Function	GA	DE	CMA-ES	GWO	MFO	SCA	WOA	GJO	FOX	POA	jSO	L-SHADE- cnEpSin	TSA
f_1	Mean	1.014e+10	3.281e+07	6.610e+08	1.209e+08	2.684e+08	3.909e+08	3.184e+09	7.232e+09	2.095e+06	7.009e+09	1.031e+07	3.587e+07 +
	Std	1.723e+09	4.984e+06	1.253e+08	2.707e+08	5.835e+09	1.166e+08	2.709e+09	1.094e+09	4.775e+05	2.748e+08	8.487e+06	2.554e+07
f_2	Mean	9.473e+11	3.534e+08	6.070e+10	1.293e+10	3.219e+12	3.576e+10	2.144e+11	4.529e+11	1.788e+08	4.068e+11	9.373e+08	2.799e+09 +
	Std	1.216e+11	1.007e+08	1.333e+10	1.654e+10	6.497e+11	8.658e+09	1.859e+11	1.730e+11	2.925e+07	2.668e+11	1.020e+09	2.586e+09
f_3	Mean	3.550e+11	2.785e+07	3.256e+10	4.209e+09	1.267e+12	9.319e+09	6.978e+10	1.717e+11	7.185e+07	1.181e+11	1.890e+08	3.284e+08 +
	Std	3.636e+10	9.233e+06	5.904e+09	4.747e+09	2.723e+11	2.880e+09	6.573e+10	4.731e+10	1.456e+07	6.430e+10	2.291e+08	2.774e+08
f_4	Mean	6.200e+03	1.912e+03	1.944e+03	1.909e+03	4.950e+05	1.913e+03	3.772e+03	2.037e+03	1.930e+03	2.891e+03	1.907e+03	1.909e+03 +
	Std	2.238e+03	1.307e+00	1.942e+01	2.653e+00	2.270e+05	1.397e+00	1.081e+03	1.526e+02	5.819e+00	2.966e+03	6.658e-01	1.353e+00
f_5	Mean	7.264e+06	3.310e+06	4.807e+04	4.747e+05	2.421e+07	6.592e+05	1.783e+06	1.064e+07	3.633e+05	1.414e+05	2.391e+04	4.305e+04 -
	Std	2.477e+06	1.033e+06	1.210e+04	3.275e+05	1.248e+07	4.199e+05	2.365e+06	8.111e+06	2.324e+05	7.052e+04	1.135e+04	1.535e+04
f_6	Mean	1.448e+05	8.570e+03	3.410e+03	2.184e+04	4.190e+07	1.223e+04	1.282e+04	1.118e+06	1.089e+04	2.166e+04	3.225e+03	4.402e+03 -
	Std	7.988e+04	2.024e+03	5.710e+02	9.360e+03	3.004e+07	4.152e+03	9.718e+03	2.202e+06	8.314e+03	1.173e+04	5.736e+02	1.154e+03
f_7	Mean	8.016e+06	8.630e+05	3.752e+04	9.711e+04	1.699e+08	2.965e+05	2.436e+05	5.519e+06	7.886e+04	2.030e+05	1.167e+04	1.679e+04 -
	Std	5.268e+06	3.138e+05	7.002e+03	1.079e+05	7.555e+07	1.475e+05	4.902e+05	5.219e+06	5.600e+04	3.658e+05	2.944e+03	4.466e+03
f_8	Mean	2.430e+03	2.312e+03	2.345e+03	2.324e+03	2.541e+03	2.341e+03	2.553e+03	2.374e+03	3.040e+03	2.390e+03	2.326e+03	2.322e+03
	Std	1.546e+01	6.696e+00	2.194e+00	6.521e+00	7.228e+01	3.002e+00	1.083e+02	1.370e+01	3.350e+02	2.789e+01	1.499e+00	3.838e+00
f_9	Mean	1.050e+04	2.666e+03	4.574e+03	3.209e+03	1.564e+04	4.015e+03	6.906e+03	8.670e+03	2.724e+03	8.377e+03	2.719e+03	2.903e+03 +
	Std	1.087e+03	1.028e+01	1.914e+02	5.675e+02	2.576e+03	2.549e+02	2.900e+03	1.701e+03	4.654e+01	2.053e+03	5.965e+01	1.349e+02
f_{10}	Mean	4.761e+03	3.155e+03	3.232e+03	3.223e+03	6.437e+03	3.549e+03	3.801e+03	3.820e+03	3.344e+03	3.795e+03	3.281e+03	3.343e+03 +
	Std	2.785e+02	2.520e+01	3.526e+01	7.190e+01	1.797e+03	1.043e+02	4.394e+02	1.640e+02	1.170e+02	4.034e+02	1.040e+02	1.152e+02
+/-/-	Avg. ranks	10/0/0	7/2/1	7/0/3	6/4/0	10/0/0	9/1/0	10/0/0	7/3/0	9/1/0	5/2/3	6/1/3	-
Avg. ranks	Avg. ranks	11.6	4.3	5.9	5.6	12.9	7.2	9.3	10.7	5.4	8.8	2.8	2.3

Table 13 Experimental results and statistical analyses on 10-D CEC2022. f_1 : Unimodal function; $f_2 - f_5$: Multimodal functions; $f_6 - f_8$: Hybrid functions; $f_9 - f_{12}$: Composite functions

Function	GA	DE	CMA-ES	GWO	MFO	SCA	WOA	GIO	FOX	POA	jSO	L-SHADE-cnEpSIn	TSA	
f_1	Mean	6.386e+03+	1.439e+03+	4.147e+02+	3.463e+02+	2.082e+04+	4.150e+02+	3.623e+03+	1.376e+03+	3.213e+02+	5.668e+02+	3.001e+02	3.017e+02≈	3.004e+02
f_2	Std	1.739e+03	4.506e+02	3.104e+01	3.982e+01	4.524e+03	5.693e+01	2.331e+03	1.432e+03	8.844e+01	4.353e+02	2.384e+01	2.748e+00	2.268e-01
f_2	Mean	5.013e+02+	4.113e+02	4.152e+02+	4.143e+02+	6.655e+02+	4.252e+02+	4.769e+02+	4.696e+02+	4.568e+02+	4.182e+02+	4.008e+02	4.014e+02	4.123e+02
f_3	Std	2.399e+01	1.661e+00	2.214e+00	1.759e+01	1.441e+02	1.058e+01	7.400e+01	1.801e+01	3.567e+01	2.490e+01	1.669e+00	3.492e+00	2.075e+01
f_3	Mean	6.001e+02+	6.000e+02	6.000e+02+	6.000e+02+	6.003e+02+	6.000e+02+	6.000e+02+	6.000e+02+	6.000e+02+	6.000e+02	6.000e+02	6.000e+02	6.000e+02
f_4	Std	1.844e-02	9.250e-08	6.226e-04	3.451e-04	9.638e-02	1.173e-03	3.766e-03	2.814e-02	2.797e-05	1.623e-02	4.401e-08	6.884e-06	6.394e-06
f_4	Mean	8.009e+02+	8.010e+02+	8.010e+02+	8.005e+02+	8.005e+02≈	8.011e+02+	8.004e+02≈	8.006e+02+	8.004e+02≈	8.001e+02	8.003e+02≈	8.003e+02≈	8.003e+02≈
f_5	Std	1.511e-01	1.586e-01	1.901e-01	3.931e-01	2.004e-01	9.538e-02	2.551e-01	2.166e-01	3.343e-01	5.189e-02	7.916e-02	8.339e-02	9.924e-02
f_5	Mean	9.010e+02+	9.001e+02≈	9.003e+02+	9.001e+02≈	9.058e+02+	9.001e+02≈	9.028e+02+	9.006e+02+	9.033e+02+	9.005e+02+	9.000e+02	9.000e+02	9.001e+02
f_6	Std	1.702e-01	4.209e-02	8.019e-02	1.560e-01	9.444e-01	2.174e-02	1.939e+00	4.219e-01	1.645e+00	5.857e-01	4.062e-04	1.603e-03	1.733e-01
f_6	Mean	4.118e+05+	5.019e+04+	4.058e+03	3.754e+04≈	7.519e+07+	9.082e+04+	2.990e+04≈	3.064e+04≈	4.234e+04+	2.408e+04≈	3.250e+03	7.744e+03	2.669e+04
f_7	Std	2.736e+05	1.789e+04	8.170e+02	1.836e+04	8.412e+07	4.012e+04	2.261e+04	1.108e+04	1.556e+04	1.099e+04	1.090e+03	3.498e+03	1.302e+04
f_7	Mean	2.089e+03+	2.036e+03+	2.078e+03+	2.037e+03+	2.708e+03+	2.062e+03+	2.199e+03+	2.188e+03+	2.286e+03+	2.033e+03+	2.029e+03	2.037e+03+	2.031e+03
f_8	Std	1.814e+01	5.537e+00	1.588e+01	5.809e+00	3.877e+02	1.030e+01	1.189e+02	9.438e+01	1.436e+02	6.059e+00	1.869e+00	4.350e+00	2.303e+01
f_8	Mean	2.513e+03+	2.234e+03+	2.228e+03≈	2.513e+03+	7.383e+07+	2.302e+03+	3.827e+03+	3.937e+03+	2.465e+03+	2.226e+03≈	2.222e+03	2.226e+03≈	2.227e+03
f_9	Std	5.563e+02	3.753e+00	2.939e+00	5.277e+02	1.118e+08	3.756e+01	1.043e+03	7.234e+02	1.970e+02	6.168e+00	4.154e+00	8.840e-01	2.333e+00
f_9	Mean	2.656e+03≈	2.626e+03≈	2.582e+03≈	2.564e+03≈	2.840e+03+	2.342e+03+	2.654e+03+	2.721e+03+	2.700e+03+	2.488e+03≈	2.300e+03	2.300e+03	2.598e+03
f_{10}	Std	8.223e+01	8.948e+01	1.317e+02	1.706e+02	7.355e+01	5.419e+01	1.767e+02	9.364e+01	1.782e+02	1.756e+02	1.637e-01	6.580e-01	1.496e+02
f_{10}	Mean	2.629e+03≈	2.602e+03	2.606e+03≈	2.639e+03≈	2.826e+03+	2.604e+03	2.819e+03+	2.686e+03≈	3.090e+03+	2.637e+03≈	2.600e+03	2.601e+03	2.674e+03
f_{11}	Std	1.763e+01	1.474e+00	8.785e-01	5.961e+01	1.539e+02	1.497e+00	2.804e+02	7.547e+01	5.106e+02	5.671e+01	1.242e+00	1.524e+00	1.260e+02
f_{11}	Mean	2.638e+03	2.617e+03	2.823e+03+	2.782e+03+	3.093e+03+	2.605e+03	2.762e+03+	2.710e+03+	2.919e+03+	2.607e+03	2.600e+03	2.600e+03	2.645e+03
f_{12}	Std	5.244e+00	9.755e+00	3.772e+02	3.625e+02	1.978e+02	1.248e+00	3.033e+02	2.815e+02	4.524e+02	9.109e+00	6.751e-02	2.390e-01	1.907e+02
f_{12}	Mean	2.888e+03+	2.866e+03≈	2.867e+03≈	2.892e+03+	2.875e+03+	2.957e+03+	2.881e+03+	3.015e+03+	2.868e+03+	2.867e+03+	2.869e+03+	2.866e+03	2.866e+03

Table 13 (continued)

Function	GA	DE	CMA-ES	GWO	MFO	SCA	WOA	GIO	FOX	POA	jSO	L-SHADE-cnEpSin	TSA
Std	5.039e+00	4.112e-01	5.724e-01	2.516e+00	1.037e+01	3.212e+01	7.804e+01	3.176e+01	1.179e+02	2.661e+00	1.254e+00	2.017e+00	1.424e+00
+/-	9/2/1	5/3/4	7/4/1	6/6/0	12/0/0	7/2/3	10/2/0	10/2/0	11/1/0	6/4/2	1/1/10	2/3/7	-
Avg. ranks	9.9	5.7	6.7	6.3	12.8	6.4	9.8	9.7	9.5	5.4	1.3	3.1	4.5

Table 14 Experimental results and statistical analyses on 20-D CEC2022

Function	GA	DE	CMA-ES	GWO	MFO	SCA	WOA	GJO	FOX	POA	jSO	L-SHADE- cnEpSin	TSA
f_1	Mean	2.814e+04+	8.257e+03+	2.562e+03+	6.466e+02+	6.074e+02+	2.159e+03+	9.975e+03+	6.267e+04+	3.026e+02+	4.676e+03+	5.171e+02+	5.828e+02+
	Std	2.946e+03	1.619e+03	3.943e+02	3.189e+02	3.454e+03	7.592e+02	2.084e+03	1.184e+04	8.080e+01	2.646e+03	1.345e+02	1.581e+02
f_2	Mean	1.030e+03+	4.527e+02+	5.171e+02+	4.942e+02+	6.599e+02+	5.125e+02+	7.153e+02+	3.691e+03+	4.510e+02 ≈	6.179e+02+	4.809e+02+	4.788e+02+
	Std	1.448e+02	1.881e+00	1.183e+01	3.869e+01	7.345e+01	1.029e+01	1.151e+02	1.153e+03	5.690e+00	9.372e+01	9.323e+00	7.225e+00
f_3	Mean	6.005e+02+	6.000e+02+	6.000e+02+	6.001e+02+	6.000e+02+	6.000e+02+	6.002e+02+	6.012e+02+	6.000e+02+	6.000e+02+	6.000e+02+	6.000e+02
	Std	1.007e-01	1.075e-05	3.840e-03	1.153e-02	6.397e-02	7.343e-03	8.237e-02	2.971e-01	1.787e-05	1.746e-01	1.324e-03	3.122e-03
f_4	Mean	8.038e+02+	8.040e+02+	8.039e+02+	8.011e+02+	8.016e+02+	8.022e+02+	8.039e+02+	8.022e+02+	8.006e+02 ≈	8.008e+02+	8.015e+02+	8.016e+02+
	Std	—	—	—	—	—	—	—	—	—	—	—	8.009e+02
f_5	Mean	3.342e-01	3.749e-01	3.804e-01	8.933e-01	7.998e-01	9.006e+02	9.067e+02+	9.006e+02+	9.027e+02≈	9.236e+02+	9.021e+02≈	9.001e+02
	Std	9.067e+02+	9.012e+02≈	9.031e+02≈	9.006e+02	—	—	—	—	—	—	—	9.021e+02
f_6	Mean	9.765e-01	3.924e-01	7.364e-01	6.701e-01	3.227e+00	2.176e-01	3.702e-01	4.378e+00	5.253e-01	1.011e+00	1.011e-01	5.151e-02
	Std	5.294e+08+	1.762e+08+	5.443e+06+	2.262e+05+	8.398e+04≈	5.011e+06+	5.810e+07+	1.119e+09+	1.558e+05+	5.012e+05+	2.355e+04	2.644e+04
f_7	Mean	1.379e+08	5.958e+07	1.916e+06	6.544e+05	3.982e+04	2.949e+06	7.955e+07	7.646e+08	4.315e+04	1.201e+06	3.578e+03	4.120e+03
	Std	3.047e+03+	2.571e+03+	2.267e+03+	2.080e+03≈	3.664e+03+	2.146e+03+	2.445e+03+	4.784e+03+	2.415e+03+	2.170e+03+	2.033e+03	2.049e+03
f_8	Mean	2.426e+02	9.828e+01	5.121e+01	3.333e+01	6.939e+02	4.251e+01	2.771e+02	5.714e+02	2.436e+02	1.214e+02	2.710e+00	6.529e+00
	Std	1.211e+07+	2.929e+05+	2.440e+03	4.847e+03+	6.238e+03+	4.002e+03+	2.597e+04+	9.899e+10+	2.325e+03	3.004e+03≈	2.300e+03	2.342e+03
f_9	Mean	3.194e+03+	2.676e+03+	2.650e+03≈	2.667e+03+	2.816e+03+	2.780e+03+	2.995e+03+	3.303e+03+	2.709e+03+	2.784e+03+	2.691e+03+	2.677e+03+
	Std	9.304e+01	1.376e+01	5.337e+00	2.328e+01	1.748e+02	3.244e+01	1.268e+02	2.857e+02	9.668e+01	7.454e+01	1.092e+01	7.468e+01
f_{10}	Mean	2.944e+03≈	3.265e+03≈	3.355e+03≈	3.960e+03≈	4.800e+03+	2.799e+03≈	3.623e+03≈	4.953e+03+	4.808e+03+	3.530e+03≈	2.764e+03	2.770e+03
	Std	—	—	—	—	—	—	—	—	—	—	—	3.283e+03
f_{11}	Mean	2.352e+01	8.744e+02	1.140e+03	1.553e+03	1.350e+03	5.524e+01	1.336e+03	1.017e+03	7.979e+02	4.432e+00	2.558e+00	8.240e+02
	Std	2.990e+03+	2.623e+03+	2.620e+03+	3.234e+03+	2.612e+03+	2.618e+03+	4.625e+03+	2.812e+03+	2.782e+03+	2.603e+03+	2.606e+03	
f_{12}	Mean	8.880e+01	1.102e+01	1.989e+00	8.295e+00	7.567e+02	3.649e+00	3.222e+02	6.320e+02	4.505e+02	1.600e+02	2.950e+00	3.008e+00
	Std	3.172e+03+	2.940e+03	2.955e+03≈	2.964e+03≈	3.287e+03+	3.074e+03+	3.084e+03+	3.079e+03+	3.655e+03+	3.015e+03	2.979e+03≈	2.964e+03
+/-	Avg.	11/1/0	9/2/1	7/4/1	11/1/0	10/1/1	10/2/0	12/0/0	8/3/1	9/2/1	6/1/5	6/1/5	—
	ranks	10.8	6.8	6.8	5.3	12.6	6.2	9.8	9.6	6.0	7.3	2.7	3.5

Acknowledgements The authors would like to thank the support of Engineering Research Center of Big Data Application in Private Health Medicine of Fujian Universities, Putian University Putian, Fujian 351100, China Putian Electronic Information Industry Research Institute, Putian University, Putian, Fujian 351100, China (Putian Science and Technology Plan Project 2023GJGZ003) and the anonymous reviewers and the editor for their careful reviews and constructive suggestions to help us improve the quality of this paper.

Funding This work was supported by the Startup Fund for Advanced Talents of Putian University (2023013), Fujian Provincial Natural Science Foundation of China (2022J011179), Sanming University National Natural Science Foundation of China Breeding Project (PYT2103), Sanming University introduces high-level talents to start scientific research funding support project (21YG01).

References

- Sharma P, Raju S (2023) Metaheuristic optimization algorithms: a comprehensive overview and classification of benchmark test functions. *Soft Comput* 2023:1–64
- Bouaouda A, Sayouti Y (2022) Hybrid meta-heuristic algorithms for optimal sizing of hybrid renewable energy system: a review of the state-of-the-art. *Arch Comput Methods Eng* 29(6):4049–4083
- Darvishpoor S, Darvishpoor A, Escarcega M, Hassanalian M (2023) Nature-inspired algorithms from oceans to space: A comprehensive review of heuristic and meta-heuristic optimization algorithms and their potential applications in drones. *Drones* 7(7):427
- Kaur S, Kumar Y, Koul A, Kumar Kamboj S (2023) A systematic review on metaheuristic optimization techniques for feature selections in disease diagnosis: open issues and challenges. *Arch Comput Methods Eng* 30(3):1863–1895
- Rajwar K, Deep K, Das S (2023) An exhaustive review of the metaheuristic algorithms for search and optimization: taxonomy, applications, and open challenges. *Artif Intell Rev* 2023:1–71
- Wilson RC, Bonawitz E, Costa VD, Ebitz RB (2021) Balancing exploration and exploitation with information and randomization. *Curr Opin Behav Sci* 38:49–56
- Alorfi A (2023) A survey of recently developed metaheuristics and their comparative analysis. *Eng Appl Artif Intell* 117:105622
- Pan J-S, Hu P, Snášel V, Chu S-C (2023) A survey on binary metaheuristic algorithms and their engineering applications. *Artif Intell Rev* 56(7):6101–6167
- Hashim FA, Hussien AG (2022) Snake optimizer: a novel metaheuristic optimization algorithm. *Knowl-Based Syst* 242:108320
- Price KV (2013) Differential evolution. *Handbook of optimization: from classical to modern approach*. Springer, Cham, pp 187–214
- Holland JH (1992) Genetic algorithms. *Sci Am* 267(1):66–73
- Dasgupta D, Yu S, Nino F (2011) Recent advances in artificial immune systems: models and applications. *Appl Soft Comput* 11(2):1574–1587
- Simon D (2008) Biogeography-based optimization. *IEEE Trans Evol Comput* 12(6):702–713
- Civicioglu P (2013) Backtracking search optimization algorithm for numerical optimization problems. *Appl Math Comput* 219(15):8121–8144
- Meng Z, Pan J-S (2016) Monkey king evolution: a new memetic evolutionary algorithm and its application in vehicle fuel consumption optimization. *Knowl-Based Syst* 97:144–157
- Amali D, Dinakaran M (2019) Wildebeest herd optimization: a new global optimization algorithm inspired by wildebeest herding behaviour. *J Intel Fuzzy Syst* 37(6):8063–8076
- Veytsari EF et al (2022) A new optimization algorithm inspired by the quest for the evolution of human society: human felicity algorithm. *Expert Syst Appl* 193:116468
- Ahmadianfar I, Bozorg-Haddad O, Chu X (2020) Gradient-based optimizer: a new metaheuristic optimization algorithm. *Inf Sci* 540:131–159
- Zhang Y, Jin Z, Mirjalili S (2020) Generalized normal distribution optimization and its applications in parameter extraction of photovoltaic models. *Energy Convers Manage* 224:113301
- Abualigah L, Diabat A, Mirjalili S, Abd Elaziz M, Gandomi AH (2021) The arithmetic optimization algorithm. *Comput Methods Appl Mech Eng* 376:113609
- Ahmadianfar I, Heidari AA, Gandomi AH, Chu X, Chen H (2021) Run beyond the metaphor: an efficient optimization algorithm based on Runge Kutta method. *Expert Syst Appl* 181:115079
- Qais MH, Hasanien HM, Turky RA, Alghuwainem S, Tostado-Vélez M, Jurado F (2022) Circle search algorithm: a geometry-based metaheuristic optimization algorithm. *Mathematics* 10(10):1626
- Ahmadianfar I, Heidari AA, Noshadian S, Chen H, Gandomi AH (2022) Info: an efficient optimization algorithm based on weighted mean of vectors. *Expert Syst Appl* 195:116516
- Abdel-Basset M, El-Shahat D, Jameel M, Abouhawwash M (2023) Exponential distribution optimizer (EDO): a novel math-inspired algorithm for global optimization and engineering problems. *Artif Intell Rev* 2023:1–72
- Bai J, Li Y, Zheng M, Khatir S, Benaisa B, Abualigah L, Wahab MA (2023) A sinh cosh optimizer. *Knowl-Based Syst* 2023:111081
- Van Laarhoven PJ, Aarts EH, van Laarhoven PJ, Aarts EH (1987) Simulated annealing. Springer, Cham
- Qais MH, Hasanien HM, Alghuwainem S (2020) Transient search optimization: a new meta-heuristic optimization algorithm. *Appl Intell* 50:3926–3941
- Faramarzi A, Heidarnejad M, Stephens B, Mirjalili S (2020) Equilibrium optimizer: a novel optimization algorithm. *Knowl-Based Syst* 191:105190
- Pereira JLJ, Francisco MB, Diniz CA, Oliver GA, Cunha SS Jr, Gomes GF (2021) Lichtenberg algorithm: a novel hybrid physics-based meta-heuristic for global optimization. *Expert Syst Appl* 170:114522
- Hashim FA, Hussain K, Houssein EH, Mabrouk MS, Al-Atabay W (2021) Archimedes optimization algorithm: a new metaheuristic algorithm for solving optimization problems. *Appl Intell* 51:1531–1551
- Mahdavi-Meymand A, Zounemat-Kermani M (2022) Homonuclear molecules optimization (HMO) meta-heuristic algorithm. *Knowl-Based Syst* 258:110032
- Abdel-Basset M, Mohamed R, Sallam KM, Chakrabortty RK (2022) Light spectrum optimizer: a novel physics-inspired metaheuristic optimization algorithm. *Mathematics* 10(19):3466
- Hashim FA, Mostafa RR, Hussien AG, Mirjalili S, Sallam KM (2023) Fick's law algorithm: a physical law-based algorithm for numerical optimization. *Knowl-Based Syst* 260:110146
- Cheng M-Y, Sholeh MN (2023) Optical microscope algorithm: a new metaheuristic inspired by microscope magnification for solving engineering optimization problems. *Knowl-Based Syst* 279:110939
- Rao RV, Savsani VJ, Vakharia D (2011) Teaching-learning-based optimization: a novel method for constrained mechanical design optimization problems. *Comput Aided Des* 43(3):303–315

36. Askari Q, Saeed M, Younas I (2020) Heap-based optimizer inspired by corporate rank hierarchy for global optimization. *Expert Syst Appl* 161:113702
37. Askari Q, Younas I, Saeed M (2020) Political optimizer: a novel socio-inspired meta-heuristic for global optimization. *Knowl-Based Syst* 195:105709
38. Harifi S, Mohammadzadeh J, Khalilian M, Ebrahimnejad S (2021) Giza pyramids construction: an ancient-inspired metaheuristic algorithm for optimization. *Evol Intel* 14:1743–1761
39. Talatahari S, Bayzidi H, Saraei M (2021) Social network search for global optimization. *IEEE Access* 9:92815–92863
40. Ayyarao TS, Ramakrishna N, Elavarasan RM, Polumahanthi N, Rambabu M, Saini G, Khan B, Alatas B (2022) War strategy optimization algorithm: a new effective metaheuristic algorithm for global optimization. *IEEE Access* 10:25073–25105
41. Dehghani M, Trojovská E, Zuščák T (2022) A new human-inspired metaheuristic algorithm for solving optimization problems based on mimicking sewing training. *Sci Rep* 12(1):17387
42. Givi H, Hubalovska M (2023) Skill optimization algorithm: A new human-based metaheuristic technique. *Comput Mater Continua* 74(1):1
43. Guan Z, Ren C, Niu J, Wang P, Shang Y (2023) Great wall construction algorithm: a novel meta-heuristic algorithm for engineer problems. *Expert Syst Appl* 233:120905
44. Dorigo M, Birattari M, Stutzle T (2006) Ant colony optimization. *IEEE Comput Intell Mag* 1(4):28–39
45. Mirjalili S, Lewis A (2016) The whale optimization algorithm. *Adv Eng Softw* 95:51–67
46. Faramarzi A, Heidarinejad M, Mirjalili S, Gandomi AH (2020) Marine predators algorithm: a nature-inspired metaheuristic. *Expert Syst Appl* 152:113377
47. Zhao W, Zhang Z, Wang L (2020) Manta ray foraging optimization: an effective bio-inspired optimizer for engineering applications. *Eng Appl Artif Intell* 87:103300
48. Abdollahzadeh B, Soleimani Gharehchopogh F, Mirjalili S (2021) Artificial gorilla troops optimizer: a new nature-inspired metaheuristic algorithm for global optimization problems. *Int J Intell Syst* 36(10):5887–5958
49. MiarNaeimi F, Azizyan G, Rashki M (2021) Horse herd optimization algorithm: a nature-inspired algorithm for high-dimensional optimization problems. *Knowl-Based Syst* 213:106711
50. Zhong C, Li G, Meng Z (2022) Beluga whale optimization: a novel nature-inspired metaheuristic algorithm. *Knowl-Based Syst* 251:109215
51. Abdel-Basset M, Mohamed R, Jameel M, Abouhawwash M (2023) Nutcracker optimizer: a novel nature-inspired metaheuristic algorithm for global optimization and engineering design problems. *Knowl-Based Syst* 262:110248
52. Abdel-Basset M, Mohamed R, Jameel M, Abouhawwash M (2023) Spider wasp optimizer: a novel meta-heuristic optimization algorithm. *Artif Intell Rev* 2023:1–64
53. Peraza-Vázquez H, Peña-Delgado A, Merino-Treviño M, Morales-Cepeda AB, Sinha N (2024) A novel metaheuristic inspired by horned lizard defense tactics. *Artif Intell Rev* 57(3):59
54. Abdelhamid AA, Towfek S, Khodadadi N, Alhussan AA, Khafaga DS, Eid MM, Ibrahim A (2023) Waterwheel plant algorithm: a novel metaheuristic optimization method. *Processes* 11(5):1502
55. Merrikh-Bayat F (2014) A numerical optimization algorithm inspired by the strawberry plant. Preprint at <http://arxiv.org/abs/1407.7399>
56. Pan J-S, Zhang S-Q, Chu S-C, Yang H-M, Yan B (2023) Willow catkin optimization algorithm applied in the TDOA-FDOA joint location problem. *Entropy* 25(1):171
57. Kaveh A, Talatahari S, Khodadadi N (2022) Stochastic paint optimizer: theory and application in civil engineering. *Eng Comput* 2022:1–32
58. Ashrafi S, Dariane A (2011) A novel and effective algorithm for numerical optimization: melody search (MS). In: 11th international conference on hybrid intelligent systems (HIS), IEEE, pp 109–114
59. Mora-Gutiérrez RA, Ramírez-Rodríguez J, Rincón-García EA (2014) An optimization algorithm inspired by musical composition. *Artif Intell Rev* 41:301–315
60. Yuan Y, Ren J, Wang S, Wang Z, Mu X, Zhao W (2022) Alpine skiing optimization: a new bio-inspired optimization algorithm. *Adv Eng Softw* 170:103158
61. Tian Z, Gai M (2024) Football team training algorithm: a novel sport-inspired meta-heuristic optimization algorithm for global optimization. *Expert Syst Appl* 245:123088
62. Ma B, Hu Y, Lu P, Liu Y (2023) Running city game optimizer: a game-based metaheuristic optimization algorithm for global optimization. *J Comput Design Eng* 10(1):65–107
63. Lam AY, Li VO, James J (2011) Real-coded chemical reaction optimization. *IEEE Trans Evol Comput* 16(3):339–353
64. Kaveh A, Khayatazad M (2012) A new meta-heuristic method: ray optimization. *Comput Struct* 112:283–294
65. Abdechiri M, Meybodi MR, Bahrami H (2013) Gases Brownian motion optimization: an algorithm for optimization (GBMO). *Appl Soft Comput* 13(5):2932–2946
66. Khaleel MI (2023) Efficient job scheduling paradigm based on hybrid sparrow search algorithm and differential evolution optimization for heterogeneous cloud computing platforms. *Internet Things* 22:100697
67. Hasanien HM, Alsaleh I, Tostado-Véliz M, Zhang M, Alateeq A, Jurado F, Alassaf A (2024) Hybrid particle swarm and sea horse optimization algorithm-based optimal reactive power dispatch of power systems comprising electric vehicles. *Energy* 286:129583
68. Kuo R, Chiu T-H (2024) Hybrid of jellyfish and particle swarm optimization algorithm-based support vector machine for stock market trend prediction. *Appl Soft Comput* 154:111394
69. Kaur S, Awasthi LK, Sangal A, Dhiman G (2020) Tunicate swarm algorithm: a new bio-inspired based metaheuristic paradigm for global optimization. *Eng Appl Artif Intell* 90:103541
70. Houssein EH, Saber E, Ali AA, Wazery YM (2021) Opposition-based learning tunicate swarm algorithm for biomedical classification. In: 2021 17th international computer engineering conference (ICENCO), IEEE, pp 1–6
71. Sharma A, Sharma A, Dasgupta A, Jately V, Ram M, Rajput S, Averbukh M, Azzopardi B (2021) Opposition-based tunicate swarm algorithm for parameter optimization of solar cells. *IEEE Access* 9:125590–125602
72. Kanimozhi P, Aruldoss Albert Victoire T (2022) Oppositional tunicate fuzzy c-means algorithm and logistic regression for intrusion detection on cloud. *Concurr Comput Pract Exp* 34(4):e6624
73. Yasin SA, Prasada Rao P (2022) Enhanced CRNN-based optimal web page classification and improved tunicate swarm algorithm-based re-ranking. *Internet J Uncertain Fuzziness Knowl-Based Syst* 30(05):813–846
74. Suryawanshi SP, Dharmani BC (2023) Comparative study of heuristic-based support vector machine and neural network for thermogram breast cancer detection with entropy features. *Biomed Eng Appl Basis Commun* 35(02):2250047
75. Mohanan MS, Rajarathinam V (2023) Deep insight of HR management on work from home scenario during Covid pandemic situation using intelligent: analysis on it sectors in Tamil Nadu. *Int J Syst Assur Eng Manag* 14(4):1151–1182
76. Chandran V, Mohapatra P (2024) An improved tunicate swarm algorithm with random opposition based learning for global optimization problems. *OPSEARCH* 2024:1–26
77. Prabhakar SK, Won D-O (2024) SCMS: systematic conglomerated models for audio cough signal classification. *Algorithms* 17(7):302

78. Laishram R, Rabidas R (2024) Binary tunicate swarm algorithm based novel feature selection framework for mammographic mass classification. *Measurement* 235:114928
79. Levy D (1994) Chaos theory and strategy: theory, application, and managerial implications. *Strateg Manag J* 15(S2):167–178
80. Gupta J, Nijhawan P, Ganguli S (2021) Parameter extraction of solar pv cell models using novel metaheuristic chaotic tunicate swarm algorithm. *Int Trans Electric Energy Syst* 31(12):e13244
81. Fetouh T, Elsayed AM (2020) Optimal control and operation of fully automated distribution networks using improved tunicate swarm intelligent algorithm. *IEEE Access* 8:129689–129708
82. Jui JJ, Ahmad MA, Rashid MIM (2022) Levy tunicate swarm algorithm for solving numerical and real-world optimization problems. In: Proceedings of the 6th international conference on electrical, control and computer engineering: InECCE2021, Kuantan, Pahang, Malaysia, 23rd August, Springer, pp 417–427
83. Karthick M, Rukkumani V (2023) Enhanced cascaded converters for switched reluctance motor-fed electric vehicles. *IETE J Res* 2023:1–22
84. Joseph SS, Dennisan A (2023) Optimised CNN based brain tumour detection and 3D reconstruction. *Comput Methods Biomed Eng Imaging Vis* 11(3):796–811
85. Alohalia MA, Al-Mutiri F, Othman KM, Yafoz A, Alsini R, Salama AS (2024) An enhanced tunicate swarm algorithm with deep-learning based rice seedling classification for sustainable computing based smart agriculture. *AIMS Math* 9(4):10185–10207
86. Arabali A, Khajehzadeh M, Keawsawasvong S, Mohammed AH, Khan B (2022) An adaptive tunicate swarm algorithm for optimization of shallow foundation. *IEEE Access* 10:39204–39219
87. Das A (2022) Adaptive UNET-based lung segmentation and ensemble learning with CNN-based deep features for automated covid-19 diagnosis. *Multimed Tools Appl* 81(4):5407–5441
88. Arandian B, Eslami M, Khalid SA, Khan B, Sheikh UU, Akbari E, Mohammed AH (2022) An effective optimization algorithm for parameters identification of photovoltaic models. *IEEE Access* 10:34069–34084
89. Bhujang RK, Kotagi V (2023) Earth quack prediction of southern California using unsupervised clustering based ensemble deep learning model. In: 2023 international conference on ambient intelligence, knowledge informatics and industrial electronics (AIKIE), IEEE, pp 1–6
90. JadHAV S, Singh J (2023) Design of egtboost classifier for automated external skin defect detection in mango fruit. *Multimed Tools Appl* 2023:1–20
91. Jakkulla PK, Ganesh KM, Jayapal PK, Malla SJ, Chandanapalli SB, Sandhya E (2023) Selection of features using adaptive tunicate swarm algorithm with optimized deep learning model for thyroid disease classification. *Ingenierie des Systemes d'Information* 28(2):299
92. Kumar MK, Amalanathan A (2023) Optimized convolutional neural network for automatic lung nodule detection with a new active contour segmentation. *Soft Comput* 27(20):15365–15381
93. Varaprasad R, Mohan CN, Rajesh B, Kumar CR, Chowdary CS, Babu BM (2023) Attack detection scheme based on blackmailing nodes using adaptive tunicate swarm algorithm in manet-IoT environment. In: 2023 International Conference on Sustainable Computing and Smart Systems (ICSCSS), IEEE, pp 1528–1535
94. Kavitha A, Meenakshi VS. Collaborative attackers detection and route optimization by swarm intelligent-based q-learning in manets
95. Chandran V, Mohapatra P (2024) A novel reinforcement learning-inspired tunicate swarm algorithm for solving global optimization and engineering design problems. *J Ind Manag Optim* 2024:1
96. Rizk-Allah RM, Saleh O, Hagag EA, Mousa AAA (2021) Enhanced tunicate swarm algorithm for solving large-scale non-linear optimization problems. *Int J Comput Intell Syst* 14(1):189
97. Kommula BN, Kota VR (2022) An integrated converter topology for torque ripple minimization in BLDS motor using an ITSA technique. *J Ambient Intell Human Comput* 2022:1–20
98. Dayana AM, Emmanuel WS (2022) An enhanced swarm optimization-based deep neural network for diabetic retinopathy classification in fundus images. *Multimed Tools Appl* 81(15):20611–20642
99. Yuan Q, Ma C, Liu J, Gui H, Li M, Wang S (2022) Correlation analysis-based thermal error control with ITSA-GRU-a model and cloud-edge-physical collaboration framework. *Adv Eng Inform* 54:101759
100. Srinivas P, Swapna P (2022) Quantum tunicate swarm algorithm based energy aware clustering scheme for wireless sensor networks. *Microprocess Microsyst* 94:104653
101. Ragab M, Ashary EB, Sabir MFS, Bahaddad AA, Mansour RF (2022) Mathematical modelling of quantum kernel method for biomedical data analysis. *Comput Mater Contin* 71(3):1
102. Fathy A, Amer DA, Al-Dhaifallah M (2023) Modified tunicate swarm algorithm-based methodology for enhancing the operation of partially shaded photovoltaic system. *Alex Eng J* 79:449–470
103. Jeyabharathi J, Velliangiri S, Joseph S, Thanakumar I, Devadass C, Sorna C (2023) Cancer prediction using feature fusion and Taylor-TSA-based GAN with gene expression data. *Int J Pattern Recognit Artif Intell* 37(14):1
104. Lathika P, Singh DS (2024) Stochastic Bayesian approach and CTSA based rainfall prediction in Indian states. *Model Earth Syst Environ* 2024:1–10
105. Jagadeesh M, Baranidharan B (2022) Dynamic fernet: deep learning with optimal feature selection for face expression recognition in video. *Concurr Comput Pract Exp* 34(28):e7373
106. Wang J, Wang S, Li Z (2021) Wind speed deterministic forecasting and probabilistic interval forecasting approach based on deep learning, modified tunicate swarm algorithm, and quantile regression. *Renew Energy* 179:1246–1261
107. Abdolinejad F, Khayati GR, Raiszadeh R, Yaghoobi NS, Khorasani SMJ (2021) An improved optimization model for predicting pb recovery efficiency from residual of liberator cells: a hybrid of support vector regression and modified tunicate swarm algorithm. *J Mater Cycles Waste Manage* 23(5):1855–1872
108. Li L-L, Liu Z-F, Tseng M-L, Zheng S-J, Lim MK (2021) Improved tunicate swarm algorithm: solving the dynamic economic emission dispatch problems. *Appl Soft Comput* 108:107504
109. Gharehchopogh FS (2022) An improved tunicate swarm algorithm with best-random mutation strategy for global optimization problems. *J Bionic Eng* 19(4):1177–1202
110. Zhang Y, He Q, Yang L, Liu C (2022) An improved tunicate swarm algorithm for solving the multiobjective optimisation problem of airport gate assignments. *Appl Sci* 12(16):8203
111. Dohare S, Rajput R (2022) Adaptive gaussian quantum based PSA and TSA optimization for parametric optimizaiton of toughned glass on toughening machine. *Ceram Int* 48(16):22799–22807
112. Cui Y, Shi R, Dong J (2022) Cltsa: a novel tunicate swarm algorithm based on chaotic-lévy flight strategy for solving optimization problems. *Mathematics* 10(18):3405
113. Wang W, Fan C, Pan Z, Tian J (2023) Slotsa: A multi-strategy improved tunicate swarm algorithm for engineering constrained optimization problems. In: 2023 IEEE international conference on software services engineering (SSE), IEEE, pp 35–42
114. Hu G, Zheng J, Ji X, Qin X (2023) Enhanced tunicate swarm algorithm for optimizing shape of c2 rqi-spline curves. *Eng Appl Artif Intell* 121:105958
115. Liu G, Guo Z, Liu W, Cao B, Chai S, Wang C (2023) Mshotsa: a variant of tunicate swarm algorithm combining multi-strategy mechanism and hybrid Harris optimization. *PLoS ONE* 18(8):e0290117

116. Dong X, Chen N, Zhang X, Wang C, Qiao N, Long H (2023) Research on the environment and economic indicators for electricity trading. *Energy Rep* 9:1774–1783
117. Akdag O (2023) A modified tunicate swarm algorithm for engineering optimization problems. *Arab J Sci Eng* 48(11):14745–14771
118. Wang Z-C, Niu J-C (2023) Wind power output prediction: a comparative study of extreme learning machine. *Front Energy Res* 11:1267275
119. Si T, Miranda PB, Nandi U, Jana ND, Mallik S, Maulik U, Qin H (2024) Opposition-based chaotic tunicate swarm algorithms for global optimization. *IEEE Access* 2024:1–10
120. Chen Y, Dong W, Hu X (2024) Imatsa—an improved and adaptive intelligent optimization algorithm based on tunicate swarm algorithm. *AI Commun* 2024:1–22
121. Zhou K, Guan R, Hou L (2023) Optimal control of turbine speed control system based on improved tunicate swarm algorithm. In: 2023 China automation congress (CAC), IEEE, pp 2745–2750
122. Althaqafi T (2024) Mathematical modeling of a hybrid mutated tunicate swarm algorithm for feature selection and global optimization. *AIMS Math* 9(9):24336–24358
123. Bhimavarapu U (2024) Optimized automated detection of diabetic retinopathy severity: integrating improved multithresholding tunicate swarm algorithm and improved hybrid butterfly optimization. *Health Inf Sci Syst* 12(1):42
124. Du C, Zhang J (2024) An enhanced tunicate swarm algorithm with symmetric cooperative swarms for training feedforward neural networks. *Symmetry* 16(7):20738994
125. Chandran V, Mohapatra P (2024) A novel multi-strategy ameliorated quasi-oppositional chaotic tunicate swarm algorithm for global optimization and constrained engineering applications. *Helion* 10(10):1
126. Tizhoosh HR (2005) Opposition-based learning: a new scheme for machine intelligence. In: International conference on computational intelligence for modelling, control and automation and international conference on intelligent agents, web technologies and internet commerce (CIMCA-IAWTIC'06), vol 1. IEEE, pp 695–701
127. Tang R, Fong S, Dey N (2018) Metaheuristics and chaos theory. *Chaos theory*. InTech, pp 182–196
128. Viswanathan GM, Afanasyev V, Buldyrev SV, Havlin S, da Luz MG, Raposo EP, Stanley HE (2000) Lévy flights in random searches. *Phys A* 282(1–2):1–12
129. Mirjalili S, Mirjalili SM, Lewis A (2014) Grey wolf optimizer. *Adv Eng Softw* 69:46–61
130. Chouhan N, Jain S (2020) Tunicate swarm grey wolf optimization for multi-path routing protocol in IoT assisted WSN networks. *J Ambient Intell Human Comput* 2020:1–17
131. Shobana Nageswari C, Kumar V, Vini Antony Grace N, Thiagarajan J (2023) Tunicate swarm-based grey wolf algorithm for fetal heart chamber segmentation and classification: a heuristic-based optimal feature selection concept. *J Intell Fuzzy Syst* 44(1):1029–1041
132. Jeysri J, Kowsigan M (2023) Adaptive fuzzy-region growing fusion and improved CNN-ANFIS-based automated segmentation and classification of cervical cancer. *Concurr Comput Pract Exp* 35(3):1
133. Ramasamy V, Ramalingam MM, Chitraivel M (2023) Energy efficient secured-quality of service routing protocol for mobile ad hoc network using multi-objective optimization. *Indon J Electric Eng Comput Sci* 31(3):1486–1495
134. Moosavi SHS, Bardsiri VK (2019) Poor and rich optimization algorithm: a new human-based and multi populations algorithm. *Eng Appl Artif Intell* 86:165–181
135. KL BJ, et al. (2021) Chronological poor and rich tunicate swarm algorithm integrated deep maxout network for human action and abnormality detection. In: 2021 fourth international conference on electrical, computer and communication technologies (ICECCT), IEEE, pp 1–9
136. Kumari RR, Kumar VV, Naidu KR (2021) Optimized dwt based digital image watermarking and extraction using RNN-LSTM
137. Shabani A, Asgarian B, Salido M, Gharebaghi SA (2020) Search and rescue optimization algorithm: a new optimization method for solving constrained engineering optimization problems. *Expert Syst Appl* 161:113698
138. Wan C (2021) TSSR algorithm based battery space optimization on thermal management system. *Int J Green Energy* 18(12):1203–1218
139. Houssein EH, Helmy BE-D, Elngar AA, Abdelminaam DS, Shaban H (2021) An improved tunicate swarm algorithm for global optimization and image segmentation. *IEEE Access* 9:56066–56092
140. Mirjalili S, Gandomi AH, Mirjalili SZ, Saremi S, Faris H, Mirjalili SM (2017) Salp swarm algorithm: a bio-inspired optimizer for engineering design problems. *Adv Eng Softw* 114:163–191
141. Chelliah J, Kader N (2021) Optimization for connectivity and coverage issue in target-based wireless sensor networks using an effective multiobjective hybrid tunicate and salp swarm optimizer. *Int J Commun Syst* 34(3):e4679
142. Boobalan J, Malleswaran M (2022) Secure cross layer energy supplementing adhoc on-demand multipath distance vector (scses-aomdv) routing protocol for energy efficient design of wireless sensor networks. *Adhoc Sens Wirel Netw* 54:1
143. Mirjalili S (2016) Sca: a sine cosine algorithm for solving optimization problems. *Knowl-Based Syst* 96:120–133
144. Awad A, Abdel-Mawgoud H, Kamel S, Ibrahim AA, Jurado F (2021) Developing a hybrid optimization algorithm for optimal allocation of renewable DGs in distribution network. *Clean Technol* 3(2):409–423
145. Sameera K, Swarnalatha P (2023) Optimization with deep learning classifier-based foliar disease classification in apple trees using IoT network. *Int J Image Graph* 2023:2550015
146. Kumari MRR, Kumar VV, Naidu KR (2023) Digital image watermarking using DWT-SVD with enhanced tunicate swarm optimization algorithm. *Multimed Tools Appl* 82(18):28259–28279
147. Tayarani-N M-H, Akbarzadeh-T M (2008) Magnetic optimization algorithms a new synthesis. In: 2008 IEEE congress on evolutionary computation (IEEE World congress on computational intelligence), IEEE, pp 2659–2664
148. Gupta S, Dave M (2021) Product recommendation system using tunicate swarm magnetic optimization algorithm-based black hole renyi entropy fuzzy clustering and k-nearest neighbour. *J Inf Knowl Manag* 20(03):2150033
149. Arora S, Singh S (2019) Butterfly optimization algorithm: a novel approach for global optimization. *Soft Comput* 23:715–734
150. Daniel J, Francis SFV, Velliangiri S (2021) Cluster head selection in wireless sensor networks using tunicate swarm butterfly optimization algorithm. *Wireless Netw* 27:5245–5262
151. Manoj K, Dhas DAS (2022) Automated brain tumor malignancy detection via 3d MRI using adaptive-3-d u-net and heuristic-based deep neural network. *Multimedia Syst* 28(6):2247–2273
152. Mirjalili S (2015) Moth-flame optimization algorithm: a novel nature-inspired heuristic paradigm. *Knowl-Based Syst* 89:228–249
153. Renukadevi M, Anita EM, Mohana Geetha D (2021) An efficient privacy-preserving model based on Omftsfa for query optimization in crowdsourcing. *Concurr Comput Pract Exp* 33(24):e6447
154. Kumar V, Kushwaha S (2023) Hybrid metaheuristic model based performance-aware optimization for map reduce scheduling. *Int J Comput Appl* 45(12):776–788

155. Diaz P, Jiju JE (2022) Feature selection and feature weighting using tunicate swarm genetic optimization algorithm with deep residual networks. *Int J Swarm Intell Res (IJSIR)* 13(1):1–16
156. Sharma S, Mishra V, Tripathi MM (2022) A novel energy efficient hybrid meta-heuristic approach (neema) for wireless body area network. *Int J Commun Syst* 35(13):e5249
157. Yang X-S (2012) Flower pollination algorithm for global optimization. In: International conference on unconventional computing and natural computation, Springer, pp 240–249
158. Yu C, Huang H, Wei X (2022) Tunicate swarm algorithm based difference variation flower pollination algorithm. In: International conference on intelligent computing, Springer, pp 80–96
159. Singh JP, Gupta AK (2022) An optimized routing technique in wireless sensor network using aquila optimizer. *Int J Intel Eng Syst* 12(4):10–22266
160. Singh JP, Gupta AK (2022) Energy aware cluster head selection and multipath routing using whale-based tunicate swarm algorithm (wtsa) for wireless sensor network. *New Rev Inf Netw* 27(1):1–29
161. Dhiman G, Garg M, Nagar A, Kumar V, Dehghani M (2021) A novel algorithm for global optimization: rat swarm optimizer. *J Ambient Intell Humaniz Comput* 12:8457–8482
162. Mohana Dhas M, Suresh Singh N (2022) Blood cell image denoising based on tunicate rat swarm optimization with median filter. In: Evolutionary computing and mobile sustainable networks: proceedings of ICECMSN 2021, Springer, pp 33–45
163. Shadravan S, Naji HR, Bardsiri VK (2019) The sailfish optimizer: a novel nature-inspired metaheuristic algorithm for solving constrained engineering optimization problems. *Eng Appl Artif Intell* 80:20–34
164. Muthu Ganesh V, Nithiyantham J (2022) Heuristic-based channel selection with enhanced deep learning for heart disease prediction under wban. *Comput Methods Biomed Biomed Engin* 25(13):1429–1448
165. Salgotra R, Singh U (2019) The naked mole-rat algorithm. *Neural Comput Appl* 31:8837–8857
166. Singh S, Mittal N, Singh U, Salgotra R, Zagaria A, Singh D (2022) A novel hybrid tunicate swarm naked mole-rat algorithm for image segmentation and numerical optimization. *Comput Mater Continua* 71(2):1
167. Singh P, Singh P, Mittal N, Singh U, Singh S (2023) An optimum localization approach using hybrid tsnmra in 2d wsns. *Comput Netw* 226:109682
168. Torczon V (1997) On the convergence of pattern search algorithms. *SIAM J Optim* 7(1):1–25
169. Khajehzadeh M, Keawsawasvong S, Sarir P, Khailany DK (2022) Seismic analysis of earth slope using a novel sequential hybrid optimization algorithm. *Period Polytech Civil Eng* 66(2):355–366
170. Kennedy J, Eberhart R (1995) Particle swarm optimization. In: Proceedings of ICNN'95-international conference on neural networks, vol 4. IEEE, pp 1942–1948
171. Sharma A, Sharma A, Jately V, Averbukh M, Rajput S, Azzopardi B (2022) A novel tsa-pso based hybrid algorithm for gmpp tracking under partial shading conditions. *Energies* 15(9):3164
172. Shang F, Zhang Y, Wang R, Wu X, Fan D (2023) Optimization modulation method of seven-level shePWM inverter based on tsa-pso. In: 2023 3rd international conference on electrical engineering and mechatronics technology (ICEEMT), IEEE, pp 207–211
173. Hunter JS (1986) The exponentially weighted moving average. *J Qual Technol* 18(4):203–210
174. Divya S, Padma Suresh L, John A (2022) Hybrid optimization algorithm-based generative adversarial network for change detection using pre-operative and post-operative mri. *Int J Pattern Recognit Artif Intell* 36(07):2251007
175. Divya S, Padma Suresh L, John A (2022) Enhanced deep-joint segmentation with deep learning networks of glioma tumor for multi-grade classification using mr images. *Pattern Anal Appl* 25(4):891–911
176. Rao R (2016) Jaya: a simple and new optimization algorithm for solving constrained and unconstrained optimization problems. *Int J Ind Eng Comput* 7(1):19–34
177. Kumar KA, Boda R (2022) A computer-aided brain tumor diagnosis by adaptive fuzzy active contour fusion model and deep fuzzy classifier. *Multimed Tools Appl* 81(18):25405–25441
178. Doraiswami PR, Sarveshwaran V, Swamidasan ITJ, Sorna SCD (2022) Jaya-tunicate swarm algorithm based generative adversarial network for covid-19 prediction with chest computed tomography images. *Concurr Comput Pract Exp* 34(23):e7211
179. Mohammadi-Balani A, Nayeri MD, Azar A, Taghizadeh-Yazdi M (2021) Golden eagle optimizer: a nature-inspired metaheuristic algorithm. *Comput Ind Eng* 152:107050
180. James S, Renjith V (2022) Design of safety zone and optimal risk identification of undesired events during loading and unloading of lng terminal using tsa-geo: A hybrid strategy. *Process Integr Optim Sustain* 6(3):791–807
181. Sangeetha Francelin VF, Daniel J, Velliangiri S (2022) Intelligent agent and optimization-based deep residual network to secure communication in uav network. *Int J Intell Syst* 37(9):5508–5529
182. Passino KM (2002) Biomimicry of bacterial foraging for distributed optimization and control. *IEEE Control Syst Mag* 22(3):52–67
183. Guan S, Wang J, Wang X, Shi M, Lin W, Chen W (2022) Dynamic hyperparameter tuning-based path tracking control for robotic rollers working on earth-rock dam under complex construction conditions. *Autom Constr* 143:104576
184. Dhiman G, Kumar V (2017) Spotted hyena optimizer: a novel bio-inspired based metaheuristic technique for engineering applications. *Adv Eng Softw* 114:48–70
185. Das A (2022) Designing green IoT communication by adaptive spotted hyena tunicate swarm optimization-based cluster head selection. *Trans Emerg Telecommun Technol* 33(11):e4595
186. Heidari AA, Mirjalili S, Faris H, Aljarah I, Mafarja M, Chen H (2019) Harris hawks optimization: algorithm and applications. *Futur Gener Comput Syst* 97:849–872
187. Barshandeh S, Masdari M, Dhiman G, Hosseini V, Singh KK (2022) A range-free localization algorithm for IoT networks. *Int J Intell Syst* 37(12):10336–10379
188. Saremi S, Mirjalili S, Lewis A (2017) Grasshopper optimisation algorithm: theory and application. *Adv Eng Softw* 105:30–47
189. Antony Asir Daniel V, Jeha J (2023) An optimal modified faster region CNN model for diagnosis of liver diseases from ultrasound images. *IETE J Res* 2023:1–18
190. Sadollah A, Eskandar H, Kim JH (2015) Water cycle algorithm for solving constrained multi-objective optimization problems. *Appl Soft Comput* 27:279–298
191. Krishnan N et al (2023) Water cycle tunicate swarm algorithm based deep residual network for virus detection with gene expression data. *Comput Methods Biomed Eng Imaging Vis* 11(5):1641–1651
192. Karimkashi S, Kishk AA (2010) Invasive weed optimization and its features in electromagnetics. *IEEE Trans Antennas Propag* 58(4):1269–1278
193. Singh G, Nagpal A (2023) Hfcvo-dmn: Henry fuzzy competitive verse optimizer-integrated deep maxout network for incremental text classification. *Computation* 11(1):13
194. Wang T, Yang L (2018) Beetle swarm optimization algorithm: theory and application. Preprint <http://arxiv.org/abs/1808.00206>
195. Kumar L, Kumar P (2023) Bita-based secure and energy-efficient multi-hop routing in iot-wsn. *Cybern Syst* 54(6):809–835

196. Hashim FA, Houssein EH, Mabrouk MS, Al-Atabany W, Mirjalili S (2019) Henry gas solubility optimization: a novel physics-based algorithm. *Futur Gener Comput Syst* 101:646–667
197. Arumugasamy M, Arokiasamy A (2023) Tunicate henry gas solubility optimization-based deep residual network for fruit ripeness classification. *Concurr Comput Pract Exp* 35(2):e7490
198. Jia H, Peng X, Lang C (2021) Remora optimization algorithm. *Expert Syst Appl* 185:115665
199. Gupta AD, Rout RK (2023) Rotee: Remora optimization and tunicate swarm algorithm-based energy-efficient cluster-based routing for eh-enabled heterogeneous wsns. *Int J Commun Syst* 36(2):e5372
200. Brammya G, Praveena S, Ninu Preetha N, Ramya R, Rajakumar B, Binu D (2019) Deer hunting optimization algorithm: a new nature-inspired meta-heuristic paradigm. *Comput J* 2019:bxy133
201. Roshan R, Rishi OP (2023) Design and development of multi-objective hybrid clustering framework for smart city in India using internet of things. *J Inf Knowl Manag* 22(01):2250064
202. Iniyavan R, Vijayalakshmi B (2023) A novel channel estimation model for broadband wireless communication system using hybrid heuristic-based invariable step-size zero-attracting nlms algorithm. *Int J Intell Robot Appl* 7(2):370–384
203. Askarzadeh A (2016) A novel metaheuristic method for solving constrained engineering optimization problems: crow search algorithm. *Comput Struct* 169:1–12
204. Kiran U, Kumar K (2023) An hybrid heuristic optimal relay selection strategy for energy efficient multi hop cooperative cellular communication. *Ad Hoc Netw* 140:103058
205. Ghaemi M, Feizi-Derakhshi M-R (2014) Forest optimization algorithm. *Expert Syst Appl* 41(15):6676–6687
206. Ravikumar C et al (2023) Developing novel channel estimation and hybrid precoding in millimeter-wave communication system using heuristic-based deep learning. *Energy* 268:126600
207. Gomes GF, da Cunha SS, Acelotti AC (2019) A sunflower optimization (SFO) algorithm applied to damage identification on laminated composite plates. *Eng Comput* 35:619–626
208. Disney DA, Merline A (2023) An improved fuzzy logic-based small cell deployment in noma-hetnet: a novel sun flower-based tunicate swarm optimization-oriented multi objective concept. *Sādhanā* 48(2):67
209. Bansal JC, Sharma H, Jadon SS, Clerc M (2014) Spider monkey optimization algorithm for numerical optimization. *Mem Comput* 6:31–47
210. Dayana AM, Emmanuel WS, Linda CH (2023) Feature fusion and optimization integrated refined deep residual network for diabetic retinopathy severity classification using fundus image. *Multimed Syst* 29(3):1629–1650
211. Dhiman G, Kumar V (2019) Seagull optimization algorithm: theory and its applications for large-scale industrial engineering problems. *Knowl-Based Syst* 165:169–196
212. Balaji C, Suresh D (2024) Eeg and speech signal based multi-class recognition manoeuvre by exploiting a hyb-sgts and a dual stage deep cnn architecture for an early diagnosis of hc, ad and pd neurological diseases. *Int J Biomed Eng Technol* 44(4):348–366
213. Hayyolalam V, Kazem AAP (2020) Black widow optimization algorithm: a novel meta-heuristic approach for solving engineering optimization problems. *Eng Appl Artif Intell* 87:103249
214. Pahuja S, Jindal P (2024) Joint metaheuristics-based optimisation in wireless cooperative network. *Int J Wireless Mobile Comput* 26(3):291–301
215. Sadeq HT, Abdulazeez AM (2022) Giant trevally optimizer (GTO): a novel metaheuristic algorithm for global optimization and challenging engineering problems. *IEEE Access* 10:121615–121640
216. Zhao Q, Shi Y (2024) Prediction of unconfined compressive strength of stabilized sand using machine learning methods. *Indian Geotech J* 2024:1–18
217. Li S, Chen H, Wang M, Heidari AA, Mirjalili S (2020) Slime mould algorithm: a new method for stochastic optimization. *Futur Gener Comput Syst* 111:300–323
218. Mishra J, Tiwari M (2024) IoT-enabled ECG-based heart disease prediction using three-layer deep learning and meta-heuristic approach. *SIVIP* 18(1):361–367
219. Azizi M, Talatahari S, Gandomi AH (2023) Fire hawk optimizer: a novel metaheuristic algorithm. *Artif Intell Rev* 56(1):287–363
220. Minu M, Rani P, Sonthi VK, Shankar G, Mohan E, Rajesh A (2024) An innovative privacy preservation and security framework with fog nodes in enabled vanet system using hybrid encryption techniques. *Peer-to-Peer Netw Appl* 2024:1–25
221. Sharma I, Kumar V (2022) Multi-objective tunicate search optimisation algorithm for numerical problems. *Int J Intell Eng Inf* 10(2):119–144
222. El-Sehiemy RA (2022) A novel single/multi-objective frameworks for techno-economic operation in power systems using tunicate swarm optimization technique. *J Ambient Intell Humaniz Comput* 13(2):1073–1091
223. Rizk-Allah RM, Hagag EA, El-Fergany AA (2023) Chaos-enhanced multi-objective tunicate swarm algorithm for economic-emission load dispatch problem. *Soft Comput* 27(9):5721–5739
224. Al-Wesabi FN, Obayya M, Hilal AM, Castillo O, Gupta D, Khanna A (2022) Multi-objective quantum tunicate swarm optimization with deep learning model for intelligent dystrophinopathies diagnosis. *Soft Comput* 2022:1–16
225. Liu Z-F, Zhao S-X, Zhao S-L, You G-D, Hou X-X, Yu J-L, Li L-L, Chen B (2023) Improving the economic and environmental benefits of the energy system: a novel hybrid economic emission dispatch considering clean energy power uncertainty. *Energy* 285:128668
226. Menesy AS, Sultan HM, Hassan MH, Elsayed SK, Kamel S (2021) Calculating optimal parameters of proton exchange membrane fuel cell. In: 2021 IEEE CHILEAN conference on electrical, electronics engineering, information and communication technologies (CHILECON), IEEE, pp 1–9
227. Singh P, Pandit M, Srivastava L (2021) Enviro-economic sizing of a grid-connected hybrid energy system using tunicate swarm algorithm. In: 2021 IEEE 2nd international conference on electrical power and energy systems (ICEPES), IEEE, pp 1–6
228. Ajayi O, Heymann R (2022) Tunicate swarm algorithm-trained multi-layered perceptron for data centre energy demand forecasting and relative percentage contribution analysis of input parameters. *J Eng Design Technol* 20(5):1172–1187
229. Nguyen TT, Le KH, Phan TM, Duong MQ (2021) An effective reactive power compensation method and a modern metaheuristic algorithm for loss reduction in distribution power networks. *Complexity* 2021:1–21
230. Rajesh P, Shajin FH, Cherukupalli K (2021) An efficient hybrid tunicate swarm algorithm and radial basis function searching technique for maximum power point tracking in wind energy conversion system. *J Eng Design Technol* 2021:1
231. Ajayi O, Heymann R, Okampo E (2021) Marine predators algorithm and tunicate swarm algorithm for power system economic load dispatch. In: Proceedings of the 11th annual international conference on industrial engineering and operations management, Singapore, pp 120–133
232. Sathish K, Ananthapadmanabha T (2021) Power quality enhancement in distribution system integrated with renewable energy sources using hybrid rbfnn-tsa technique. In: 2021 7th international conference on electrical energy systems (ICEES), IEEE, pp 189–194

233. Abd El-Sattar H, Sultan HM, Kamel S, Menesy AS, Rahmann C (2021) Optimal design of hybrid stand-alone microgrids using tunicate swarm algorithm. In: 2021 IEEE international conference on automation/XXIV congress of the Chilean association of automatic control (ICA-ACCA), IEEE, pp 1–6
234. Sharma A, Dasgupta A, Tiwari SK, Sharma A, Jately V, Azzopardi B (2021) Parameter extraction of photovoltaic module using tunicate swarm algorithm. *Electronics* 10(8):878
235. Aribowo W, Muslim S, Suprianto B, Haryudo SI et al (2021) Tunicate swarm algorithm-neural network for adaptive power system stabilizer parameter. *Sci Technol Asia* 2021:50–63
236. Nguyen V, Doan T, Do K, Le H, Phan V (2021) Power generation cost optimization for thermal power plants considering prohibited operation zones and power losses. In: AIP conference proceedings, vol. 2406. AIP Publishing
237. Ganti PK, Naik H, Barada MK (2021) Hybrid tsa-rbfnn based approach for mppt of the solar pv panel under the effects of tilt angles variations and environmental effects. *Int J Energy Res* 45(14):20104–20131
238. Mansoor M, Mirza AF, Long F, Ling Q (2021) An intelligent tunicate swarm algorithm based mppt control strategy for multiple configurations of pv systems under partial shading conditions. *Adv Theor Simul* 4(12):2100246
239. Tayab UB, Yang F, Metwally ASM, Lu J (2022) Solar photovoltaic power forecasting for microgrid energy management system using an ensemble forecasting strategy. *Energy Sour A: Recov Utilizat Environ Effects* 44(4):10045–10070
240. Ge L, Liu J, Du T, Zhao C, Pian R, Liu W (2022) Size optimization of wind-pv-diesel-hydrogen-ice system for island microgrid. In: 2022 IEEE power & energy society general meeting (PESGM), IEEE, pp 1–5
241. Patnaik S, Sarangi B, Tripathy R, Nayak MR, Viswavandy M (2022) Strategic placement of pv and wtg in low power distribution system for improving system efficacy. In: 2022 international conference on intelligent controller and computing for smart power (ICICCSP), IEEE, pp 1–6
242. Vishal G, Pradeep J (2022) Improved performance of pmsm using tunicate swarm optimization. In: 2022 international conference on emerging smart computing and informatics (ESCI), IEEE, pp 1–5
243. Tayeb JH, Islam MR, Shafiqullah M, Gani SMA, Hossain MI (2022) Robust power system stabilizer for multi-machine power networks using tunicate swarm algorithm. In: 2022 second international conference on artificial intelligence and smart energy (ICAIS), IEEE, pp 1761–1766
244. Hossen MS, Islam MR, Shafiqullah M, Fahim-Ul-Haque M, Ali A (2022) Tunicate swarm algorithm for power system stability enhancement in a smib-upfc network. In: 2022 second international conference on artificial intelligence and smart energy (ICAIS), IEEE, pp 1767–1772
245. Hien CT, Ha PT, Phan-Van TH, Pham TM (2022) Multi-period economic load dispatch with wind power using a novel metaheuristic, GMSARN. *Int J* 16:165–173
246. Larouci B, Ayad ANEI, Alharbi H, Alharbi TE, Boudjella H, Tayeb AS, Ghoneim SS, Abdelwahab SAM (2022) Investigation on new metaheuristic algorithms for solving dynamic combined economic environmental dispatch problems. *Sustainability* 14(9):5554
247. Fathy A, Ferahtia S, Rezk H, Yousri D, Abdelkareem MA, Olabi A (2022) Optimal adaptive fuzzy management strategy for fuel cell-based dc microgrid. *Energy* 247:123447
248. Zhou M, Zhu Z, Hu F, Bian K, Lai W, Hu T (2022) Short-term commercial load forecasting based on peak-valley features with the tsa-elm model. *Energy Sci Eng* 10(8):2622–2636
249. Krishnakumar R, Ravichandran C (2022) Reliability and cost minimization of renewable power system with tunicate swarm optimization approach based on the design of pv/wind/fc system. *Renew Energy Focus* 42:266–276
250. Sholikhah EN, Windarko NA, Sumantri B (2022) Tunicate swarm algorithm based maximum power point tracking for photovoltaic system under non-uniform irradiation. *Int J Electric Comput Eng* 12(5):4559–4570
251. Li G, Yin S, Yang H (2022) A novel crude oil prices forecasting model based on secondary decomposition. *Energy* 257:124684
252. Memon AS, Laghari J, Bhayo MA, Khokhar S, Chandio S, Memon MS (2023) Tunicate swarm algorithm based optimized pid controller for automatic generation control of two area hybrid power system. *J Intell Fuzzy Syst* 45(2):2565–2578
253. Madupu HS, Chinda PR, Kotni S (2023) A novel tunicate swarm algorithm for optimal integration of renewable distribution generation in electrical distribution networks considering extreme load growth. *J Electric Eng Technol* 18(4):2709–2722
254. Sharma B, Rizwan M, Anand P (2023) Optimal design of renewable energy based hybrid system considering weather forecasting using machine learning techniques. *Electr Eng* 105(6):4229–4249
255. Saha A, Dash P, Chiranjeevi T, Ram Babu N (2024) Implementation of combined hydrogen aqua electrolyser-fuel cell and redox-flow-battery under restructured situation of agc employing tsa optimized pdn (fopi) controller. *J Taibah Univ Sci* 18(1):2334004
256. Rashidi R, Hatami A, Moradi M, Liang X (2024) Optimal multi-microgrids energy management through information gap decision theory and tunicate swarm algorithm. *IEEE Access* 2024:1
257. Anand P, Sharma B, Rizwan M (2024) Size optimization of grid-tied hybrid energy system by employing forecasted meteorological data. *Mapan* 39(3):739–750
258. Islam MR, Azam MS, Hossen MS, Islam MS, Worku MY, Shahriar MS, Shafiqullah M (2024) Power system stability enhancement through optimal pss design, e-Prime-advances in electrical engineering. *Electron Energy* 9:100735
259. Verma S, Kaur S, Rawat DB, Xi C, Alex LT, Jhanji NZ (2021) Intelligent framework using IoT-based WSNS for wildfire detection. *IEEE Access* 9:48185–48196
260. Verma S, Kaur S, Sharma AK, Kathuria A, Piran MJ (2020) Dual sink-based optimized sensing for intelligent transportation systems. *IEEE Sens J* 21(14):15867–15874
261. Sharma S, Mishra V, Tripathi MM (2021) Intelligent-routing algorithm for wireless body area networks (i-raw). *Int J Commun Syst* 34(17):e4984
262. Dogra R, Rani S, Verma S, Garg S, Hassan MM (2021) Torm: tunicate swarm algorithm-based optimized routing mechanism in IoT-based framework. *Mobile Netw Appl* 2021:1–9
263. Avdhesh Yadav S, Poongodi T (2022) A novel optimized routing technique to mitigate hot-spot problem (north) for wireless sensor network-based internet of things. *Int J Commun Syst* 35(16):e5314
264. Khan S, Singh YV, Singh P, Singh RS et al (2022) An optimized artificial intelligence system using IoT biosensors networking for healthcare problems. *Comput Intell Neurosci* 2022:1
265. Subramani N, Perumal SK, Kallimani JS, Ulaganathan S, Bharagava S, Meckanizi S (2022) Controlling energy aware clustering and multihop routing protocol for IoT assisted wireless sensor networks. *Concurr Comput Pract Exp* 34(21):e7106
266. Gupta S, Singh NP (2022) Energy hole mitigation through optimized cluster head selection and strategic routing in internet of underwater things. *Int J Commun Syst* 35(15):e5283
267. Raj S, Rajesh R (2024) Securing rpl networks with enhanced routing efficiency with congestion prediction and load balancing strategy. *Int J Adv Comput Sci Appl* 15(8):1
268. Taher F, Elhoseny M, Hassan MK, El-Hasnony IM (2022) A novel tunicate swarm algorithm with hybrid deep learning

- enabled attack detection for secure iot environment. *IEEE Access* 10:127192–127204
269. Chaudhary S, Hiranwal S, Gupta C (2022) Graph signal processing and tunicate swarm optimization based image steganography using hybrid chaotic map based image scrambling. *J Discret Math Sci Cryptogr* 25(7):2159–2171
270. Singh G, Nagpal A (2022) A text classification optimization framework for prodigious datasets. In: *ICT with intelligent applications: proceedings of ICTIS 2022*, vol 1. Springer, pp 677–691
271. Aljebreen M, Alrayes FS, Maray M, Aljameel SS, Salama AS, Motwakel A (2023) Modified equilibrium optimization algorithm with deep learning-based ddos attack classification in 5g networks. *IEEE Access* 2023:c1
272. Katib I, Assiri FY, Abdushkour HA, Hamed D, Ragab M (2023) Differentiating chat generative pretrained transformer from humans: detecting chatgpt-generated text and human text using machine learning. *Mathematics* 11(15):3400
273. Seth R, Sharaff A (2023) Sentiment data analysis for detecting social sense after covid-19 using hybrid optimization method. *SN Comput Sci* 4(5):568
274. Krishnasamy S, Alotaibi MB, Alehaideb LI, Abbas Q (2023) Development and validation of a cyber-physical system leveraging efdpn for enhanced WSN-IoT network security. *Sensors* 23(22):9294
275. Singh JP, Kumar M (2023) Conditional autoregressive-tunicate swarm algorithm based generative adversarial network for violent crowd behavior recognition. *Artif Intell Rev* 56(Suppl 2):2099–2123
276. Alrurban A, Alrayes FS, Kouki F, Alotaibi FA, Aljehane NO, Mohamed A (2023) Chaotic tumbleweed optimization algorithm with stacked deep learning based cyberattack detection in industrial cps environment. *Alex Eng J* 84:250–261
277. Sasaki T (2024) A secure multi-modal biometrics using deep convgru neural networks based hashing. *Expert Syst Appl* 235:121096
278. Daniel DAJ, Meena MJ (2021) A novel sentiment analysis for amazon data with tsa based feature selection. *Scalable Comput Pract Exp* 22(1):53–66
279. Diaz P, Jiju MJE (2022) A comparative analysis of meta-heuristic optimization algorithms for feature selection and feature weighting in neural networks. *Evol Intel* 15(4):2631–2650
280. Gupta R, Sharma A, Wadhwa C, Yoganathan S (2024) Improving supply chain performance administration using a novel deep learning algorithm. *Multidiscip Sci J* 6:1
281. PS ALH, Kala SP, Bindu G, Husseen A, Naresh V (2024) Customer churn prediction using tunicate swarm optimization based hybrid machine learning algorithms. In: *2024 international conference on distributed computing and optimization techniques*, IEEE, pp 1–4
282. Sharifi MR, Akbarifard S, Qaderi K, Madadi MR (2021) Comparative analysis of some evolutionary-based models in optimization of dam reservoirs operation. *Sci Rep* 11(1):15611
283. Abdelhamid M, Kamel S, Nasrat L, Shahinzadeh H, Nafisi H (2022) Adaptive coordination of distance and direction overcurrent relays in active distribution networks based on the tunicate swarm algorithm. In: *2022 12th smart grid conference (SGC)*, IEEE, pp 1–6
284. Al Duhayyim M, Albraikan AA, Al-Wesabi FN, Burbur HM, Alamgeer M, Hilal AM, Hamza MA, Rizwanullah M (2022) Modeling of artificial intelligence based traffic flow prediction with weather conditions. *Comput Mater Continua* 71(2):1
285. Kammula SK, Anand V, Singh D (2023) An energy-conscious surveillance scheme for intrusion detection in underwater sensor networks using tunicate swarm optimization. In: *International conference on information systems security*, Springer, pp 129–138
286. Pahuja S, Jindal P (2023) Swarm algorithm-based power optimization in cooperative communication network. *Int J Sens Wirel Commun Control* 13(5):285–295
287. Qiang S, Chenyu M, Dezh K (2023) The implementation of a least square support vector regression model utilizing metaheuristic algorithms for predicting undrained shear strength. *Multisc Multidisc Model Exp Design* 2023:1–14
288. Husain S, Jarndal A, Hashmi M, Ghannouchi FM (2023) Accurate, efficient and reliable small-signal modelling approaches for gan hemts. *IEEE Access* 2023:1
289. Hasan AF, Humaidi AJ, Al-Obaidi ASM, Azar AT, Ibraheem IK, Al-Dujaili AQ, Al-Mhdawi AK, Abdulmajeed FA (2023) Fractional order extended state observer enhances the performance of controlled tri-copter uav based on active disturbance rejection control. In: *Mobile robot: motion control and path planning*, Springer, pp 439–487
290. Li Y, Wu Y, Zhang X, Tan X, Zhou W (2023) Unmanned bicycle balance control based on tunicate swarm algorithm optimized by neural network pid. *Int J Inf Technol Syst Approach* 16(3):1–16
291. Guo H, Feng Z, Wang X (2023) Multi-objective grasshopper optimisation algorithm applied to design dna sequences. In: *2023 15th international conference on advanced computational intelligence (ICACI)*, IEEE, pp 1–8
292. Alnifai MM (2023) Intelligent modulation recognition of communication signal for next-generation 6g networks. *Comput Mater Continua* 74(3):1
293. Zhou Z, Ma Z, Wang Y, Zhu Z (2023) Fabric wrinkle rating model based on resnet18 and optimized random vector functional-link network. *Text Res J* 93(1–2):172–193
294. Kamalkumar V, Lal Raja Singh R (2023) Optimum transistor sizing of cmos differential amplifier using tunicate swarm algorithm. *J Circ Syst Comput* 32(03):2350051
295. He B, Armaghani DJ, Lai SH (2023) Assessment of tunnel blasting-induced overbreak: a novel metaheuristic-based random forest approach. *Tunn Undergr Space Technol* 133:104979
296. Mei X, Li C, Cui Z, Sheng Q, Chen J, Li S (2023) Application of metaheuristic optimization algorithms-based three strategies in predicting the energy absorption property of a novel aseismic concrete material. *Soil Dyn Earthq Eng* 173:108085
297. Barua A, Jeet S, Mishra M, Kumari K, Priyadarshini M, Pradhan S, Saha S (2023) Weight optimization of plastic injection moulded electrical wire casing thermoplastic using hybrid rsm-tunicate swarm algorithm. In: *E3S Web of Conferences*, vol 453. EDP Sciences, p 01052
298. Liu X, Zhang Y, Lei S, Yang S (2023) Estimating the mechanical properties of high-performance concrete via automated and ensembled machine learning methods. *Mater Today Commun* 37:107386
299. Kala P, Sharma A, Jately V, Joshi J, Yang Y (2024) An initial solution based selective harmonic elimination method for multilevel inverter. *CPSS Transactions on Power Electronics and Applications*
300. Wang L (2024) Estimating high-performance concrete compressive strength with support vector regression in hybrid method. *Multisc Multidisc Model Exp Design* 7(1):477–490
301. Alyami M, Khan M, Javed MF, Ali M, Alabduljabbar H, Najeh T, Gamil Y (2024) Application of metaheuristic optimization algorithms in predicting the compressive strength of 3d-printed fiber-reinforced concrete. *Dev Built Environ* 17:100307
302. Zhai Q, Sun J, Shang Y, Wang H (2024) A novel remaining useful life prediction method based on gated recurrent unit network optimized by tunicate swarm algorithm for lithium-ion batteries. *Transactions of the Institute of Measurement and Control* 01423312241257305

303. Kengpol A, Tabkosai P (2024) Design of hybrid deep learning using tsa with ann for cost evaluation in the plastic injection industry. *Front Mech Eng* 10:1336828
304. Jeyanthi S, Venkatakrishnaiah R, Raju K (2024) Evaluation and intelligent modelling for predicting the amplitude of footing resting on geocell-based weak sand bed under vibratory load. In: *Cross-industry AI applications*, IGI Global, pp 225–244
305. Shwetha N, Priyatham M, Dalal V, Raghu J (2024) Adaptive channel equalization for digital communication with tunicate swarm algorithm. *IETE J Res* 2024:1–18
306. Sudha M, Balamurugan V, Lai W-C, Divakarachari PB (2022) Sustainable multipath routing for improving cross-layer performance in manet using an energy centric tunicate swarm algorithm. *Sustainability* 14(21):13925
307. Inamdar SR, Kallibaddi JI (2022) Route establishment in manets; ameliorated with tunicate swarm algorithm and cross layer interaction. In: *2022 international conference on distributed computing, VLSI, electrical circuits and robotics (DISCOVER)*, IEEE, pp 144–149
308. Khan S, Singh YV, Yadav PS, Sharma V, Lin C-C, Jung K-H (2023) An intelligent bio-inspired autonomous surveillance system using underwater sensor networks. *Sensors* 23(18):7839
309. Saad A, Hegazy I, El Sayed M (2023) Energy efficient clustering-based routing algorithm for internet of things. *Bull Electric Eng Inf* 12(6):3489–3498
310. Simon J, Kapileswar N, Phani Kumar P, Aarthi Elaveini M (2024) Improved geographic opportunistic routing protocol for void hole elimination in underwater IoTs: parameter tuning by tsa optimization. *Int J Commun Syst* 37(3):e5659
311. Chander S, Vijaya P (2020) Tunicate swarm-based black hole entropic fuzzy clustering for data clustering using covid data. In: *2020 IEEE 17th India Council International Conference (INDICON)*, IEEE, pp 1–5
312. Nguyen GN, Le Viet NH, Joshi GP, Shrestha B (2020) Intelligent tunicate swarm-optimization-algorithm-based lightweight security mechanism in internet of health things. *Comput Mater Continua* 66(1):551–562
313. Awari H, Subramani N, Janagaraj A, Balasubramaniapillai Thanammal G, Thangarasu J, Kohar R (2022) Three-dimensional dental image segmentation and classification using deep learning with tunicate swarm algorithm. *Expert Syst* 2022:e13198
314. Çetinkaya MB, Duran H (2022) Performance comparison of most recently proposed evolutionary, swarm intelligence, and physics-based metaheuristic algorithms for retinal vessel segmentation. *Math Probl Eng* 2022:1–25
315. Wankhede J, Sambandam P, Kumar M (2022) Effective prediction of heart disease using hybrid ensemble deep learning and tunicate swarm algorithm. *J Biomol Struct Dyn* 40(23):13334–13345
316. Srikanth K, Ul Huq SZ, Kumar A (2022) Big data based analytic model to predict and classify breast cancer using improved fractional rough fuzzy k-means clustering and labeled ensemble classifier algorithm. *Concurr Comput Pract Exp* 34(10):1
317. Sun Y, Jen TH (2023) The impact of the teaching mode of physical activities independent courses in arts education on the physical changes and mental health of college students based on deep learning analysis. *Eurasian J Educ Res* 105(105):140–158
318. Mahaveerakannan R, Dhar M, Goswami S, Krishna PG, Jayanthi K, Kumar MS (2023) Analysis of lung cancer for developing smart healthcare with the help of bgwo based tsa-xgboost model. In: *2023 international conference on self sustainable artificial intelligence systems (ICSSAS)*, IEEE, pp 910–916
319. Akram SW, Kumar AS (2023) Parkinson's disease diagnosis from t1 and t2 weighted magnetic resonance images using fblstmnet architecture. *Multimed Tools Appl* 2023:1–28
320. Abdulla S, Ragab M (2023) Tunicate swarm algorithm with deep convolutional neural network-driven colorectal cancer classification from histopathological imaging data. *Electron Res Arch* 31(5):2793–2812
321. Poonguzhalai R, Ahmad S, Sivasankar PT, Babu SA, Joshi P, Joshi GP, Kim SW (2023) Automated brain tumor diagnosis using deep residual u-net segmentation model. *Comput Mater Continua* 74(1):2179–2194
322. Laishram R, Rabidas R (2023) Optimized hyperbolic tangent function-based contrast-enhanced mammograms for breast mass detection. *Expert Syst Appl* 213:118994
323. Gandikota HP (2023) CT scan pancreatic cancer segmentation and classification using deep learning and the tunicate swarm algorithm. *PLoS ONE* 18(11):e0292785
324. Laxminarayananamma K, Krishnaiah R, Sammulal P (2024) Idrcnn: a novel deep learning network model for pancreatic ductal adenocarcinoma detection on computed tomography. *Int J Electric Comput Eng Syst* 15(1):1–11
325. Digumarthi J, Gayathri V, Pitchai R (2023) Cardiac arrhythmia detection from ECG signal using siamese adversarial neural network. *Multimed Tools Appl* 2023:1–28
326. Ganesan P, Ramesh G, Falkowski-Gilski P, Falkowska-Gilska B (2024) Detection of Alzheimer's disease using otsu thresholding with tunicate swarm algorithm and deep belief network. *Front Physiol* 15:1380459
327. Kengpol A, Klunngien J (2024) An intelligent risk assessment on prediction of covid-19 pandemic using dnn and tsa: an empirical case study in Thailand. *Expert Syst Appl* 2024:124311
328. Palaniswamy T (2024) An automated metaheuristic tunicate swarm algorithm based deep convolutional neural network for bone age assessment model. *Ain Shams Eng J* 2024:102942
329. Lavanya K, Mahendran A, Selvanambi R, Mazzara M, Hemanth JD (2023) Tunicate swarm algorithm with deep learning based land use and cover change detection in nallamalla forest india. *Appl Sci* 13(2):1173
330. Saranya N, Srinivasan K, Pravin Kumar S (2023) Fbcnn-tsa: an optimal deep learning model for banana ripening stages classification. *J Intell Fuzzy Syst* 44(3):5257–5273
331. Kumar KV, Kumar YD, Godla SR, Al Ansari MS, El-Ebiary YAB, Muniyandy E (2024) Enhancing water quality forecasting reliability through optimal parameterization of neuro-fuzzy models via tunicate swarm optimization. *Int J Adv Comput Sci Appl* 15(3):1
332. Javed MF, Siddiq B, Onyelowe K, Khan WA, Khan M (2024) Metaheuristic optimization algorithms-based prediction modeling for titanium dioxide-assisted photocatalytic degradation of air contaminants. *Results Eng* 23:102637
333. Harik GR, Lobo FG (1999) A parameter-less genetic algorithm. In: *Proceedings of the 1st annual conference on genetic and evolutionary computation*, vol 1. GECCO'99, Morgan Kaufmann Publishers Inc., San Francisco, CA, USA, pp 258–265
334. Storn R, Price K (1997) Differential evolution—a simple and efficient heuristic for global optimization over continuous spaces. *J Global Optim* 11:341–359
335. Hansen N, Müller SD, Koumoutsakos P (2003) Reducing the time complexity of the derandomized evolution strategy with covariance matrix adaptation (cma-es). *Evol Comput* 11(1):1–18
336. Chopra N, Mohsin Ansari M (2022) Golden jackal optimization: a novel nature-inspired optimizer for engineering applications. *Expert Syst Appl* 198:116924. <https://doi.org/10.1016/j.eswa.2022.116924>
337. Mohammed H, Rashid T (2023) Fox: a fox-inspired optimization algorithm. *Appl Intell* 53(1):1030–1050. <https://doi.org/10.1007/s10489-022-03533-0>
338. Trojovský P, Dehghani M (2022) Pelican optimization algorithm: a novel nature-inspired algorithm for engineering applications. *Sensors*. <https://doi.org/10.3390/s22030855>

-
- 339. Brest J, Maučec MS, Bošković B (2017) Single objective real-parameter optimization: algorithm JSO, IN. IEEE Cong Evol Comput (CEC) 2017:1311–1318. <https://doi.org/10.1109/CEC.2017.7969456>
 - 340. Awad NH, Ali MZ, Suganthan PN (2017) Ensemble sinusoidal differential covariance matrix adaptation with euclidean neighborhood for solving cec2017 benchmark problems, in. IEEE Cong Evol Comput 2017:372–379. <https://doi.org/10.1109/CEC.2017.7969336>
 - 341. Wolpert DH, Macready WG (1997) No free lunch theorems for optimization. IEEE Trans Evol Comput 1(1):67–82

Springer Nature or its licensor (e.g. a society or other partner) holds exclusive rights to this article under a publishing agreement with the author(s) or other rightsholder(s); author self-archiving of the accepted manuscript version of this article is solely governed by the terms of such publishing agreement and applicable law.